DOE/PC/90044--T2
(DE95001146)
Distribution Category UC-109

HIGH OCTANE ETHERS FROM SYNTHESIS GAS-DERIVED ALCOHOLS

Final Technical Report
September 25, 1990-December 24, 1993

Kamil Klier and Richard G. Herman

Zettlemoyer Center for Surface Studies
and Department of Chemistry
LEHIGH UNIVERSITY
Bethlehem, PA 18015

May 1994

PREPARED FOR THE

U. S. DEPARTMENT OF ENERGY
PITTSBURGH ENERGY TECHNOLOGY CENTER

Contract No. DE-AC22-90PC90044

Disclaimer

EXECUTIVE SUMMARY

The objective of the research was to develop the methodology for the catalytic synthesis of ethers, primarily methyl isobutyl ether (MIBE) and methyl tertiary butyl ether (MTBE), directly from alcohol mixtures that are rich in methanol and 2-methyl-1-propanol (isobutanol). The overall scheme involves gasification of coal, purification and shifting of the synthesis gas, higher alcohol synthesis, and direct synthesis of ethers. The last stage of the synthesis involves direct coupling of synthesis gas-derived methanol and isobutanol that has been previously demonstrated by us to occur over superacid catalysts to yield MIBE and smaller amounts of MTBE at moderate pressures and a mixture of methanol and isobutene at low pressures.

The effectiveness of solid acid catalysts for the conversion of methanol and isobutanol mixtures to ethers or precursors to ethers was investigated. The target ethers are those which possess beneficial fuel additive characteristics such as high octane or high cetane values for use in gasoline or diesel fuels, respectively. In addition, these ethers possess environmentally beneficial properties in that they are oxygenates and their use in automotive fuels reduces carbon monoxide emissions. Indeed, the use of oxygenated fuels is required in many major metropolitan areas during winter months.

Several very selective novel reactions have been discovered over the course of this work. H-Mordenite can selectively convert, at relatively low temperatures, i.e. 90-150°C, the methanol in the methanol/isobutanol mixture to dimethyl ether (DME) while leaving the isobutanol unconverted. Acidic ion-exchange resins, particularly Nafion-H, have been shown to directly couple the two alcohols to MIBE selectively at 90°C.

Sulfate-modified zirconia converts isobutanol selectively, in high yield, in the presence

of an equimolar amount of methanol, to isobutene with minimal conversion of methanol. This essentially converts the methanol/isobutanol mixture to a methanol/isobutene mixture that is the direct feedstock in the current commercial process for MTBE production. This highly selective and novel reaction is the critical step in the efficient production of MTBE from C_1 sources such as coal, natural gas, and biomass.

The direct conversion of methanol and isobutanol to MTBE, although thermodynamically viable, has been found to be kinetically unfavored over other acid catalyzed reactions. The conversion, however, may be realized in a 2-step process utilizing the high selectivity of sulfate-modified zirconia catalyst for the initial dehydration of isobutanol to isobutene. Then the methanol/isobutene mixture can be converted, at lower temperature over Amberlyst-15, to MTBE. Because the initial isobutanol dehydration occurs in the presence of methanol, the need for a costly alcohol separation step following higher alcohol synthesis is eliminated.

The sulfate-modified zirconia was characterized extensively. The treatment of the zirconia precursor with sulfate was found to be crucial as the sulfate-free zirconia was found to be totally inactive for the methanol-isobutanol reactions even at elevated temperatures. The addition of sulfate was also found to stabilize the high surface area of the catalyst. X-ray photoelectron spectroscopy (XPS) of pyridine adsorbed on ZrO_2/SO_4^{2-} shows the presence of both Bronsted and Lewis type acid centers. Aqueous titration of water-treated sulfated zirconia revealed that all of the sulfate groups can be converted to mono-protic surface Brönsted acid.

TABLE OF CONTENTS

LIST OF FIGURES

LIST OF TABLES

I. Background of C_5 Ether Synthesis

Due to U.S. federal legislation aimed at environmental improvements of the transportation industry, reformulated gasolines are being developed that contain lower content of aromatic hydrocarbons and increased levels of organic oxygenates. At the present time, the preferred oxygenate is methyl tertiary butyl ether (MTBE) because it compensates for the loss in octane number due to a reduction in aromatics, reduces the vapor pressure of the gasoline fuel, and provides for partial abatement of vehicle tailpipe hydrocarbon and carbon monoxide emissions (1).

Currently, MTBE is manufactured from methanol and isobutene *via* a liquid phase synthesis over acid resin catalysts, as represented by Equation 1, where isobutene is obtained as a side product from petroleum refinery FCC units (2-4). Although older FCC units could produce 8 wt% C_4 products in their output (5), the typical FCC refinery product slate now contains 1.4 wt% C_4 compounds (6), and improved processes utilizing catalytic additives such as improved ZSM-5 tend to decrease the yield of C_3 and C_4 olefins in the light ends still further (7). Thermal cracking of isobutane in the light ends can also be carried out to obtain isobutene (6). In any case, the availability of refinery supplied isobutene is limited.

$$(CH_3)_2C{=}CH_2 \; + \; CH_3OH \; \rightarrow \; (CH_3)_3C\text{-}O\text{-}CH_3 \qquad (1)$$

Since MTBE is now the seventh largest produced synthetic organic chemical today (8) and has also been the fastest growing catalytic process during the last decade, a ready supply of both methanol and isobutene is needed. Indeed, it has been predicted that due to continuing and increasing clean air restrictions, the demand for oxygenates (ethers and alcohols) in fuels could increase more than 10-fold by the year 2001 (9). To put this in perspective, the U.S. National Research Council states that the demand for oxygenates may

approach 1 million barrels/day by the year 2000, a level equivalent to nearly 10% of current U.S. petroleum production (1). Various alternatives have been sought for increasing the availability of isobutene, and one source of C_4 is butane from natural gas. Although the butane content in natural gas is low, this source of C_4 is increasingly gaining importance. Among the processes that have been developed for the synthesis of pure isobutene is the endothermic dehydration of tertiary butanol (10).

Another possible source of isobutene for ether synthesis is dehydration of isobutanol, produced from synthesis gas as represented by Equation 2. Methanol and isobutanol are the predominant products formed from H_2/CO synthesis gas over alkali promoted Cu/ZnO-based catalysts (11-15). Since the two alcohols are produced together, direct coupling of these two alcohols to produce high octane ethers provides an attractive path to C_5 ethers. It has been shown (16,17) that over acid catalysts, the dominant reaction is direct coupling that results in the formation of methyl isobutyl ether (MIBE), Equation 3.

$$(CH_3)_2CHCH_2OH \rightarrow (CH_3)_2C=CH_2 + H_2O \quad (2)$$

$$(CH_3)_2CHCH_2OH + CH_3OH \rightarrow (CH_3)_2CHCH_2\text{-}O\text{-}CH_3 + H_2O \quad (3)$$

However, if a selective catalyst were found for converting isobutanol to isobutene followed by a reaction with methanol, a desirable route to high octane MTBE from natural gas or coal-derived synthesis gas would be provided. Such a process would alleviate isobutene dependence on petroleum feedstocks. The objective of this research was to develop the methodology for the catalytic synthesis of high value ethers, primarily MTBE and MIBE, from alcohol mixtures that are rich in methanol and isobutanol.

A. Selection of the Organic Resin Catalysts

Since the current commercial catalysts used for the liquid phase synthesis of MTBE from methanol and isobutene are strong acid resin catalysts, this type of catalyst was studied here for the gas phase synthesis of ethers. Task 1 of this research was centered on acid organic resins, principally those containing comparisons of the catalytic behavior of $-SO_3H$ acid functional groups. The two general groups of these resins are

(i) polystyrene ion exchange resins, and

(ii) fluorocarbon sulfonic acid (FSA) polymers.

The first group contains polymeric catalysts such as Amberlyst-15, Purolite C-150, and Bio-Rad AG 50W X-2, all of which were tested for the reaction of isobutene with methanol at 75°C and 0.1 MPa to form MTBE, as well as for ether synthesis *via* alcohol coupling at 90°C and 0.1 MPa. This group of catalysts consists of sulfonated forms of polystyrene crosslinked with divinylbenzene. Amberlyst-15 and Purolite are macroreticular forms of the polystyrene type resins. The second group of FSA polymers was developed by duPont under the name of Nafion, and similar materials were subsequently developed by Dow Chemical Co. Both are copolymers of tetrafluoroethylene and fluorinated vinyl ethers that contain fluorosulfonyl groups, and the molecular structures of these are given below:

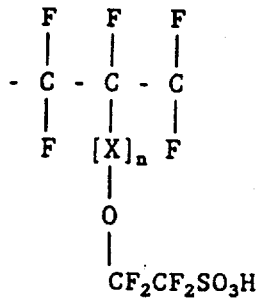

I. Dow Chemical Company

II. Du Pont Nafion

I; n = 0

II; n = 1, 2, 3 -- with X = $-O-CF_2-CF(CF_3)-$

B. Experimental Testing of the Catalysts

The catalysts were tested for ether synthesis from binary methanol/isobutanol, as well as methanol/isobutene, reactant mixtures in the vapor phase in a continuous flow stainless steel bench-scale reactor system that is automated so that testing can be carried out under continuous operation at designed experimental conditions. A schematic of the reaction system is shown in Figure 1. The furnace consists of three independent heating elements and maintained a very constant steady state temperature. Typically N_2/He gas is utilized as the carrier/inlet gas, and the alcohol mixture was added at the top of the reactor *via* a Gilson high pressure pump. Later experiments, in particular those with inorganic catalysts, used a ISCO high pressure piston pump provided by Air Products and Chemicals, Inc. In certain experiments, independent flows of methanol and isobutanol were employed by utilizing both pumps, and this allowed the molar ratio of the two alcohols to be easily varied during the experiments. The conversion and product composition were monitored by periodic sampling, e.g. semi-hourly, of the exit stream by gas chromatographic analysis using in-line, heated, automated sampling valves. In addition, the liquid product collected was sometimes subjected to subsequent analyses by GC, NMR, and GC/MS.

The dedicated Hewlett-Packard Model 5890 Series II gas chromatograph (HP GC) has automated heated Valco sampling valves, both thermal conductivity (TCD) and flame ionization (FID) detectors, both packed column and capillary column (a 25 m x 0.32 mm ID wall coated open tube (WCOT) capillary column with a chemically bound 5.0 um thick methyl silicon coating) capabilities, and is interfaced and controlled by a PC data station (Gateway 2000 personal computer system) using a complete package of menu-driven chromatographic software (Chrom Perfect) from Justice Innovations, Inc. At the same time, the GC is interfaced with a Hewlett-Packard Model 3396 Series II recorder/integrator, that

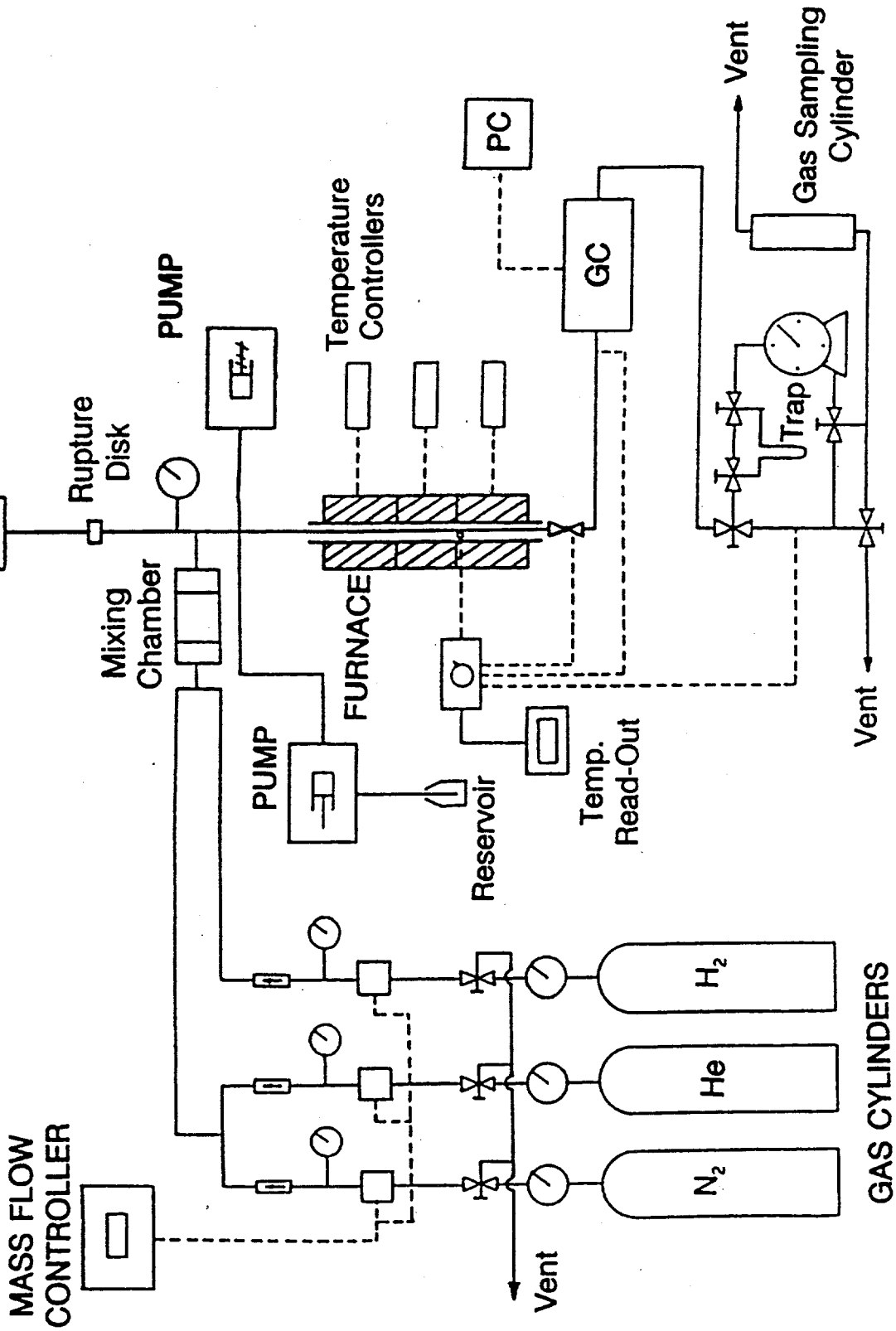

Figure 1. Schematic of the reaction system

can produce a hard copy of each chromatogram and listing of the associated integrated peak areas.

The catalytic results are presented in two forms. One presentation of the data is in the form of rate of formation of each of the products, with the units of mol of product/kg catal/hr. This is also referred to as the space time yield or the productivity. In this case, the % conversion and % selectivity of each reactant can be directly calculated if the space time yields of all significant products are plotted, as they are in this report.

The second representation of the experimental data is %yield of each of the products. This latter quantity is defined as (% conversion of one of the reactants x % product selectivity)/100. Thus, for 50% conversion of isobutanol to isobutene with 75% selectivity, the %yield would be 37.5%. It can also be directly calculated from the rate of formation, i.e. %yield = (rate of formation of product/rate of reactant flow) x 100. For example, with the usual reactant of methanol = isobutanol = 1.72 mol/kg cat/hr formation of 0.645 mol isobutene/kg catal/hr under the present reaction conditions = 37.5 %yield. This last definition of %yield, as written, presumes that one mole of reactant forms one mole of product, e.g. isobutanol to isobutene (or MIBE). However, two moles of methanol can form one mole of dimethylether. In this case, it must be clear whether the %yield refers to comparisons of products containing the methyl group from methanol or molar conversions of methanol to products. As an example, the formation of 0.129 mol DME/kg catal/hr (20% conversion of methanol with 75% selectivity to DME) would correspond to a %yield of 15% because 0.258 mol of methanol/kg catal/hr would be converted to DME. If the basis were moles of products formed that contain one or more methyl groups derived from methanol, then the %yield of DME would be 7.5% ((0.129/1.72) x 100).

II. MTBE Synthesis From Methanol and Isobutene over Resin Catalysts

A. Comparison of Acidic Ion-Exchange Resin Catalysts

The present commercial process for the production of MTBE involves the liquid phase addition of methanol to isobutene over the acidic ion exchange Amberlyst-15 resin in the temperature range of 50-90°C, Figure 2. A study of this reaction over several acidic ion exchange resins in the vapor phase was conducted to provide a comparison of the relative activity of other catalysts toward MTBE production. This reaction might also be important in the coupling of methanol and isobutanol in which the acid-catalyzed dehydration of isobutanol to isobutene may be followed by methanol addition to isobutene to yield MTBE. The conditions chosen for this reaction were those used by Baba et al. (18):

Catalyst Weight	0.25 g (dry)
Temperature	75°C
Total Pressure	0.1 MPa (1 atm)
N_2/He/MeOH/i-Butene	2/1/1
Total Space Velocity	2.0 mol gas/g cat/hr

The acidic ion exchange resins used in this study were Amberlyst-15, Purolite C-150, and BioRad AG 50W X-2. The Amberlyst was obtained in dry form from Rohm and Haas, the manufacturer, and was used without pretreatment. Both the Purolite and BioRad resins were originally in an extremely wet form and had to be dried at 90°C overnight prior to loading the reactor. The catalyst bed was diluted with 3 cm^3 of Pyrex beads. The results of the MTBE synthesis over these catalysts using the conditions listed above are given in Table 1, where the conversion of isobutene to MTBE is given. The most striking aspects of these results are that the macroreticular resins Amberlyst and Purolite were active while the gel-type resin BioRad was completely inactive. The macroreticular resins are characterized by a rigid structure with well-defined pores that allow easy access to internal acid sites for most liquid and vapor phase organic molecules (19). The gel type resins are

produced in a manner that results in a structure that is inherently *nonporous* (19). Gel-type resins swell when exposed to liquid phase polar solvents, such as alcohols. This swelling should open the interior of the resin particle to reactants (19,20). It has been established that gel-type resins are active in liquid phase reactions, but are poor catalysts for vapor phase reactions (20,21). The MTBE synthesis results also show that the commercially used catalyst Amberlyst-15 is more active in producing MTBE on a weight basis than Purolite. Both Amberlyst-15 and Purolite C-150 were 100% selective towards MTBE formation with no trace of other products being observed.

Table 1. MTBE synthesis *via* methanol and isobutene coupling at 75°C and 0.1 MPa. Total flow rates (alcohol reactants plus N_2/Hc carrier gas) for the three tests were the following: Purolite C-150 = 1950 mol/kg/hr, BioRad = 1975 mol/kg/hr, and Amberlyst-15 = 2015 mol/kg/hr.

Catalyst	Feed Rate (mol/kg/hr)	Space Time Yield (mol/kg/hr)	Conversion (%)
Purolite 0.2559 g	MeOH = 490 i-Butene = 485	MTBE = 76.6	15.8
BioRad 0.2587 g	MeOH = 485 i-Butene = 465	MTBE = 0.0	0.0
Amberlyst-15 0.2526 g	MeOH = 495 i-Butene = 495	MTBE = 121.4	24.6

B. Temperature Dependence of MTBE Synthesis Over Purolite C-150

After finding that Purolite C-150 was an active and selective MTBE catalyst, some additional tests were performed in order to ascertain its activity profile with respect to temperature and reactant gas hourly space velocity. The steady state activities, in terms of

Figure 2. The present commercial process for the production of MTBE

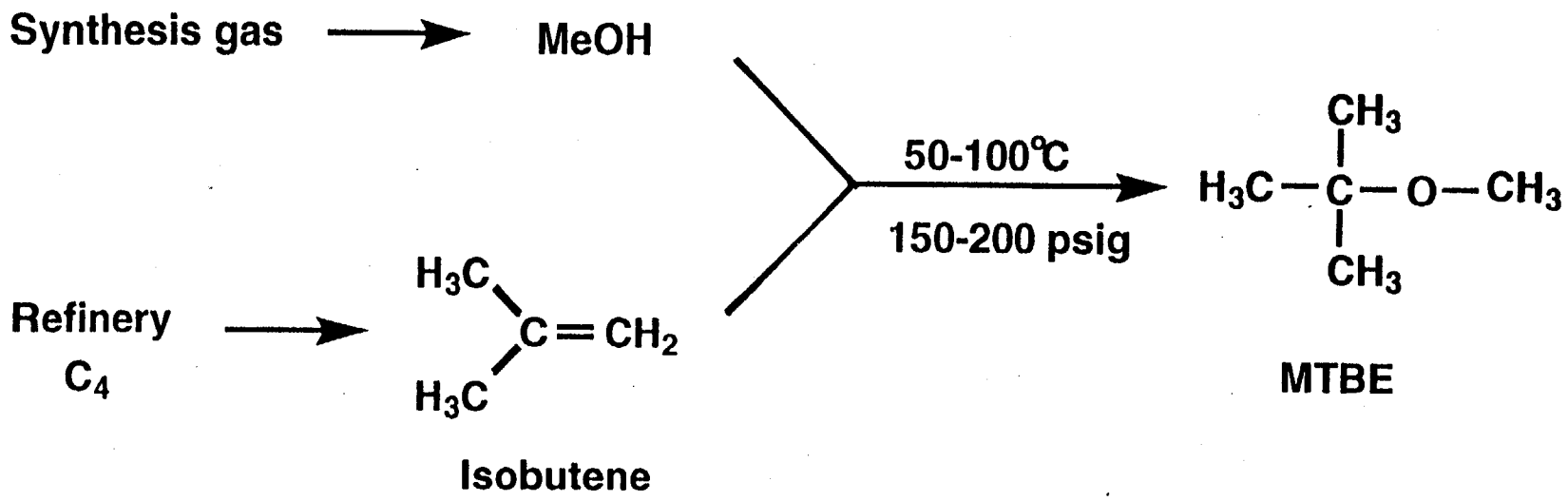

Catalyst: Amberlyst-15 (Sulfonated polystyrene ion exchange resin)

% conversion of isobutent to MTBE, of Purolite C-150 for MTBE synthesis at temperatures between 75-105°C under the same conditions as those used above are given in Table 2. The maximum productivity of MTBE was found at 85°C.

Table 2. Results of methanol and isobutene coupling over Purolite C-150 as a function of temperature at 0.1 MPa (catalyst weight = 0.26 g).

Temperature	Feed Rate (mol/kg/hr)	Productivity (mol/kg/hr)	Conversion (%)
75°C	MeOH = 490 i-Butene = 470 N_2/He = 970	MTBE = 72.6	15.4
85°C	MeOH = 490 i-Butene = 470 N_2/He = 970	MTBE = 90.5	19.2
95°C	MeOH = 490 i-Butene = 470 N_2/He = 970	MTBE = 79.9	16.9
105°C	MeOH = 490 i-Butene = 470 N_2/He = 970	MTBE = 65.8	14.0

C. Space Velocity Dependence Over Purolite C-150

The effects of varying reactant space velocity on the conversion of the reactants over Purolite C-150 at 75°C are presented in Table 3. The activity of the catalyst responds quite well to changing the space velocity of the reactants. Starting with a reactant space velocity of about 500 mol/kg cat/hr, the conversion of each reactant was 36%. Approximately doubling the space velocity essentially decreased the conversion of each reactant by half, i.e. of isobutene to 15.5%. Doubling the space velocity once again decreased the reactant conversions by approximately half, i.e. of isobutene to 7.4%.

Table 3. Results of methanol and isobutene coupling to form MTBE over Purolite C-150 as a function of reactant space velocity at 0/1 MPa and 75°C (catalyst weight = 0.25 g).

Reactant GHSV (mol/kg/hr)	Feed Rate (mol/kg/hr)	Conversion (%)
Low (510)	MeOH = 245 i-Butene = 265 N_2/HE = 485	36.0
Medium (975)	MeOH = 490 i-Butene - 485 N_2/He = 975	15.5
High (1930)	MeOH = 975 i-Butene = 955 N_2/He = 1960	7.4

III. Ether Synthesis From Methanol and Isobutanol Over Resin Catalysts

A. Ether Synthesis via Coupling of Methanol and Isobutanol

This work included testing of various solid acid catalysts for the direct coupling of methanol and isobutanol to ethers. The first stage of catalyst testing involved the use of commercially available acidic ion exchange resins and is discussed below. The second stage of catalyst testing involved the use of various inorganic solid acids that included zeolites, clays, oxides, mixed oxides, and supported acid systems.

In order to study the coupling of methanol and isobutanol to ethers in a systematic manner, it was found necessary to develop a standardized set of reaction conditions. Thermodynamic calculations of the direct coupling of methanol and isobutanol indicate that low temperatures, i.e. 50-90°C, are necessary to achieve favorable selectivity to desired products, especially MTBE and MIBE (17). All of the ion exchange resins are thermally stable within this temperature range, and 90°C was chosen for the reaction temperature in order to maximize conversion. Low pressure, i.e. 0.1MPa, was utilized in these reactions in light of the findings of Nunan et al. (16,17) that indicated lower pressures favored greater isobutene formation, the precursor of MTBE. The alcohol partial pressure was chosen such that no condensation would occur within the reaction system, and this was determined empirically under reaction conditions. The ratio of methanol to isobutanol used in the feed was investigated using Amberlyst-15 as a catalyst. Initially, a molar ratio of MeOH/i-BuOH = 2/1 was used for the feed. Then the same experimental conditions were used except that the MeOH/i-BuOH ratio was changed to 1/1, which is the stoichiometric ratio of the desired reaction. The 1/1 reactant mixture yielded more ether products than the 2/1 mixture, and therefore the 1/1 molar alcohol ratio was chosen for the standard test reaction. Alcohol feed rate and total gas flow were similar to those described by Nunan et al. (16,17).

The catalyst bed was diluted to 20 cm^3 with Pyrex beads. A summary of the experimental conditions is given below:

Catalyst weight	5.00 g (dry)
Reaction temperature	90°C
Total Pressure	0.1 MPa
Molar ratio MeOH/iBuOH	1/1
MeOH flow rate	1.72 mol/kg cat/hr
i-BuOH flow rate	1.72 mol/kg cat/hr
He + N_2 flow rate	16 mol/kg cat/hr

Product Analysis

The acid catalyzed reaction of the two alcohols usually results in a complex mixture of products. The following product abbreviations are used in this report:

DME:	Dimethylether
MTBE:	Methyl tertiary butyl ether
MIBE:	Methyl isobutyl ether
TIBE:	Tertiary butyl isobutyl ether
DIBE:	Di-isobutyl ether.

These products are obtained by the following reactions:

$$2\ MeOH \rightarrow DME + H_2O \quad (4)$$

$$MeOH + i\text{-}BuOH \rightarrow MTBE + H_2O \quad (5)$$

or

$$MeOH + i\text{-}Butene \rightarrow MTBE \quad (1)$$

$$MeOH + i\text{-}BuOH \rightarrow MIBE + H_2O \quad (3)$$

$$i\text{-}Butene + i\text{-}BuOH \rightarrow TIBE \quad (6)$$

$$2\ i\text{-}BuOH \rightarrow DIBE + H_2O. \quad (7)$$

The isobutene shown in some of the above reactions originated from the isobutanol reactant:

i-BuOH → i-Butene + H_2O. (2)

The acid catalyzed dehydration of isobutanol was studied previously by several workers and is known to result in a mixture of butenes, i.e. isobutene, 1-butene, *cis*- and *trans*-2-butene (22,23). It will be shown herein that among these butenes, isobutene is the dominant product formed. Mechanistically, reactions 2-5, and 7 may involve oxonium ion intermediates. Reactions 1, 2, and 6 may require carbenium ions to be formed. These intermediates will be considered later in this report from a perspective of the dominant reaction pathways that operate to control the selectivity of the synthesis reactions that yield ethers and olefins.

Activity and Selectivity of Ion Exchange Resins

The results of the standard test over the four ion exchange resins at steady state activity are shown in Table 4 in terms of the conversions of the reactant alcohols. In this test the microsaddles (MS) form of Nafion-H was used.

Table 4. Activities of the resin catalysts in the MeOH + i-BuOH standard test.

Catalyst	Methanol Conversion (%)	Isobutanol Conversion (%)
Amberlyst-15	9.1	10.2
BioRad	4.9	5.4
Nafion MS	1.4	1.4
Purolite C-150	9.2	9.9

All catalyst testing runs reached steady state conversion levels after the first hour of reaction. All catalysts studied were most selective for MIBE production. Relative overall

activity followed the order Amberlyst-15 ≈ Purolite C-150 > BioRad > Nafion MS. One interesting observation is that the BioRad AG 50W x-2 resin was quite active in the reaction between methanol and isobutanol but was observed to be inactive for methanol and isobutene conversion (cf. Table 1). The presence of isobutanol at a temperature much below its boiling point may allow it to be absorbed enough by the BioRad gel resin to cause swelling of the polymer matrix. This would render the active sites in the interior of the resin particle to be accessible. This evidently did not occur with gas phase isobutene, which possibly explains the sharp differences in the activities of this resin with different reactants. Product selectivities for the different catalysts are illustrated in Figure 3. Water is, of course, the major product of these dehydration reactions, but it is not included in the selectivity analysis. The butenes are shown as the sum of isobutene and the linear *trans*-2-butene and *cis*-2-butene, where 88-91% of the total was isobutene except for Nafion where the linear butenes were not detectable. Under the standard reaction conditions, Nafion appears to be the most selective catalyst for MIBE production. The other catalysts produce significant amounts of MTBE, along with the other ethers TIBE, DIBE, and DME. The higher selectivity of Nafion towards MIBE formation may be due to the distinctly different nature of the acid sites of Nafion. The fluorosulfonic acid groups of Nafion contrast with the sulfonic acid groups of the other ion exchange resins tested in this study.

Figure 4 gives the ratios of MTBE to isobutene, MIBE to DME, and MIBE to MTBE produced over the catalysts and illustrates the effectiveness of the catalysts for MIBE formation. In addition, a low MTBE/isobutene ratio in the case of Nafion MS suggests that even when isobutene is formed in relatively high concentrations in the presence of excess methanol, it is difficult to produce MTBE under these reaction conditions.

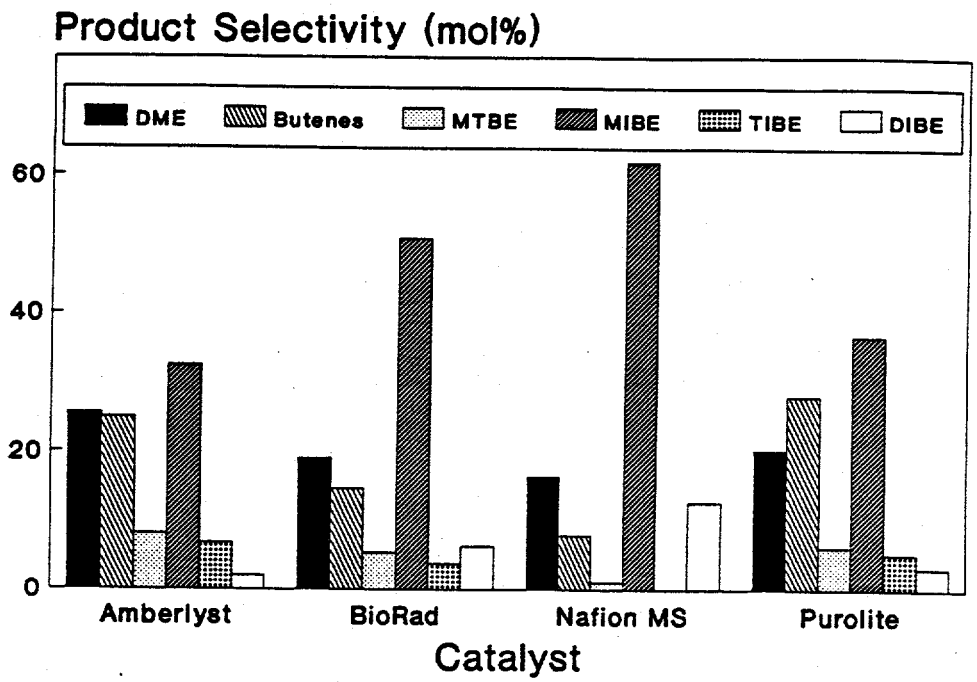

Figure 3. The product selectivities of the organic resin catalysts at 90°C and 0.1 MPa with methanol/isobutanol = 1/1 reactants.

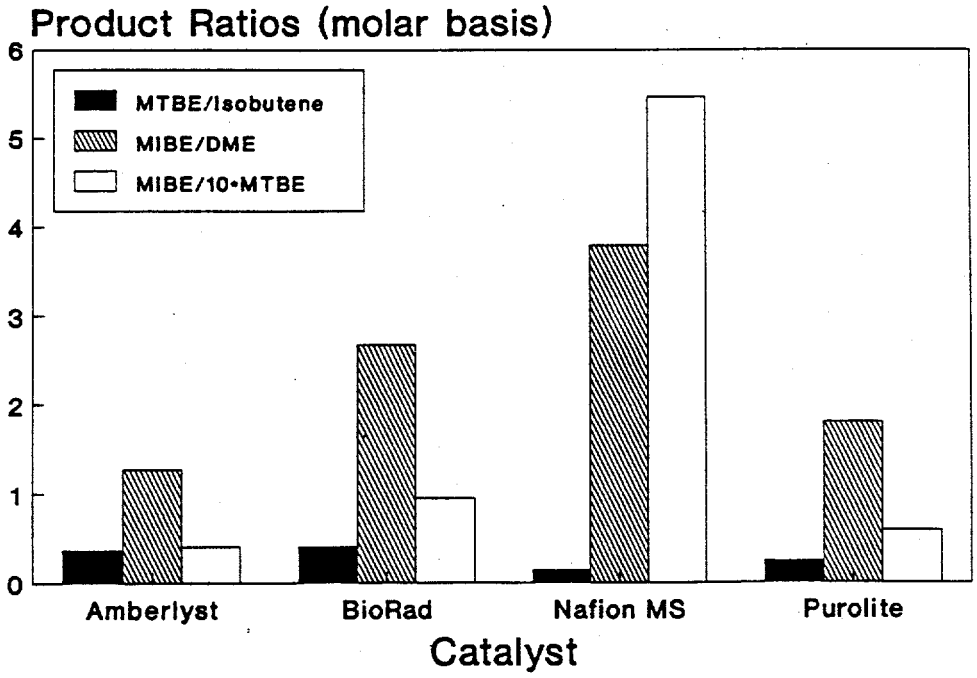

Figure 4. The product ratios of MTBE/isobutene, MIBE/DME, and MIBE/MTBE over the organic resin catalysts at 90°C and 0.1 MPa with methanol/isobutanol = 1/1 reactants.

B. High Temperature Testing of Nafion-H MS and Nafion-K

For comparison with both organic resins and the inorganic catalysts, the Nafion-H MS catalyst test was repeated under standard conditions and was extended to higher temperatures. Table 5 shows activities of Nafion-H MS at 90, 125, 150, and 175°C.

Table 5. Activities of the Nafion-H MS catalyst in the MeOH + i-BuOH standard test as a function of temperature.

Temperature (°C)	Methanol Conversion (%)	Isobutanol Conversion (%)
90	1.4	1.5
125	28.2	31.6
150	60.3	99.6
175	59.3	98.2

Conversion at 90°C compared well with the previous catalytic test (Table 4). Upon increasing the temperature to 125°C, conversion increased to ≈30% for both methanol and isobutanol with methyl isobutylether (MIBE) and DME as major products. A few minor products were not identified at this temperature. At higher temperatures (150 and 175°C), methanol conversion, predominantly to DME (MIBE selectivity decreased at higher temperature), increased to ≈60%, whereas isobutanol was almost completely converted, predominantly to isobutene. It must be noted that at 150 and 175°C a large number of small unidentified peaks in the analytical gas chromatogram were seen. Upon unloading the catalyst from the reactor, the previously light yellow catalyst had changed color to black. It had a greasy "film" over it and smelled "oily". Apparently, due to its very strong acidity, Nafion-H at 150°C and above is able to catalyze extensive isomerization and oligomerization.

To probe the significance of the acid groups in the Nafion-H resin, a portion of

Nafion-H was exchanged to its potassium form, designated as Nafion-K. To achieve the ion exchange 10 g of Nafion-H was immersed in 75 ml of 1 M potassium nitrate (KNO_3) and stirred for approximately 45 min. The solution was strongly acidic dur to the exchange of H^+ for K^+. A new portion of potassium nitrate was added after the previous was decanted and the catalyst was washed with distilled water. The procedure was repeated until full exchange was reached, as determined by testing the pH of the exchannge solution. Four portions of KNO_3 were needed for total exchange of the Nafion-H. Finally, the Nafion-K resin washed in distilled water and allowed to dry overnight at 90°C.

In contrast to the results in Table 5 for Nafion-H MS, Nafion-K showed no activity at all over this temperature range. This indicates that a catalyst possessing appreciable acidity is necessary for the reactions discussed above. The tested Nafion-K also retained its light yellow color, even after being subjected to reaction conditions at 175°C, indicating the color change of Nafion-H was due to either thermal decomposition of the SO_3H groups (assuming the SO_3K group does not) or to hydrocarbonaceous deposits on the Nafion-H resin.

C. Nafion-H MS Activity Dependence on Sodium Content

The objective of this study was to further investigate the role that the concentration of acid sites has on the activity of the Nafion-H MS catalyst.

To 0.52 g of Nafion-H MS was added 5.2 ml of 0.016 M sodium chloride solution. Since Nafion-H MS has 0.89 meq H^+/g, the added sodium chloride was equivelent to 18% of the acid sites. The catalyst was left to equilibrate with the NaCl solution overnight. The pH was measured before and after equilibration, and the difference was taken to correspond to the amount of sodium exchanged into the Nafion-H MS catalyst. The experimentally

determined degree of exchange was 18%. The catalyst was then washed in distilled water until a neutral pH was obtained. Following this, the sample was filtered, dried at 100°C for 3 hr, and then left to cool in air. The following experimental conditions were used for the testing of the non-exchanged catalyst and the Na^+ exchanged sample:

Temperature	90°C
Pressure	1 atm
Methanol feed	5.7 mol/kg cat/hr
Isobutanol feed	5.7 mol/kg cat/hr
Helium (+N_2 trace)	52.7 mol/kg cat/hr
Catalyst weight	0.5 g

Table 6 shows that both the non-exchanged and the 18% exchanged Nafion-H MS produced three major products, e.g. MIBE, DME and isobutene. In both cases, MIBE was the dominant product. The yield of MIBE only decreased 10% with the sample having 18% less acidic sites available.

Table 6. Productivity over Non-exchanged and 18% Exchanged Nafion-H MS

Compound	Productivity over non-exchanged Nafion-H (mol/kg cat/hr)	Yield over 18% Na^+ exchanged Nafion-H (mol/kg cat/hr)
MIBE	0.050	0.045
DME	0.015	0.015
Isobutene	0.009	0.013

It was shown in the previous experiment that 100% exchange of Nafion-H with potassium resulted in a 100% activity loss. Therefore, a more extensive series of experiments should be carried out with partially exchanged Nafion-H samples where 25-90% of the acid groups would be exchanged with Na^+ or K^+ and the effect on activity and selectivity would then be determined.

D. Characterization of New Amberlyst Catalysts

Three newew Amberlyst solid acid resin catalysts, designated as Amberlyst-35, -36, and -1010, were obtained from Rohm and Haas. These newer Amberlyst catalysts have polymeric structures similar to that of the Amberlyst-15 resin that was extensively studied earlier in this project, e.g. see Figure 5. The main differences in these new catalysts compared to Amberlyst-15 are that the Amberlyst-35 and -36 resins are more thermally stable and have higher acidity, while the Amberlyst-1010 resin has a much higher surface area, smaller average pore size, and lower concentration of acid sites. The new catalysts were characterized by means of surface area, swelling properties, and concentration of acid sites.

Surface Area Measurements

Surface areas were measured using a Micromeritics Gemini 2360 Surface Area Analyzer with nitrogen gas as the adsorbate at -196°C. The Amberlyst catalysts were dried at 90°C overnight under nitrogen atmosphere prior to the surface area measurements. Results were obtained as BET multipoint and Langmuir surface areas. Data points were chosen so that p/p_o varied from 0.05 to 0.3. This yielded a linear BET plot.

Table 7 shows the results for the three Amberlyst samples. It can be seen that the Langmuir surface area results corresponded well with the values given by the manufacturer. The reason for the apparent low values determined by the BET method is not yet known. It was not specified by the manufacturer what type of surface area model was used or what adsorbate was used. The surface area of the Amberlyst-15 resin used for comparison was approximately 45 m^2/g.

Figure 5. Schematic of Amberlyst structure.

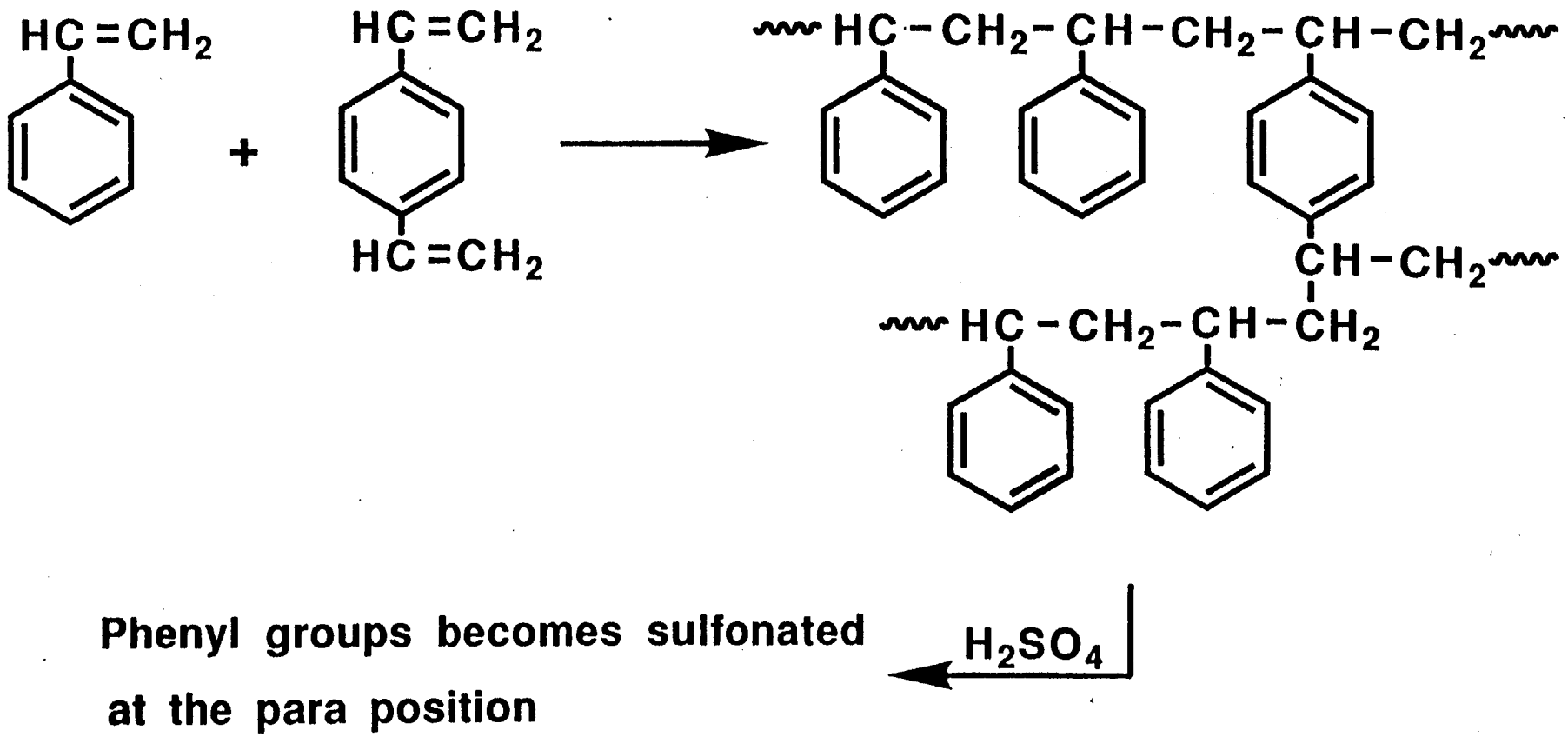

Table 7. Surface Areas of the Amberlyst Resins

Amberlyst	Manufacturer's Surface Area (m^2/g)	Experimental BET Multipoint Surface Area (m^2/g)	Experimental Langmuir Surface Area (m^2/g)
1010	540	350	570
35	44	32	50
36	35	19	31

Swelling Properties of the Resins

To measure the swelling properties of the Amberlyst samples, approximately 1.5 g of each catalyst was mixed with 4.0 ml of solvent in a graduated cylinder. The percent swelling was measured in both methanol and water. The dry volume of the resin was taken immediately following the addition of the catalyst to the solvent. After an equilibration time of 5-10 minutes, the volume of the resin was recorded once again. This final volume was the volume after swelling. The % swelling was then calculated by taking the difference of the two volumes.

Amberlyst-35 and -36 were obtained from the manufacturer in a wet form, and they were dried overnight at 90°C to remove water before the swelling experiments were carried out. Amberlyst-1010, according to the manufacturer's data, contained less than 2% water and was not dried further. Table 8 shows the results obtained from the swelling experiments. All three catalysts swelled more in water than in methanol. Amberlyst-35 and -36 were very similar in their swelling properties, but Amberlyst-1010 swelled significantly less. One possible reason for the smaller swelling of Amberlyst-1010 is that this resin has appreciably smaller average diameter of its internal pores (≈50Å) than the Amberlyst-35 and -36 resins. This indicates more cross-linking and a more rigid polymer network.

Table 8. % Swelling of Amberlyst Resins in Water and Methanol

Amberlyst	% Swelling in water	% Swelling in methanol
1010	25	22
35	58	50
36	52	42

Concentration of Acid Sites in the Resins

The ion exchange capacities provided by the manufacturer were verified by titration of the Amberlyst samples in water with 0.498 M sodium hydroxide. Amberlyst-35 and -36 resins were dried at 90°C in air overnight prior to weighing and titration, while the Amberlyst-1010 was used as received. The pH was continuously monitored throughout the titration with a pH meter, which providing an acid-base titration curve, where the inflection point gave the end point of the titration.

Table 9 includes both the manufacturer's value of the ion exchange capacities and the experimental ion exchangeable H^+ concentrations in meq/g of the dry resin, as well as the % difference involved in the experimental results. It is seen that the experimental values obtained in this laboratory agree very well with the manufacturer's specifications. Again, the Amberlyst-35 and -36 resins had very similar properties, whereas the Amberlyst-1010 had a much lower concentration of acid sites.

Table 9. Ion Exchange Titration Data for Amberlyst-1010, -35, and -36 Resins.

Amberlyst	Manufacturer's meq/g	LU Experimental meq/g	% Difference
1010	3.3	3.25	1.5
35	5.2	5.22	0.4
36	5.4	5.30	1.8

Catalytic Activities and Selectivities of the Amberlyst Catalysts

The new Amberlyst-35 and -36 catalysts were reported to be more acidic than Amberlyst-15, and the Amberlyst-1010 resin has a higher porosity (0.41 cm^3/g) than the other three resins. Higher acidity is of great interest for alcohol coupling to ethers at low temperature. Rohm and Haas information indicated that the Amberlyst-1010 and Amberlyst-15 resins are stable to 120°C, while the Amberlyst-35 and -36 resins are more thermally stable and can be used to 140°C.

The Amberlyst-1010, -35, and -36 catalysts were subjected to the standard test (p. 26) for screening catalysts for ether synthesis, where the methanol and isobutanol feed rates were both 1.72 mol.kg cat/hr. The temperature was also increased stepwise above 90°C to monitor the temperature dependence of the product formation.

In Tables 10-12, the conversion at 90°C and at some higher temperatures are reported.

Table 10. Amberlyst-1010 Activity as a Function of Temperature

Temperature (°C)	% Methanol Conversion	% Isobutanol Conversion
90	5.0	4.2
100	8.3	8.9
110	14.4	21.3
120	23.6	42.2

Table 11. Amberlyst-35 Activity as a Function of Temperature

Temperature (°C)	% Methanol Conversion	% Isobutanol Conversion
90	16.4	15.8
100	32.1	43.9
110	42.9	63.9
120	62.0	57.1
130	70.0	57.9
90	17.0	15.7

Table 12. Amberlyst-36 Activity as a Function of Temperature

Temperature (°C)	% Methanol Conversion	% Isobutanol Conversion
90	12.3	10.2
100	25.9	30.0
110	42.0	63.1
120	56.7	53.1
130	63.4	57.9
90	10.7	6.8

Amberlyst-1010 showed moderate conversion of both methanol and isobutanol. The Amberlyst-35 and -36 catalysts showed high and similar conversions at all of the reaction temperatures, but Amberlyst-35 tended to be somewhat more active than Amberlyst-36. No deactivation of the Amberlyst-35 catalyst was observed (Table 11). However, in reference to Table 12, some deactivation can be seen for Amberlyst-36, as evidenced upon lowering the reaction temperature back to 90°C after carrying out the reaction at higher temperatures. In comparison with Amberlyst-35 and -36, Amberlyst-15 converted about 10% of methanol and 10% of isobutanol at 90°C. Conversions over all of the polymer resins tested (at 90°C)

during this project are listed in Table 13. The overall order of activity follows the sequence Amberlyst-35 > Amberlyst-36 > Amberlyst-15 ≈ Purolite C-150 > BioRad AG 50W X-2 ≈ Amberlyst-1010 > Nafion-H.

Table 13. Activity of Polymeric Resin Catalysts at 90°C

Catalyst	% Methanol Conversion	% Isobutanol Conversion
Amberlyst-15	9.1	10.2
BioRad AG 50W X-2	4.9	5.4
Nafion-H	1.4	1.4
Purolite C-150	9.2	9.9
Amberlyst-1010	5.0	4.2
Amberlyst-35	16.4	15.8
Amberlyst-36	12.3	10.2

Selectivity data obtained at the reaction temperatures shown in Tables 10-12 are represented in Figures 6-8. Under the reaction conditions employed, the catalysts were generally rather non-selective, especially at the lower temperatures. At higher temperatures (e.g. ≥120°C), one product was more dominant than the others. Amberlyst-1010 formed MIBE, DME, and butenes (mainly isobutene) at 90°C, but butenes were favored at temperatures above 90°C. Amberlyst-35 mainly formed butenes at 90-110°C, but at 120°C and above DME was predominantly formed (Figure 7). Amberlyst-36 showed a similar selectivity pattern, with butenes being the favored products at 100 and 110°C and DME being the dominant product at 120 and 130°C (Figure 8). Figures 9-14 present the data as % yield of the products. Figures 9-11 give the % yields with respect to the methanol reactant, whereas Figures 12-14 give % yields with respect to isobutanol (fractional conversion times % selectivity). The trends observed in these plots are the same as for the

selectivities in Figures 6-8.

Figure 6. Selectivity for Amberlyst-1010 in mol% of Products.

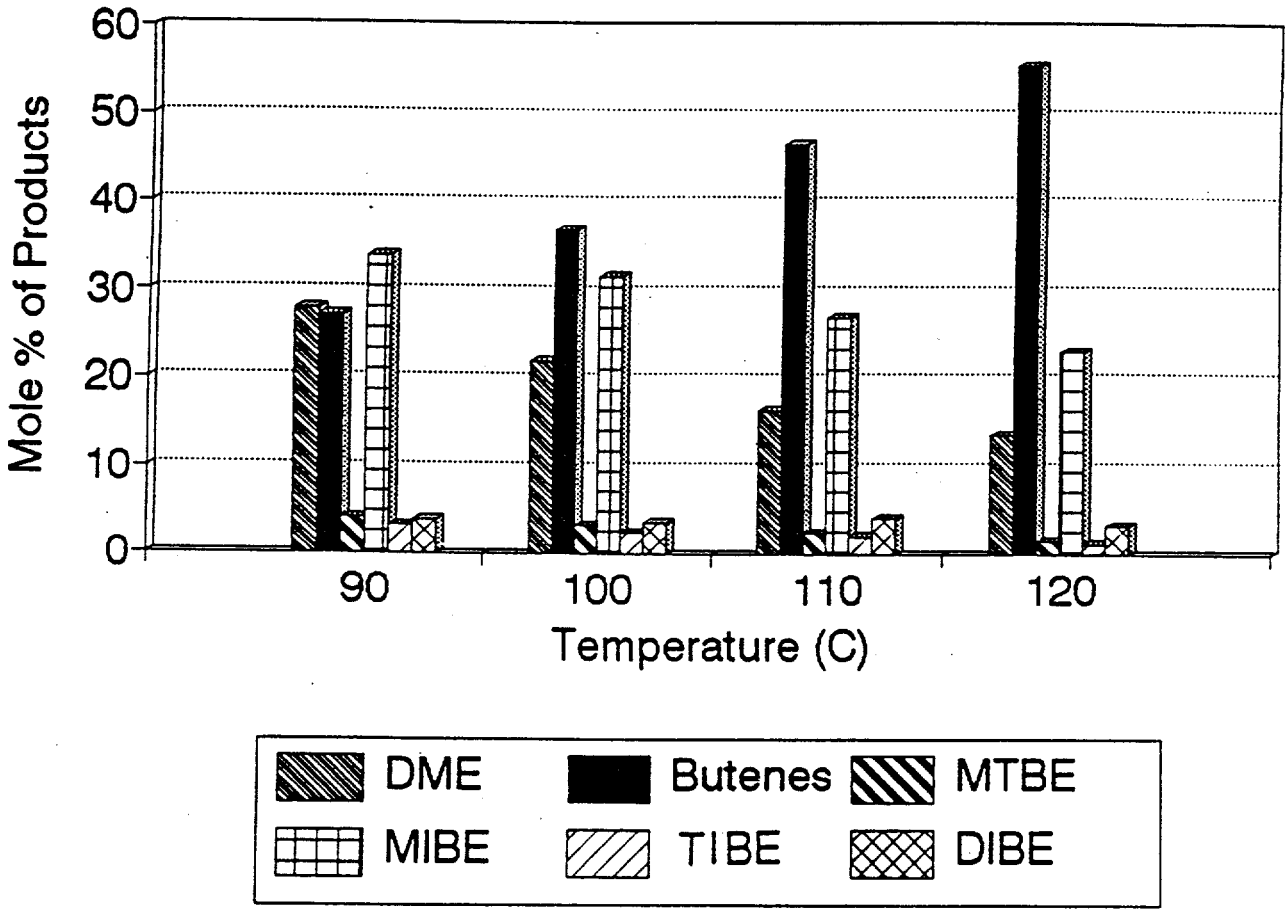

Figure 7. Selectivity for Amberlyst-35 in mol% of Products.

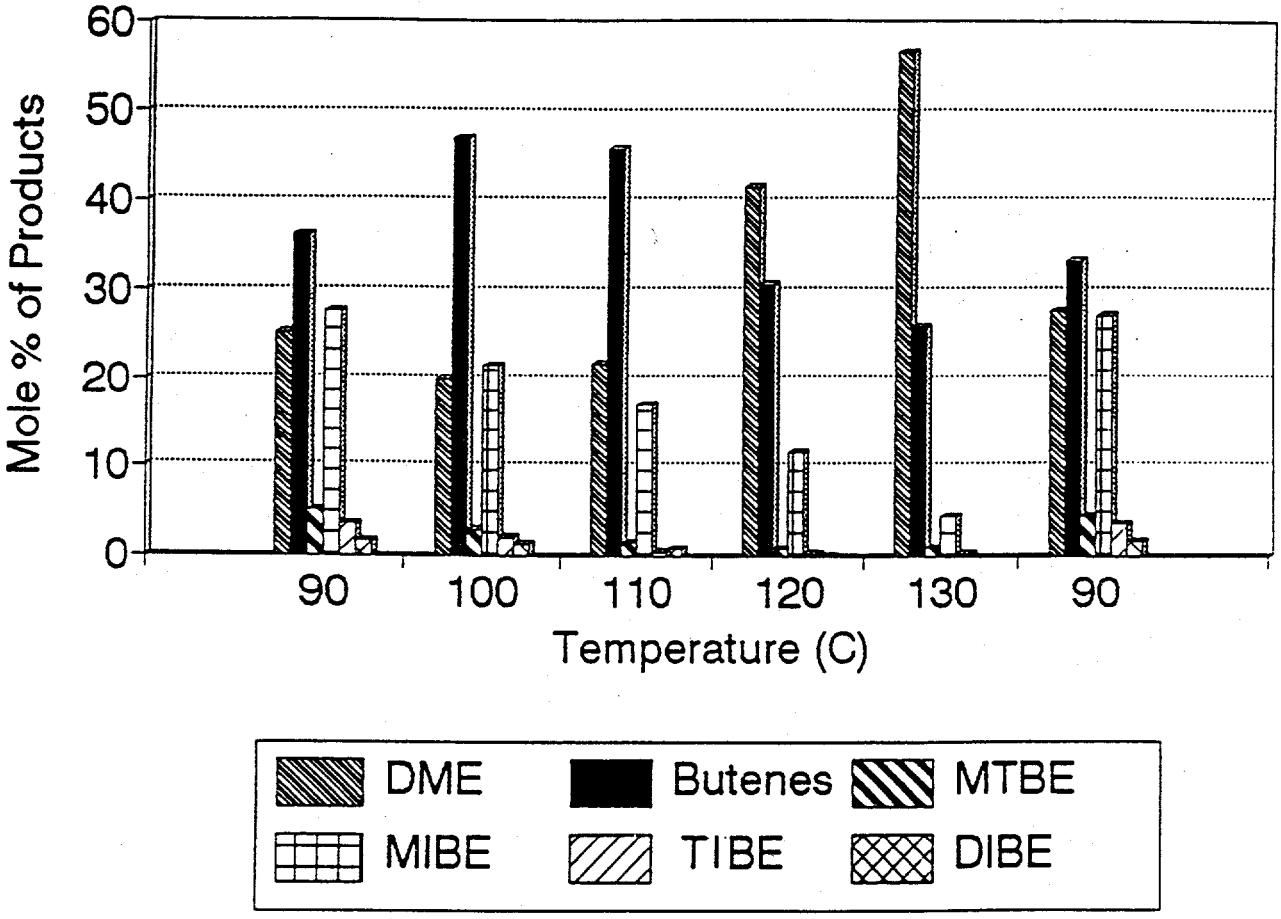

Figure 8. Selectivity for Amberlyst-36 in mol% of Products.

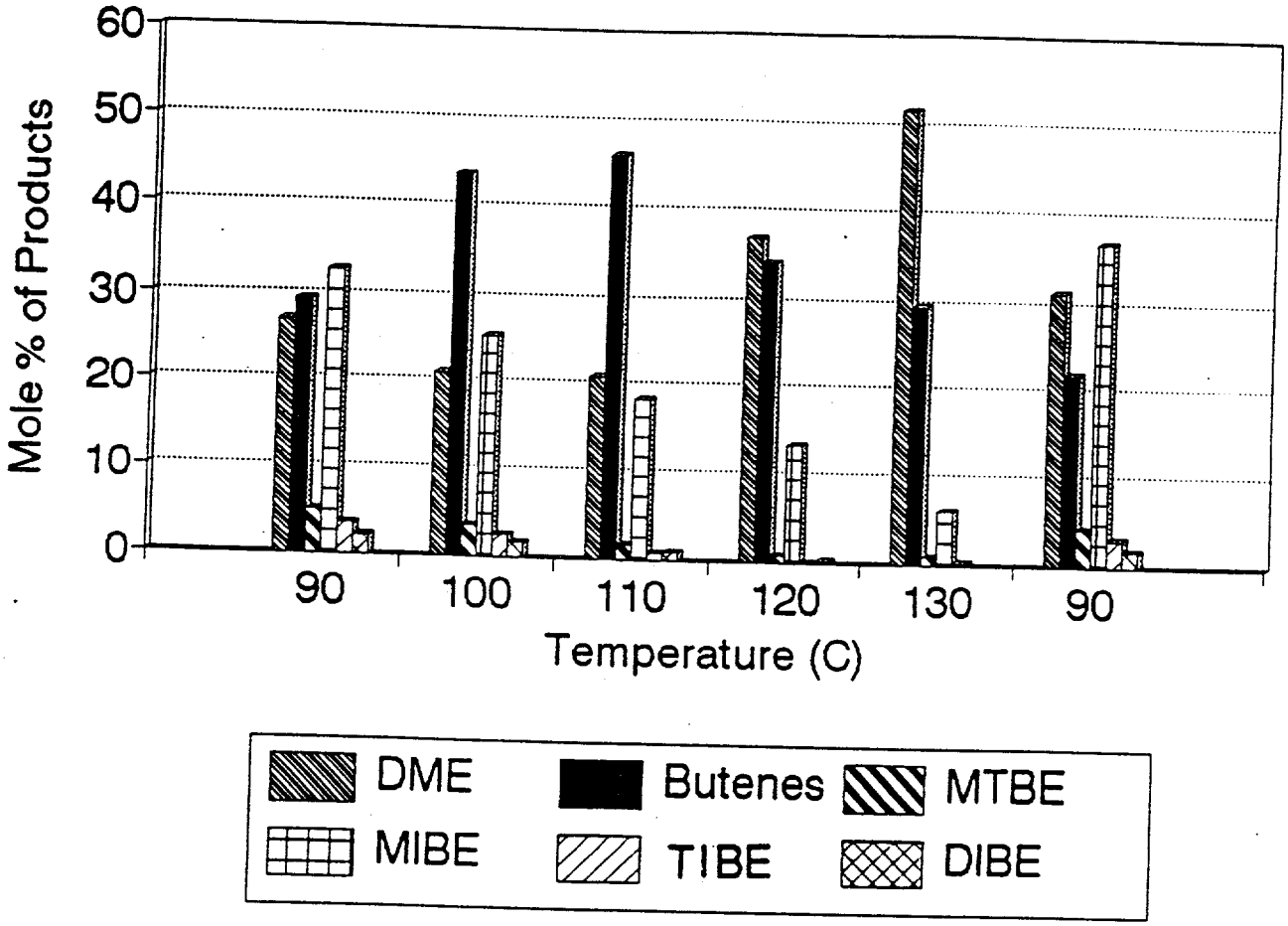

Figure 9. % Yield for Amberlyst-1010 based on Methanol Conversion.

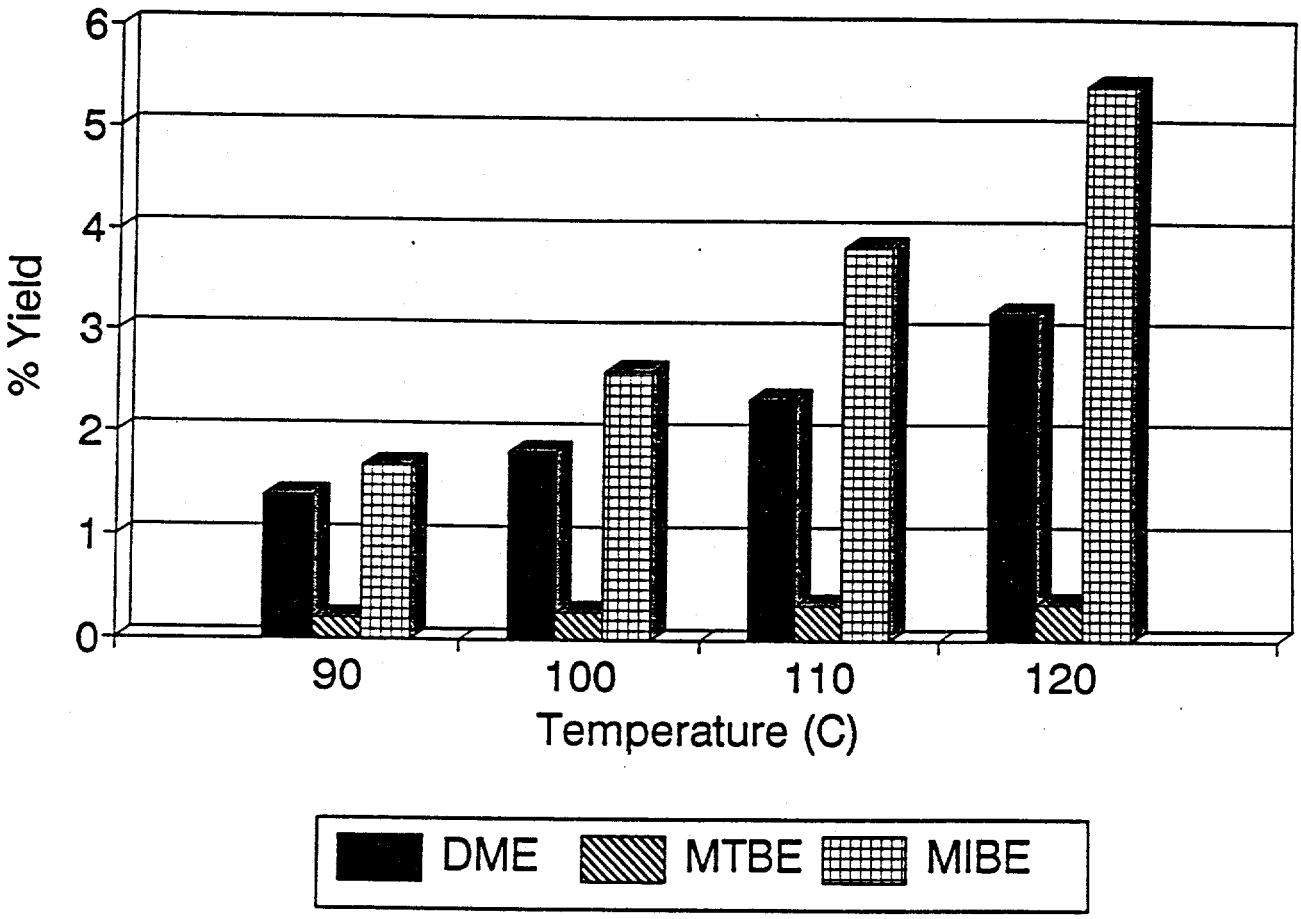

Figure 10. % Yield for Amberlyst-35 based on Methanol Conversion.

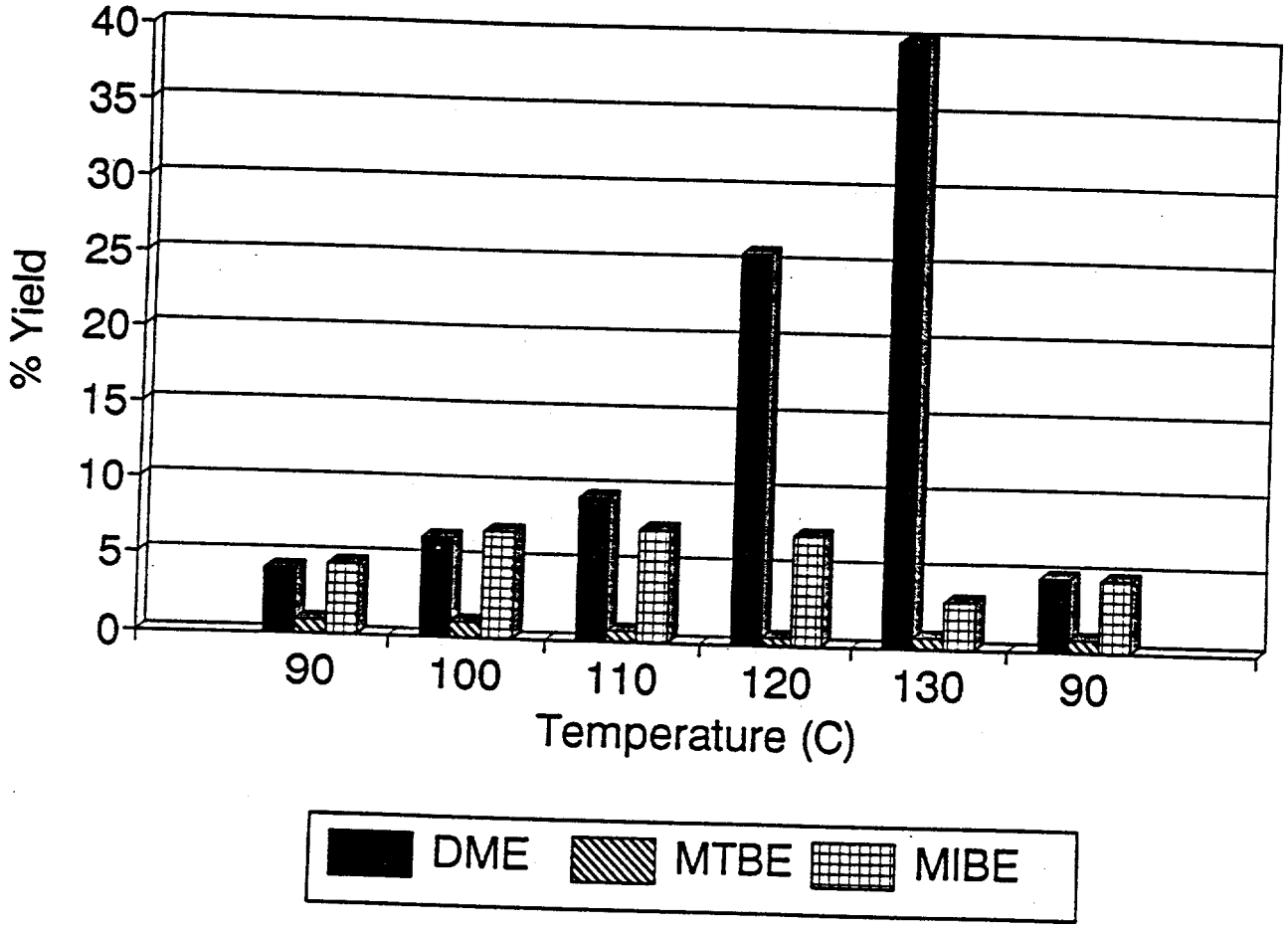

Figure 11. % Yield for Amberlyst-36 based on Methanol Conversion.

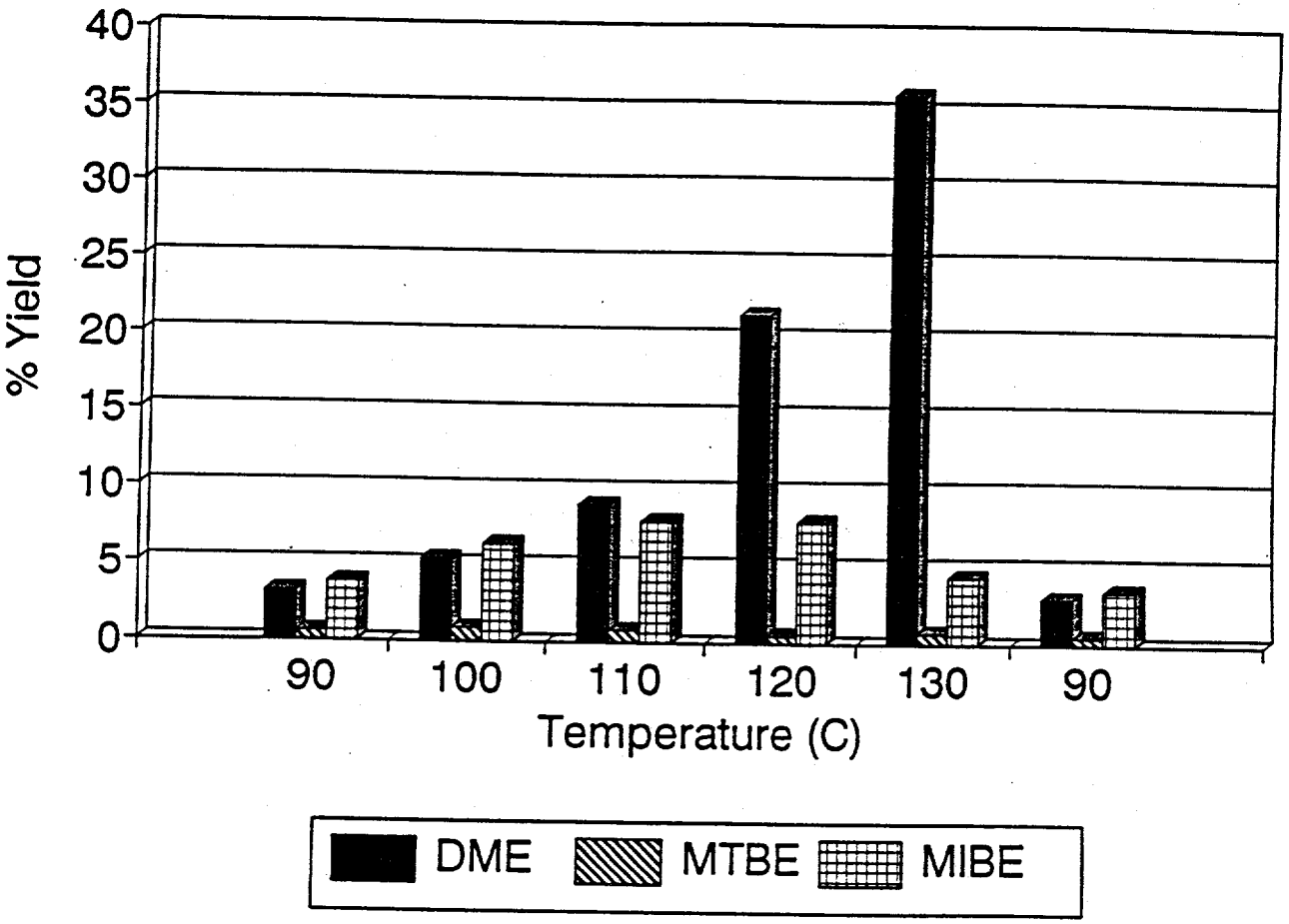

Figure 12. % Yield for Amberlyst-1010 based on Isobutanol Conversion.

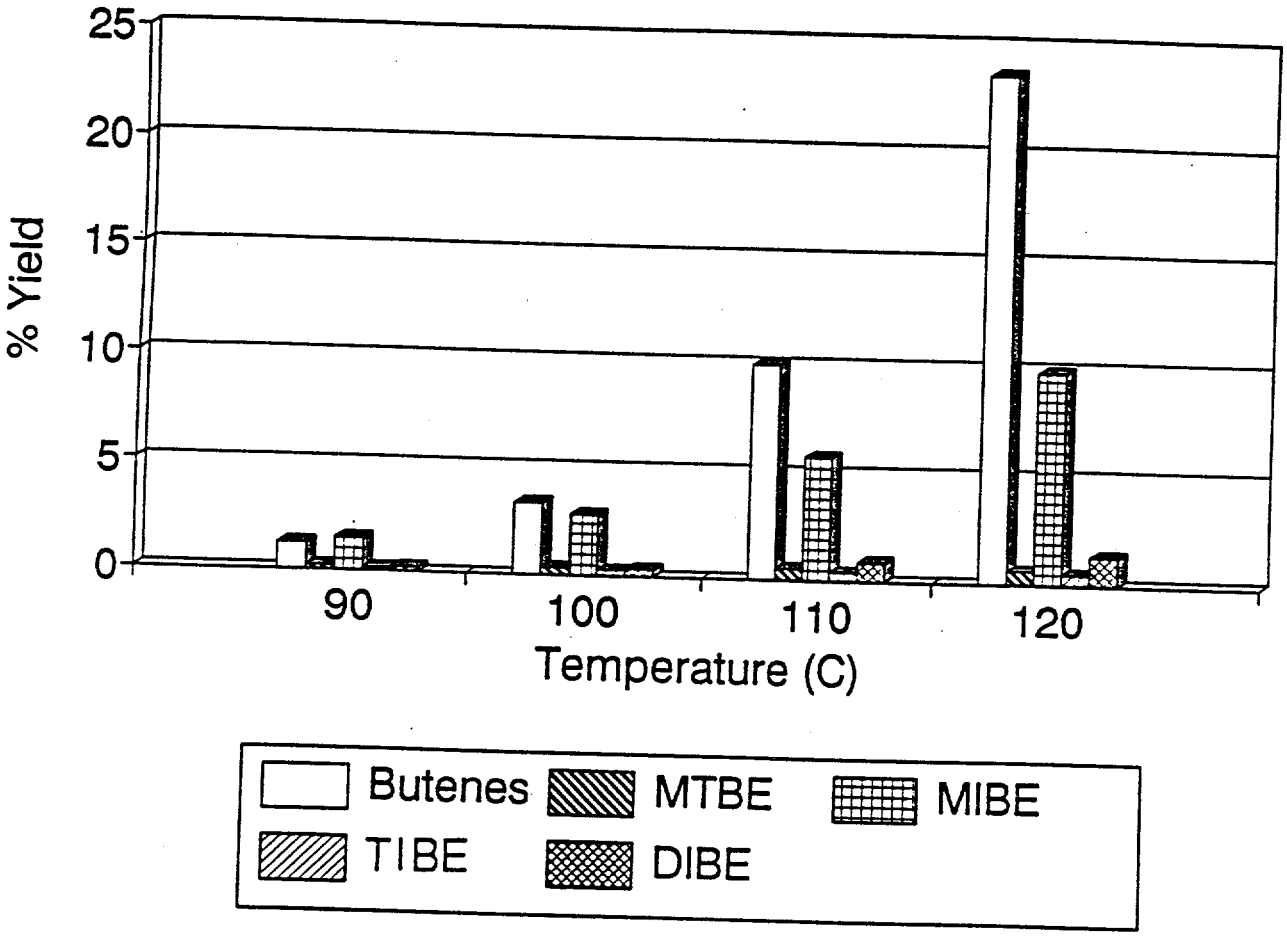

Figure 13. % Yield for Amberlyst-35 based on Isobutanol Conversion.

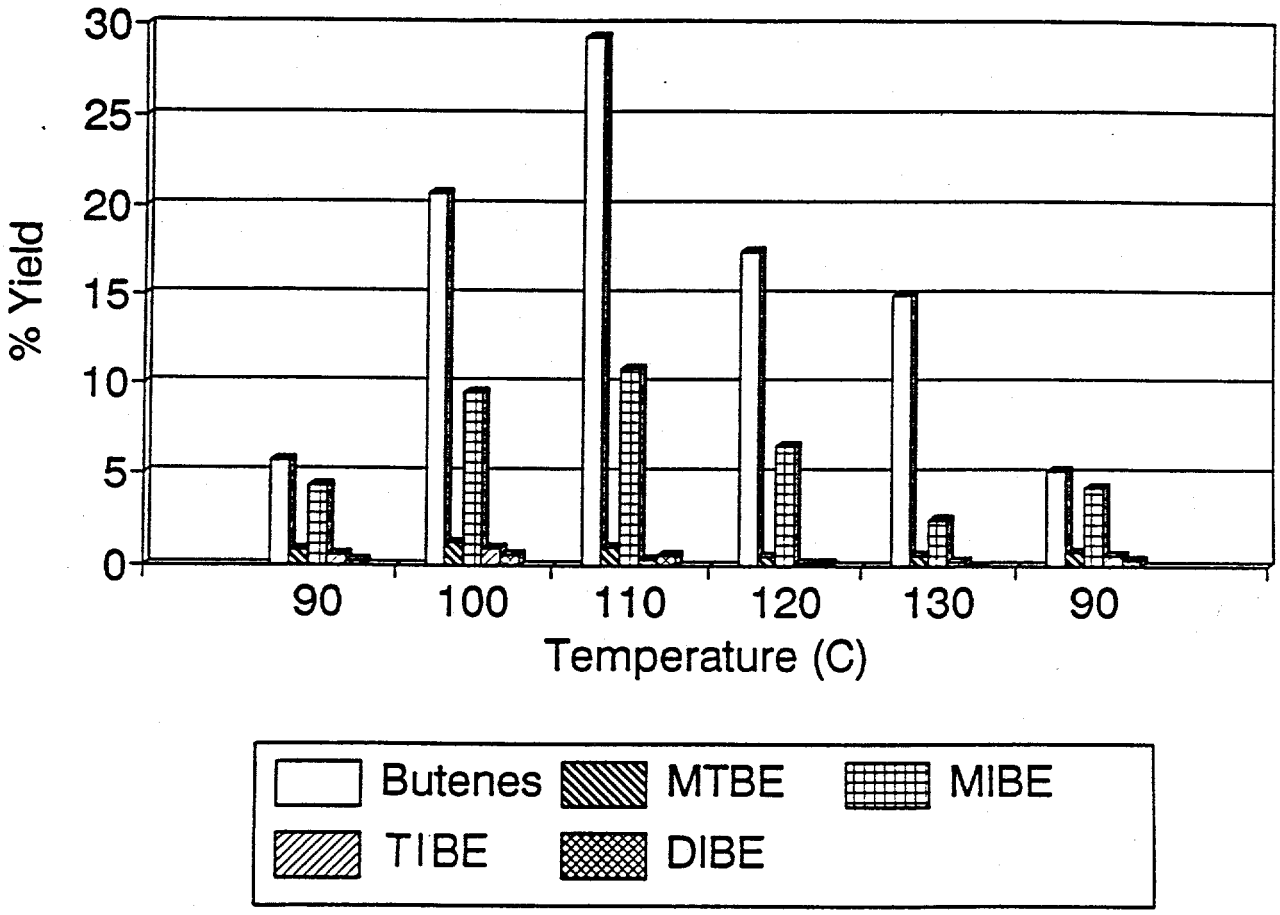

Figure 14. % Yield for Amberlyst-36 based on Isobutanol Conversion.

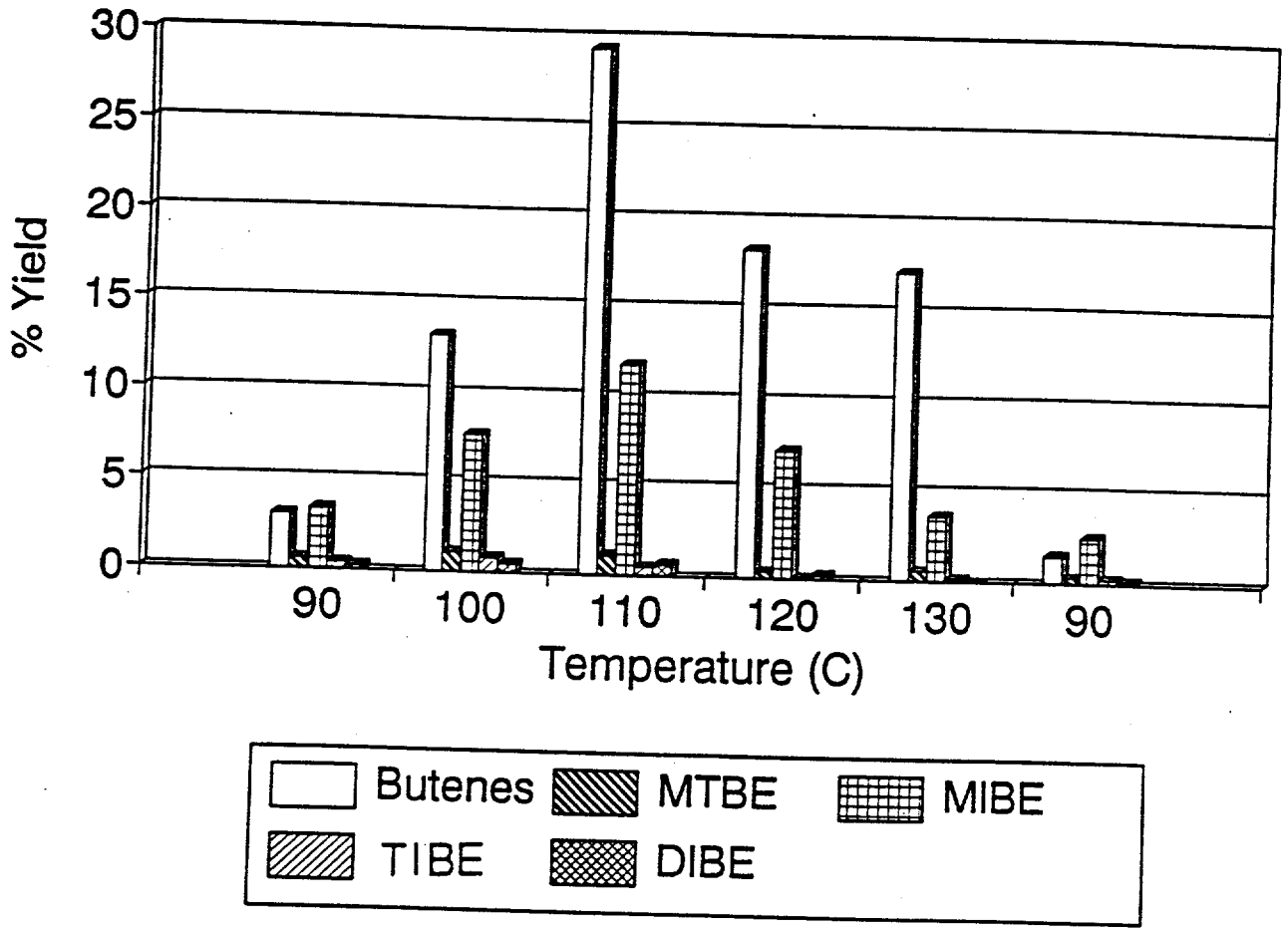

Pressure Dependence of Amberlyst-35

The reaction of methanol and isobutanol over a Nafion-H catalyst had previously been shown to be very sensitive to the total pressure (16,17). To investigate the pressure dependence of the synthesis reaction over Amberlyst-type catalysts, the active Amberlyst-35 resin was chosen. The pressure dependence study was carried out at the two reaction temperatures of 90 and 117°C.

The experiment was carried out using the following conditions:

Catalyst weight	1.0 g dry catalyst
Temperature	90 and 117°C
Total pressure at 90°C	0.1-0.65 MPa
Total pressure at 117°C	0.1-1.3 MPa
Methanol feed	10.4 mol/kg cat/hr
Isobutanol feed	5.2 mol/kg cat/hr
He + N_2	185 mol/kg cat/hr

This includes the standard temperature of 90°C and pressure of 0.1 MPa developed for testing the resin catalysts.

The results shown in Figures 15 and 16 demonstrate that the formation of butenes was very sensitive to the alcohol partial pressure. A small elevation of the alcohol pressure suppressed the formation of butenes rather drastically at both 90 and 117°C. The synthesis rates of DME, MIBE, and MTBE were not strongly affected by pressure at 90°C, although there was a trend to increase the space time yield of DME as the alcohol pressure was increased. At the reaction temperature of 117°C, all of the ethers showed increasing productivities as the pressure of the reactants was increased (Figure 16).

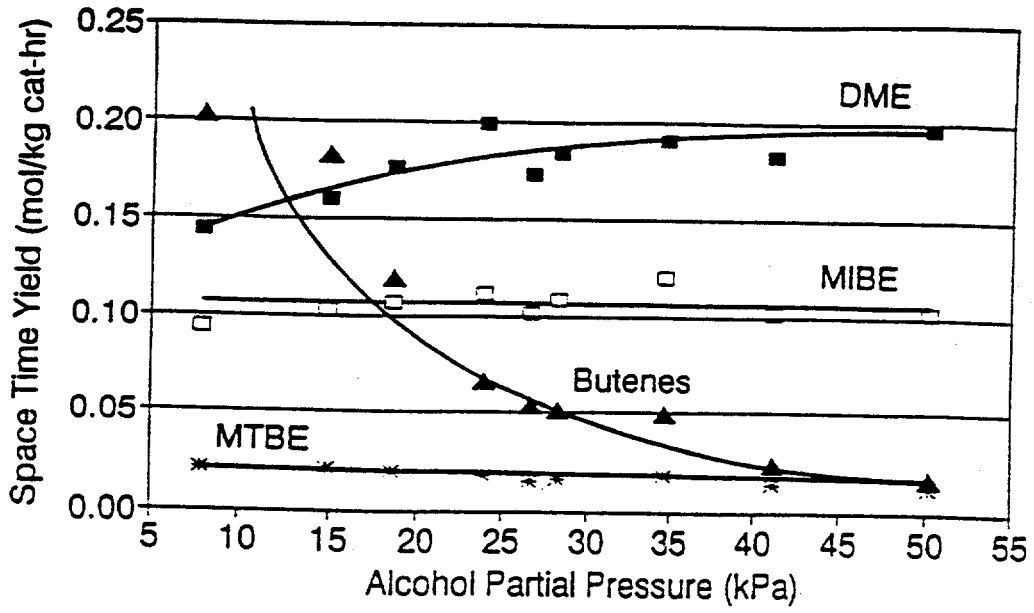

Figure 15. Space Time Yields of the Ethers and Butenes Formed Over Amberlyst-35 as a Function of the Alcohol Partial Pressure at 90°C.

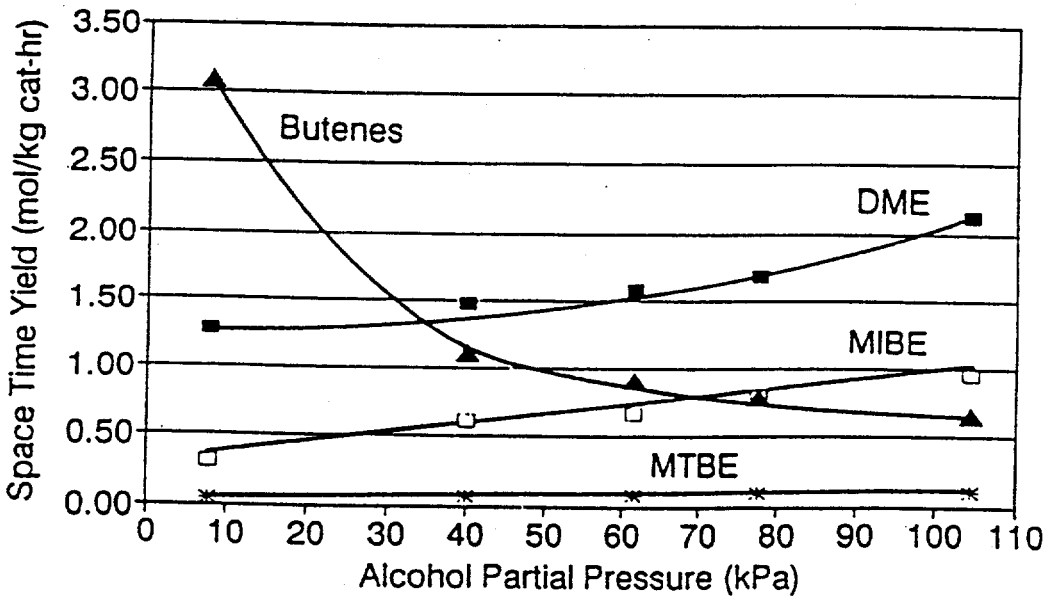

Figure 16. Space Time Yields of the Ethers and Butenes Formed Over Amberlyst-35 as a Function of the Alcohol Partial Pressure at 117°C.

E. Mechanism of MIBE Formation Over Nafion-H: Isotope Labelling Study of Ether Synthesis Over Nafion-H

The two reactant alcohols, methanol and isobutanol, can be produced from H_2/CO synthesis gas (a non-petroleum feedstock) over alkali-promoted Cu/ZnO catalysts (13,14,24). Since MTBE is an oxygenated, high octane fuel additive and MIBE has a high cetane number of 53 (25), it is desirable to shift the selectivity of the alcohol coupling reaction to control MIBE or MTBE as required by fuel composition. It has been shown that in the reaction of methanol with isobutanol, MTBE is the thermodynamically favored oxygenated product but that MIBE is the kinetically favored product (17). Therefore, an isotope labelling experiment was carried out to provide mechanistic insight into the manner in which methanol and isobutanol react together to form DME, MIBE, and MTBE and to determine if MTBE were derived from MIBE.

The methanol was purchased from MSD Isotopes and was 97.3 atom% ^{18}O enriched. Anhydrous isobutanol was purchased from Aldrich Chemical Co., Inc., and it contained the natural abundances of oxygen isotopes, i.e. 99.8% ^{16}O and 0.2% ^{18}O. Nafion-H microsaddles was the catalyst employed in this study. The alcohols were mixed in a molar ratio of 1/1 and pumped into the preheater section of the reactor at the rate of 3.4 mol/kg catalyst/hr by means of a Gilson high pressure pump. The reaction took place in a gas phase tubular downflow reactor with on-line GC analysis. Conversions of methanol and isobutanol were kept below 10% to minimize any possible secondary reactions and to keep the reaction within the differential regime. Isotopic composition analysis was accomplished off-line *via* GC/MS analysis, following the trapping and condensation of the effluent from the reactor in a dry ice cooled cold-finger. The mass spectra were compared to those of reference compounds for identification of the catalytic products (26).

The experimental testing conditions that were utilized consisted of the following:

Catalyst weight	2.00 g (dry)
Reaction temperature	90°C
Total Pressure	0.1 MPa
Molar ratio MeOH/iBuOH	1/1
Methanol flow rate	1.7 mol/kg cat/hr
Isobutanol flow rate	1.7 mol/kg cat/hr
He + N_2 flow rate	16.6 mol/kg cat/hr

The molar abundances of each ^{16}O- or ^{18}O-containing product were quantified *Via* GC/MS analyses by comparing the most intense MS peak intensities to one another. It was observed that the most abundant fragment from both DME and MIBE (easily separated by GC) was CH_3OCH_2 (after the loss of the $CH(CH_3)_2$ part of the MIBE molecule, which was further fragmented), while from MTBE it was $(CH_3)_3CO$ (after the loss of the CH_3 group). Specifically, for MIBE analysis, the peak at a mass-to-charge (m/q) ratio = 47 was normalized to the most intense peak at m/q = 45, corresponding to the CH_3-^{16}O-CH_2 fragment (26), in order to calculate the fraction of ^{18}O-containing MIBE relative to ^{16}O-containing MIBE, respectively. Likewise for MTBE, the peaks at m/q = 75 and 73 (26), corresponding to the $(CH_3)_3$-C-^{18}O and $(CH_3)_3$-C-^{16}O fragments, respectively, were used, while the m/q = 47 peak intensity, corresponding to the CH_3-^{18}O-CH_2 fragment, was compared to that of the m/q = 45 peak (CH_3-^{16}O-CH_2) for DME quantification. Other less intense MS peaks were also analyzed for further verification of the analyses.

The space time yields of the products are given in Table 14, and it is seen that MIBE was the principal product, while similar but smaller quantities of DME and isobutene were also formed. Analyzable quantities of MTBE were also formed.

Table 14

Space Time Yields of Products Formed by the Reaction of ^{18}O-Methanol and ^{16}O-Isobutanol over Nafion-H at 90°C and 101 kPa.

Product	Space-Time-Yields (mol (kg catalyst)$^{-1}$ hr^{-1})
MIBE	0.0140
DME	0.0045
Isobutene	0.0037
MTBE	0.0010
C_8-Ethers	trace

Isotopic composition of each of the oxygenates formed was determined by mass spectrometry as described. The results of these analyses are presented in Figure 17. The oxygen-containing products ^{16}O-MIBE and ^{18}O-MTBE were found with over 90% selectivity. The isotopic composition of DME of ≈92% ^{18}O demonstrates that isotopic scrambling of methanol did not occur to a significant extent over the catalyst.

These results can be summarized as follows:

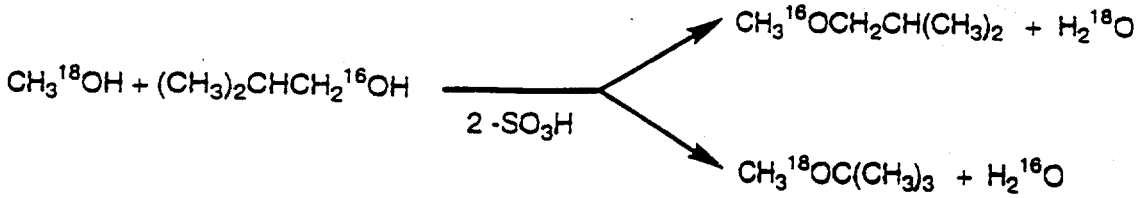

It is evident from these results that MIBE derived its oxygen from isobutanol, while MTBE obtained its oxygen from methanol. This result demonstrates that MIBE and MTBE are not formed from a common intermediate and that MTBE is not the product of isomerization of MIBE. Moreover, MIBE is produced by a kinetically controlled pathway

Figure 17. Isotopic composition of the reaction of ^{18}O-methanol and ^{16}O-isobutanol over the Nafion-H catalyst at 90°C.

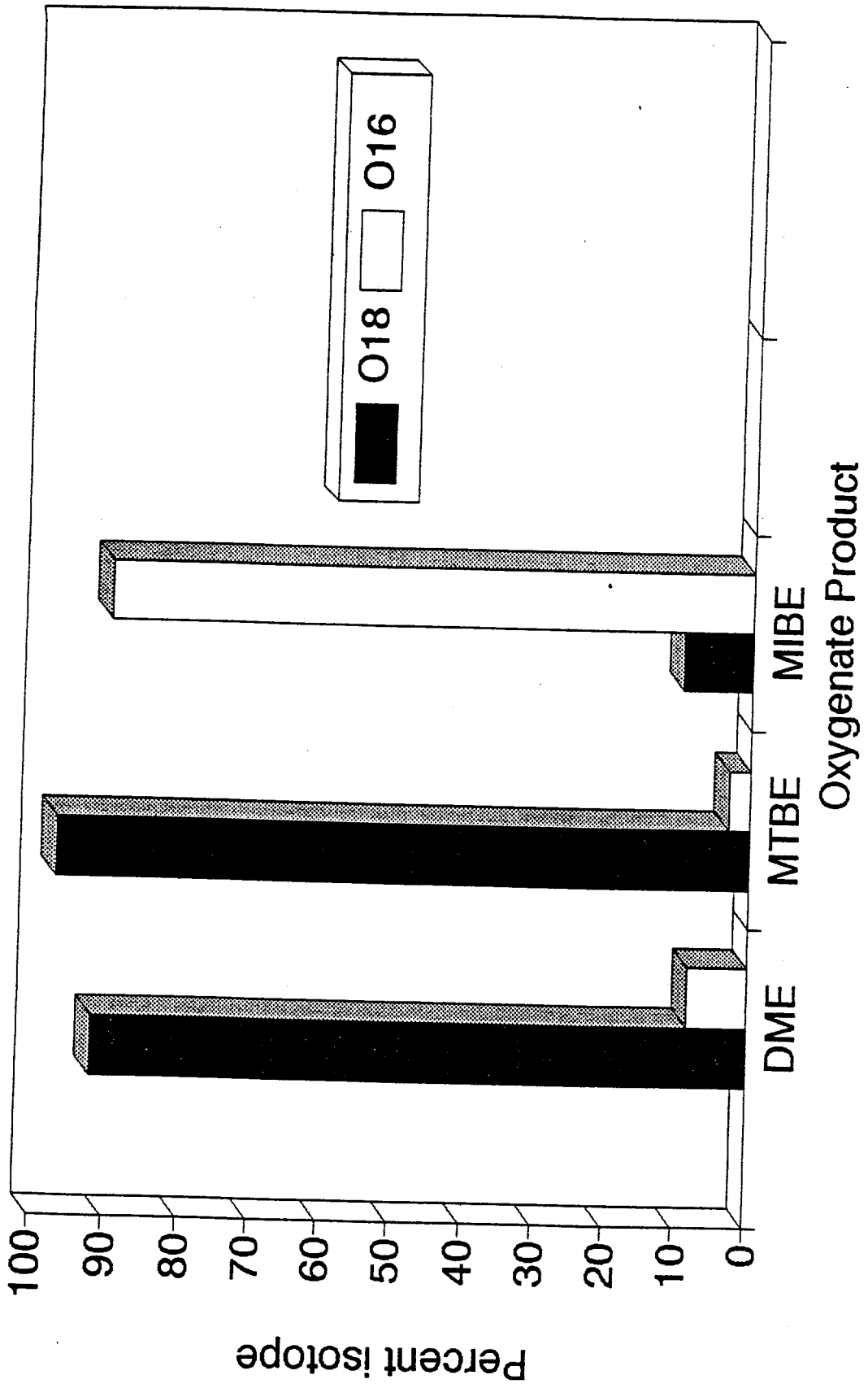

that is mechanistically more efficient than that leading to the thermodynamically more stable MTBE. These isotope discriminating reactions, taken in conjunction with those of the prior kinetic analyses (17), support a reaction scheme for MIBE that has mechanistic features of a S_N2 solution-phase reaction, but the heterogeneous synthesis exhibits distinctly different kinetics unique to surface catalyzed reactions in which both alcohols are activated by being adsorbed on the acid sites of the Nafion-H catalysts. This results in kinetics that show self-poisoning of the reaction by either alcohol at its high concentration, contrary to the kinetics of S_N2 reactions in solutions in which the rate is proportional to the concentrations of both reactants (27). In fact, the surface-catalyzed four-center reaction (involving two SO_3H surface groups and the two alcohols) exhibits a maximum rate at optimum concentrations of the reactant alcohols, which falls off when either alcohol is in excess as a negative power of the partial pressure of the excess reactant (17).

The specific mode of bonding of the alcohols to the sulfonic acid sites has not been resolved in full detail, but the current ^{18}O label flow to the products rules out the formation of isobutyl ester or isobutyl carbenium ion put forward as a possibility earlier (17), as in this case isobutanol would lose its oxygen and MIBE would gain ^{18}O from methanol, contrary to experiment. A likely type of bonding is *via* oxonium of the alcohols, with methanol oxonium suffering a rear attack by isobutanol that is just leaving its bonded state on neighboring sulfonic group; the ^{18}O-labelled H_2O is then the leaving group from methanol and the MIBE produced retains ^{16}O from isobutanol, as shown in Figure 18. The reverse attack of isobutyl oxonium by methanol is sterically hindered, in analogy with steric hindrance of the attack of isobutyl group by ethoxide in the related S_N2 reactions of alkyl halides (27).

Figure 18. The Reaction Pathway for ^{18}O-Methanol and ^{16}O-Isobutanol to Form ^{16}O-MIBE.

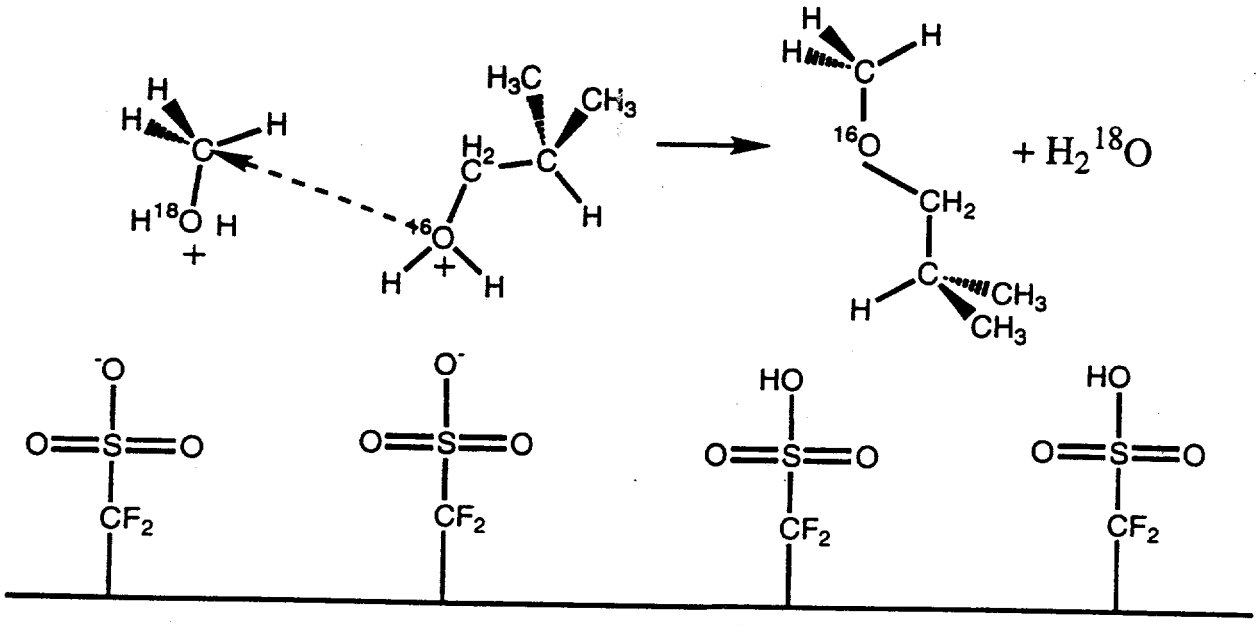

Contrary to MIBE, the MTBE contained almost exclusively oxygen originating from methanol and not isobutanol. Since isobutanol is dehydrated to isobutene by a parallel reaction, the origin of MTBE can be traced to a coupling of isobutene with methyl oxonium or isobutyl carbenium with methanol (28), as shown in Figure 19. The former path has been proposed to occur in the industrial acid-catalyzed MTBE synthesis from methanol and isobutene (29).

Figure 19. The Mechanism for Isobutanol Dehydration to Form Isobutene, with Subsequent Reaction of O^{18}-Methanol to Form O^{18}-MTBE.

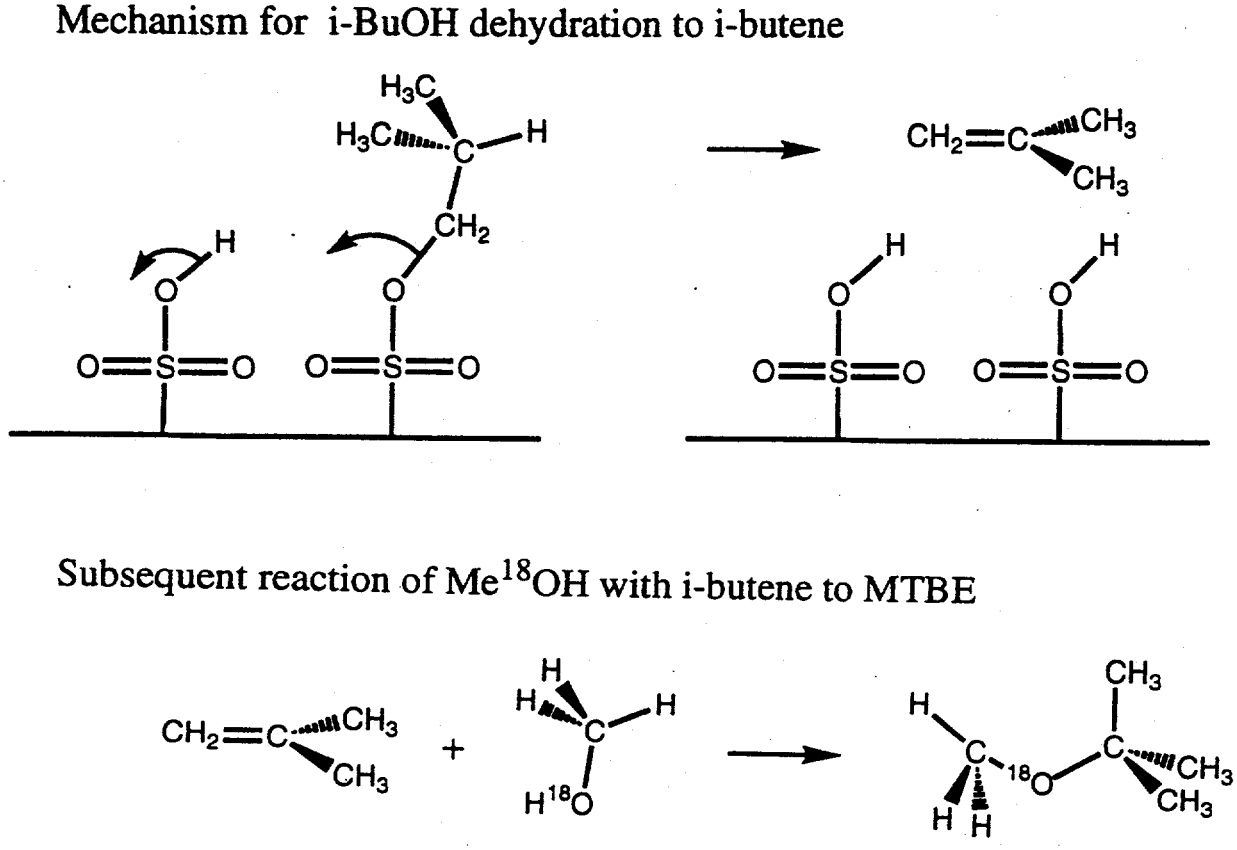

IV. Inorganic Catalysts for Direct Coupling of Alcohols to Ethers

A. Standard Test Screening of Inorganic-Based Catalysts

The inorganic catalysts tested in this section consisted of the following:

H-ZSM-5	MZ-289 provided by Mobil Res. & Dev. Co.
Catapal-B	Vista Chemical Co. (used to prepare γ-alumina)
H-Mordenite	Norton Zeolon-900
Montmorillonite	Aldrich K-10
Silica-Alumina	Davison Grade 980
Sulfated ZrO_2	Prepared in-house

These catalysts were chosen for their strong acidity, ability to be used at high temperatures, and ease of regenerability. Mordenite, montmorillonite, silica-alumina, and γ-alumina have long histories of use in the petroleum industry, e.g. as fluidized catalytic cracking (FCC), isomerization, and reforming catalysts. Sulfate-modified zirconia has received recent attention as a possible isomerization or alkylation catalyst owing to its very strong acidity that has been characterized as a superacid (30,31). The sulfating step has been claimed to stabilize the surface area and the tetragonal phase of zirconia, as well as forming strong Lewis and Brönsted acid sites (32).

H-ZSM-5 is a medium pore zeolite with interconnecting channels of the dimensions 5.3 × 5.6Å and 5.1 × 5.5Å. H-mordenite is a zeolite with two parallel straight channels. The larger of the channels is 6.5 × 7.0 Å and the smaller channel is 2.6 × 5.7 Å (33). Breck reports a total pore volume for mordenite of about 0.21 cm^3/g (34). The surface area of this H-mordenite is ≥ 350 m^2/g. Catapal-B, produced specifically for catalytic applications, is a high purity form of pseudoboehmite that is the precursor of γ-alumina. Calcination of pseudoboehmite to 500°C (for 3 hr) has been shown to result in the formation of γ-alumina, with a high surface area of typically 150-300 m^2/g, which is a solid Lewis acid, thermally stable form of alumina with a nominal molecular formula of Al_2O_3. The H-mordenite and

silica-alumina catalysts were calcined at 400°C for 4 hr, while the H-ZSM-5 catalyst was calcined in air at 400°C for 2 hr prior to loading into the reactor. A sample of γ-alumina from the Fisher Scientific Company was found to be totally inactive for any reaction of the methanol-isobutanol mixture under the reaction conditions employed.

The sulfate-modified zirconia (ZrO_2/SO_4^{2-}) was prepared as described by Hino and Arata (31). Zirconyl chloride octahydrate ($ZrOCl_2 \cdot 8H_2O$) was added to aqueous ammonia to precipitate high surface area $Zr(OH)_4$ that was washed, until free of Cl, and dried at 100°C overnight. The dried $Zr(OH)_4$, e.g. weighing ≈10 g, was placed on a folded filter paper, and 150 ml of 1 N H_2SO_4 was poured through it. The wet powder was dried at 110°C overnight and then calcined in air at 620°C for 3 hr.

The following standard test conditions were used to study the activity and selectivity of these catalysts:

Temperature	90, 125, 150, 175°C (also 200, 225, 250°C for γ-alumina)
Pressure	0.1 MPa
Methanol feed	1.72 mol/kg catalyst/hr
Isobutanol feed	1.72 mol/kg catalyst/hr
He + N_2 flow	16.0 mol/kg catalyst/hr
Catalyst weight	5.0 g

According to our standard procedure, the catalysts were diluted with 0.5 mm Pyrex beads to a total volume of 20 ml. The catalyst bed was centered in the stainless steel reactor between two glasswool plugs. The remainder of the reactor volume was filled with 3 mm Pyrex beads that served to preheat and mix the entering gas, as well as to minimize the dead volume in the reactor. The charged reactor was brought to the reaction temperature in a flow of approximately 80% He and 20% N_2. When the temperature was stabilized, the equimolar alcohol mixture was pumped into the reactor at the preset flow. The reaction was carried out at each temperature for a minimum of 6 hr. Steady state

conversions of methanol and isobutanol were usually obtained within the first 2 hr time-on-stream.

The space time yields (STY) of the major products obtained over this group of inorganic catalysts as a function of reaction temperature under steady state conditions are given in Table 15. The entry "Butenes" includes iso-, *trans*-2-, and *cis*-2-butene with isobutene predominating (greater than 65% of the butene content). When compared with the organic resin catalysts discussed previously, it is noted that higher temperatures were required with these inorganic catalysts to achieve comparable conversion.

The conversions of methanol and isobutanol, over the first four inorganic catalysts, are shown in Figure 20 and Figure 21, respectively, as a function of reaction temperature. The use of standard conditions at 90°C showed very low conversion of both methanol and isobutanol for all inorganic catalysts. Only **H-mordenite** showed significant activity at this temperature, reaching ≈10% conversion of methanol. Increasing the temperature to 125°C resulted in a large increase in methanol conversion over H-mordenite and only a minor change for the other catalysts. Further increase in temperature yielded >90% conversion of methanol over H-mordenite, while the other catalysts still exhibited below 20% methanol conversion. Of special interest with the H-Mordenite catalyst was the product selectivity pattern that demonstrated that methanol was selectively dehydrated to dimethylether (DME) at both 90 and 125°C (Figure 22). Only minor dehydration of isobutanol was seen at 150°C with >90% conversion of methanol.

Table 15. Product productivities (mol/kg cat/hr) over inorganic catalysts at 0.1 MPa as a function of temperature. Reactant feed was methanol = 1.72 mol/kg cat/hr and isobutanol = 1.72 mol/kg cat/hr.

	$T_{Reaction}$	DME	Butenes	MIBE	MTBE	C8 Ethers
H-Mordenite	90°C	0.060	------	------	------	------
	125°C	0.660	------	------	------	------
	150°C	0.830	0.068	------	------	0.004
ZrO_2/SO_4^{2-}	90°C	------	------	0.003	------	------
	125°C	0.006	0.067	0.020	0.003	0.008
	150°C	0.027	0.696	0.068	0.009	0.017
	175°C	0.103	1.290	0.049	0.007	------
Silica-Alumina	90°C	------	------	------	------	------
	125°C	0.007	0.028	0.011	0.001	0.003
	150°C	0.021	0.225	0.032	0.005	0.014
	175°C	0.039	0.943	0.049	0.007	0.016
Montmorillonite	90°C	------	------	------	------	------
	125°C	0.008	0.008	0.008	------	0.004
	150°C	0.019	0.071	0.019	0.004	0.014
	175°C	0.034	0.378	0.029	0.014	0.031
H-ZSM-5	90°C	0.005	0.001	0.012	------	------
	125°C	0.071	0.169	0.350	0.004	0.003
	150°C	0.261	0.339	0.134	0.003	0.003
	175°C	0.185	1.086	0.131	0.005	0.002
γ-Alumina	90°C	------	------	------	------	------
	125°C	0.006	------	0.007	------	------
	150°C	0.035	------	0.038	------	------
	175°C	0.118	0.002	0.160	------	------
	200°C	0.253	0.023	0.450	------	------
	225°C	0.342	0.242	0.831	------	------
	250°C	0.470	1.073	0.493	------	------

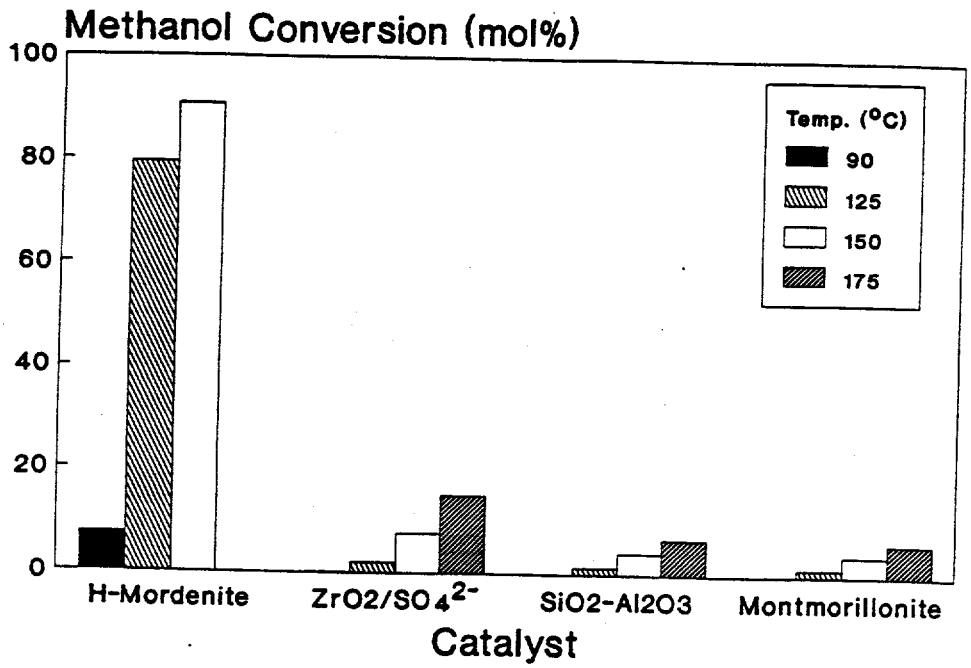

Figure 20. Conversion of methanol over four acidic inorganic catalysts under the reaction conditions given in Table 15.

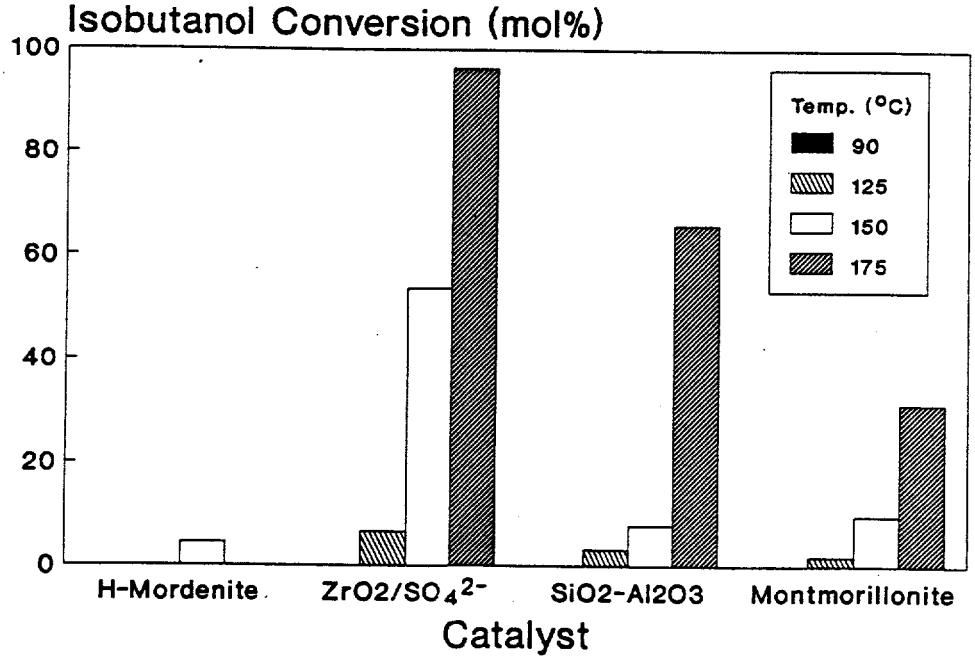

Figure 21. Conversion of isobutanol over four acidic inorganic catalysts under the reaction conditions given in Table 15.

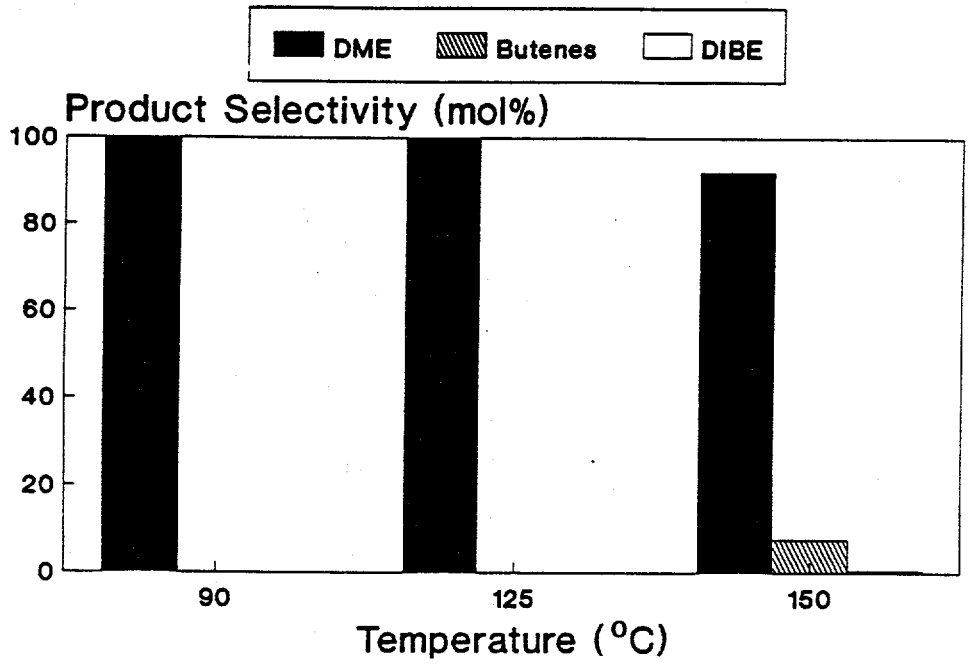

Figure 22. The product selectivity over H-mordenite from methanol/isobutanol = 1/1 reactant at 0.1 MPa as a function of temperature.

The sulfate-modified zirconia (ZrO_2/SO_4^{2-}) produced only methyl isobutyl ether at 90°C, but the yield was very low (Table 15). However, at higher temperature isobutanol was fairly selectively dehydrated to butenes in the presence of methanol (Figure 23). Indeed, at 150°C, the sulfate-modified zirconia showed 50% conversion of isobutanol, and this increased to 95% at 175°C with over 80% selectivity to butenes, principally isobutene. At the latter temperature, a small amount of C-12 product (0.5 mol%) was observed. On the other hand, non-sulfated zirconia was found to be totally inactive for the dehydration of either methanol or isobutanol over the temperature interval tested (90-175°C).

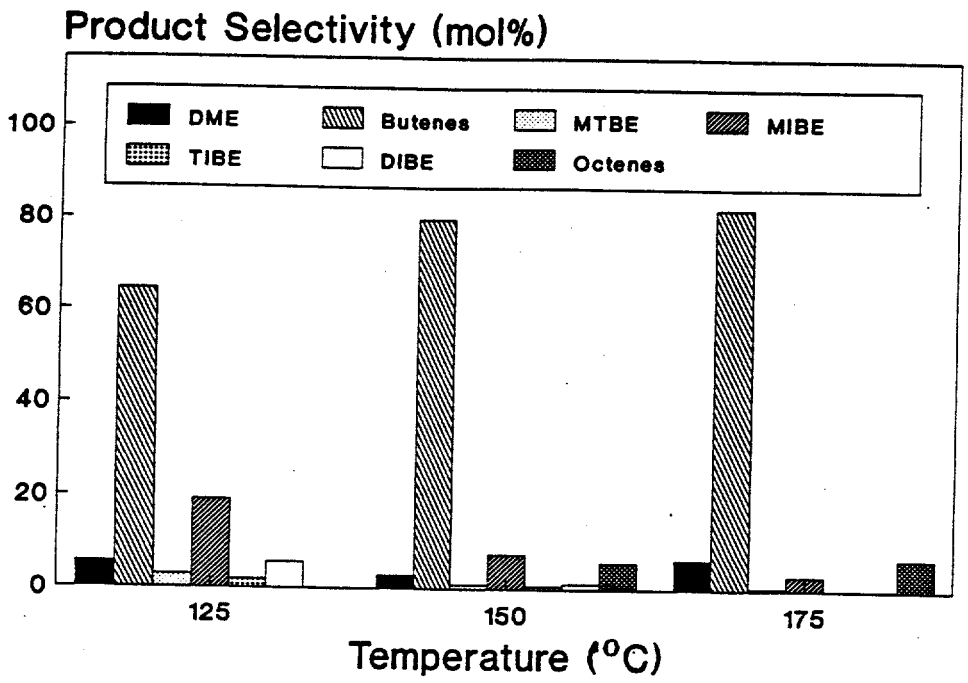

Figure 23. The product selectivity over the sulfated zirconia catalyst from methanol/isobutanol = 1/1 reactant at 0.1 MPa as a function of temperature.

Silica-alumina and montmorillonite showed no catalytic activity at 90°C, as indicated in Figures 20 and 21. However, at 175°C the two catalysts achieved 63% and 30% conversion of isobutanol, respectively, but ethers were not the dominant products. Montmorillonite showed poor selectivity toward any product at 125°C (Figure 24), but at higher temperature butenes were the dominant products. Silica-alumina was also mostly selective to butenes (Figure 25). In contrast, γ-alumina showed no significant conversion of isobutanol or methanol in this temperature range studied, i.e. 90-175°C.

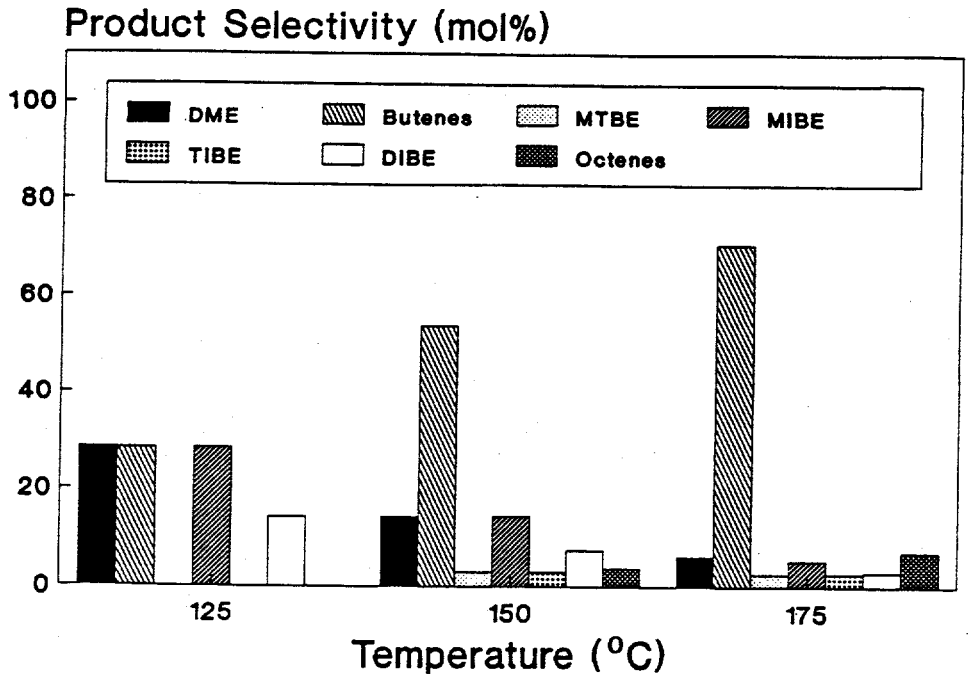

Figure 24. The product selectivity over montmorillonite from methanol/isobutanol = 1/1 reactant at 0.1 MPa as a function of temperature.

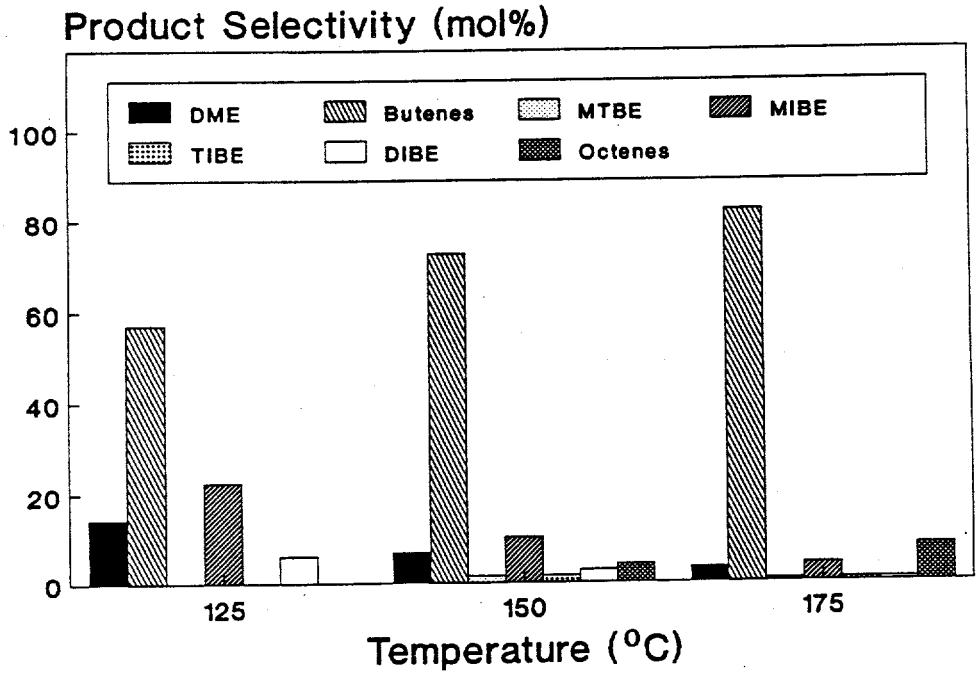

Figure 25. The product selectivity over the silica-alumina catalyst from methanol/isobutanol = 1/1 reactant at 0.1 MPa as a function of temperature.

The **H-ZSM-5 catalyst** was found to be active for isobutanol conversion to MIBE at 125°C, with the selectivity shifting toward butenes and DME as the reaction temperature was increased. At 175°C, ≈71% of the isobutanol was converted to products, with 77 mol% of the product being butenes. Figure 26 shows the STY of products, including the composition of the butenes, as a function of reaction temperature. As shown, a small amount of MTBE was formed over H-ZSM-5. This result contrasts sharply with that of H-mordenite, which had been found to be inactive for mixed ether formation from the methanol and isobutanol mixture over the temperature range studied. However, DME was formed highly selectively and in high yield with only slight conversion of isobutanol, and this could be explained in terms of "*shape selectivity*" of the H-mordenite. Although H-ZSM-5 has smaller pores than H-mordenite, it is very active for mixed ether formation and butene formation. This shows that the high selectivity toward DME formation observed over H-mordenite is not a general feature of acidic zeolites. The relative selectivities of H-Mordenite and H-ZSM-5 catalysts are discussed more extensively in Sections D-G of this chapter.

The **γ-alumina catalyst**, prepared from Catapal-B, was not very active at the lower temperatures where the other inorganic catalysts were active, and higher temperatures were needed to induce appreciable conversion of the reactants. However, the selectivity of γ-alumina is unique among the catalysts, as seen in Table 15 and Figure 27. The ethers MIBE and DME were exclusively and selectively formed between 125 and 175°C, while at higher temperatures isobutene formation became more important at 250°C, isobutene was the principal product. Additionally, small quantities of iso-octene were also seen. It is notable that the only butene formed over this γ-alumina was isobutene, whereas for all of the other catalysts, both organic and inorganic, that produced isobutene, there was always significant amounts of the linear butenes formed. The molar fraction of linear butenes of all butenes

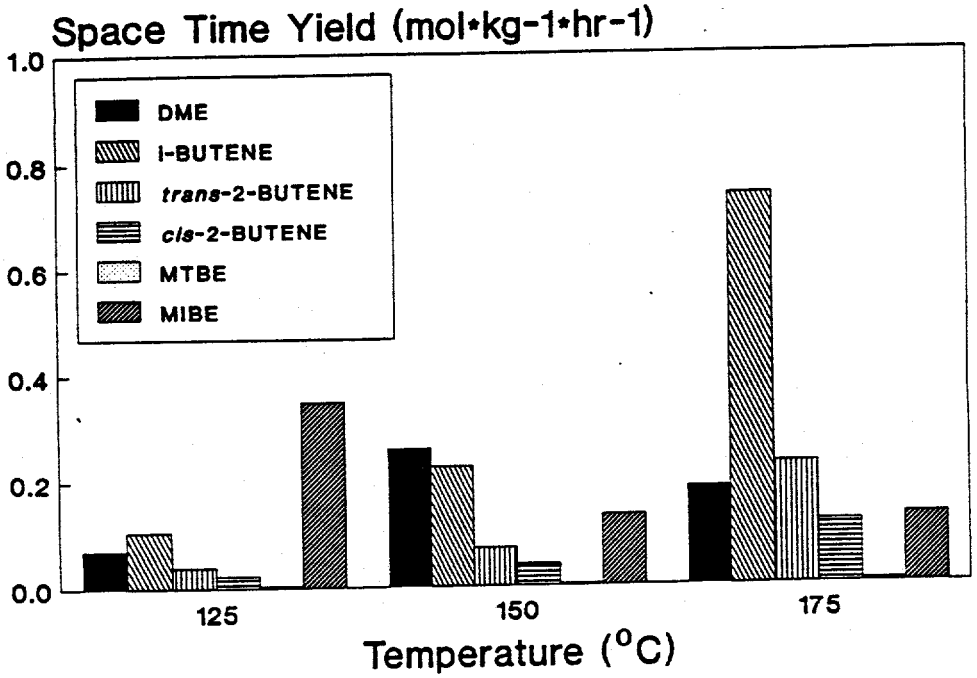

Figure 26. The product yields over the H-ZSM-5 zeolite catalyst from methanol/isobutanol = 1/1 reactant at 0.1 MPa as a function of temperature.

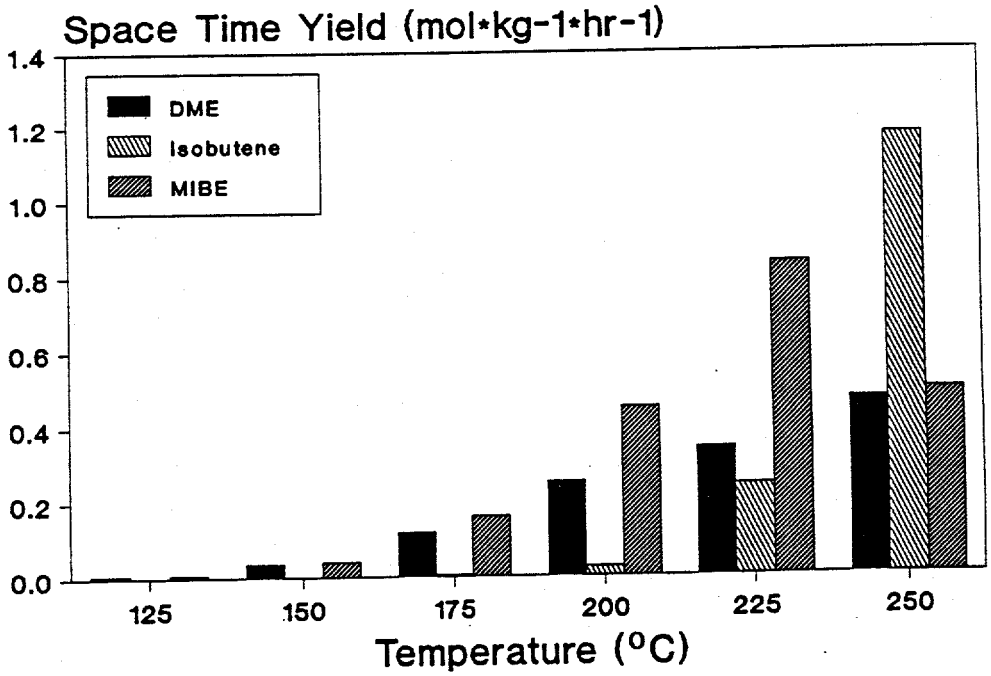

Figure 27. The product yields over the γ-alumina catalyst from methanol/isobutanol = 1/1 reactant at 0.1 MPa as a function of temperature.

formed over the inorganic catalysts, excluding γ-alumina, was about one-third.

The selectivity of isobutanol dehydration over γ-alumina had been studied by several workers (35,36), and it was found that isobutene was formed with over 95% selectivity. The pronounced selectivity of the γ-alumina may be explained by the absence of strong Brönsted acid sites on the surface of alumina (37). The γ-alumina surface has been shown to contain Lewis acid sites associated with basic sites (37). It has been proposed that the acidic and basic sites act concertedly to remove, respectively, the OH^- from the alcoholic carbon and an H^+ from the neighboring tertiary carbon of isobutanol (35,36). The presence of strong Brönsted acid sites in the other catalysts, both organic and inorganic, has been associated with carbenium ion chemistry, which leads to rearranged products in isobutanol dehydration (38). Thus, the absence of strong Brönsted acidity in γ-alumina may explain the absence of linear butenes in the product.

B. Effect of Water on the Reaction Rate Over γ-Alumina

The effect of co-feeding water with the reactant alcohols on the reaction of methanol and isobutanol over γ-alumina was investigated. The concentration and strength of Lewis acid and base sites on the surface of γ-alumina is known to depend on the extent of hydration (32,35). Other researchers have shown that Lewis acid sites on alumina can be converted to hydroxyl groups of only weak acidity upon addition of water vapor. In order to evaluate possible poisoning of the alcohol reactions over γ-alumina by water, which is always a major product of the dehydration reactions and of the ether-forming alcohol coupling reactions, testing was repeated at the standard reaction conditions over a controlled temperature range with and without water added to the alcohol feed. In addition to the standard reaction condition, the following parameters were used:

Temperature	150, 160, 170, 180°C
Water feed	0.000 mol/kg catalyst/hr (for dry feed) 0.172 mol/kg catalyst/hr (for wet feed)

The experiment began by bringing the charged reactor to 150°C under the He and N_2 flow. The 1/1 molar anhydrous mixture of methanol and isobutanol was then pumped into the reactor at the predetermined rate. The reaction temperature was raised in 10°C intervals to 180°C, collecting data at each temperature for several hours. The reaction temperature was returned to 150°C, and the yields of products were redetermined under the dry feed conditions. Following this experiment, the dry alcohol feed was stopped and the catalyst was kept under inert gas flow until all reactants had left the catalyst bed, which occurred within about two hours. A mixture of methanol, isobutanol, and water was prepared in a molar ratio of 1/1/0.1, respectively. This wet alcohol mixture was then pumped into the reactor. The productivity data were obtained under the wet conditions at the same temperatures as for the dry reactant run. After raising the reaction temperature to 180°C, the temperature was lowered to 150°C. The productivities of the products was redetermined at 150°C, after which the wet alcohol feed was stopped. After allowing the catalyst to dry out under the inert gas flow, the anhydrous 1/1 mixture of methanol and isobutanol was again pumped into the reactor at the 150°C reaction temperature.

The space time yields of the DME and MIBE and of the isobutene and iso-octene hydrocarbons produced as a function of reaction temperature from the methanol and isobutanol reaction mixture, with and without water, are presented in Figure 28. As can be seen, the productivities of DME and MIBE were higher for the dry run than for the reaction with water present. The catalyst activity and productivity were restored to about the same values as those of the fresh catalyst when the reaction conditions were returned to the dry alcohol feed at 150°C. There was apparently very little deactivation with this catalyst. The

presence of water had an inhibiting effect on the reactions, but this inhibiting effect was reversible.

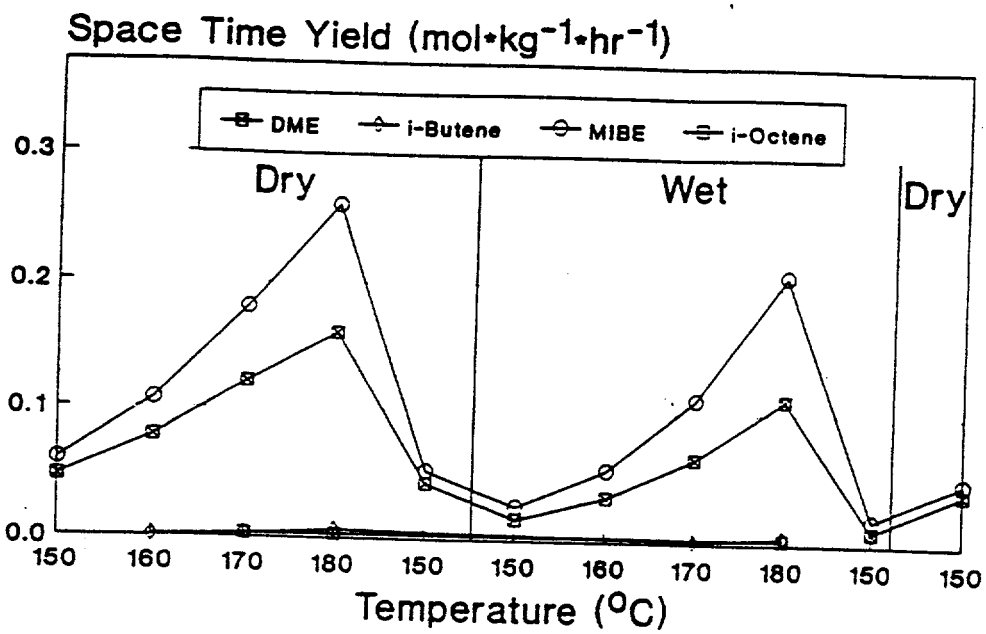

Figure 28. The effect of the methanol/isobutanol = 1/1 reactant being dry or wet on the productivity of the γ-alumina catalyst.

Conclusions From the Screening Tests

The patterns that emerge from the catalytic testing are the following:

(i) H-mordenite is a selective catalyst for dehydration of methanol to DME. Isobutanol is not converted to any ethers or dehydrated significantly to isobutene over H-mordenite under the conditions used. Evidently the pore size or shape of H-mordenite restricts the activation of isobutanol. Even though the isobutanol molecule is small enough to enter the larger channel pores of mordenite, its conversion is suppressed by one or all of the following three classic mechanisms of zeolite shape selectivity: (a) inaccessibility at low temperatures of acid centers that reside primarily in the narrow side channels of the mordenite structure (this type of size

exclusion in alcohol dehydration was first studied by Weisz et al. (39), and it should be noted that acid sites in mordenite are accessible to molecules as large as 1-methyl-2-ethylbenzene at higher temperatures (40)), (b) retardation of isobutanol transport by preferential diffusion of methanol, e.g diffusive selectivity as studied by Chen et al. (41), or (c) size restrictions on the transition states involving isobutanol, isobutyl esters, and isobutyl oxonium ions, following the concept of restricted transition state selectivity in zeolites as first proposed by Csicsery (40).

(ii) Sulfate-modified zirconia is an efficient and highly selective catalyst for the dehydration of isobutanol to isobutene, with methanol dehydration to DME being suppressed. The reasons for this selectivity pattern have not been established, but it is tentatively suggested that isobutanol is more strongly bonded than methanol to the sulfate groups on the zirconia surface so that methanol activation is suppressed. The relative bonding strength of isobutanol and methanol to the sulfate-modified zirconia would have to be more markedly different than that on Nafion H because DME and MIBE are co-products with isobutene over Nafion H but not over the sulfate-modified zirconia. An alternative explanation may be dilution of acid sites, which would disfavor ether-forming reactions since they require two adjacent acid sites. Isobutanol dehydration, while also a dual site mechanism, may only require one acid functionality adjacent to a non-acid empty adsorption site.

(iii) The overall order of activities for the dehydration reactions over the inorganic acids tested is:

$ZrO_2/SO_4^{=}$ > H-ZSM-5 zeolite > H-mordenite > SiO_2/Al_2O_3 > H-Montmorillonite > γ-Al_2O_3.

(iv) The inorganic catalysts are generally less active than the organic polymeric catalysts

at 90°C, except for the H-mordenite catalyst that is active and selective for methanol dehydration to DME. Higher temperatures are needed for significant alcohol dehydration with inorganic catalysts. In general, the organic polymeric catalysts are unstable at these higher temperatures, i.e. 120-140°C.

The yields of DME observed for the inorganic catalysts followed the order H-mordenite > montmorillonite ≈ SiO_2/Al_2O_3 ≈ ZrO_2/SO_4^{2-} > γ-Al_2O_3. The relative order of space time yields of isobutene production followed the order ZrO_2/SO_4^{2-} > SiO_2/Al_2O_3 > montmorillonite > H-mordenite ≈ γ-Al_2O_3. The selectivity behavior of the H-ZSM-5 zeolite catalyst was very strongly dependent on the reaction temperature. Probably, the most important finding of the inorganic catalyst testing is the remarkable selectivity properties of H-mordenite and ZrO_2/SO_4^{2-}. The ability of these catalysts to selectively dehydrate either methanol or isobutanol in a mixture containing both alcohols was unexpected. Even at near total conversion of one of the alcohols, the other alcohol remains essentially unconverted. The use of ZrO_2/SO_4^{2-} may lead to a new process where methanol/isobutanol streams, the major products of higher alcohol synthesis over alkali/Cu/ZnO catalysts, can be selectively dehydrated to methanol/isobutene streams that are the current feedstocks for industrial MTBE production.

C. Dehydration of Alcohols Over Silica and Zirconia Supported PW_{12} Heteropolyacid NO_2O_5, and $Fe/Mn/ZrO_2/SO_4^{2-}$ Catalysts

Supported heteropolyacids are used as heterogenous catalysts in several industrial applications. They are reported to possess strong acidic character, as well as unique selectivity characteristics. The activities and selectivities of silica-supported and zirconia-supported phosphotungstic acid, designated herein as PW_{12}/SiO_2 and PW_{12}/ZrO_2, for the standard reaction of a 1/1 molar MeOH/i-BuOH mixture were investigated. In addition,

niobic acid ($Nb_2O_5.xH_2O$) and iron-and manganese-doped sulfate modified zirconia catalysts were tested for catalytic activity.

The silica-supported phosphotungstic acid catalyst was prepared using $H_3PW_{12}O_{40}$, obtained from Fisher Scientific, Co. This compound is also sometimes referred to by others as tungstophosphoric acid or 12-polytungstophosphoric acid. Silica gel was obtained from Davison and had the following properties: Davisil grade 646, 35-60 mesh, surface area = 300 m^2/g, pore volume = 1.15 cm^3/g, and 150 Å pore size. An aqueous solution consisting of 5 g of phosphotungstic acid in 23 ml of distilled water was prepared. A 20 g portion of the silica was impregnated with this solution, with constant mixing, to make a 20% loading of phosphotungstic acid by weight. The impregnated silica, PW_{12}/SiO_2, was placed in a 100°C oven overnight. A sample of this material calcined to 200°C was also prepared. These calcination temperatures were chosen because they are below the decomposition range reported for heteropolyacids.

The zirconia-supported phosphotungstic acid catalyst, designated herein as PW_{12}/ZrO_2, was prepared in a similar manner. An aqueous solution consisting of 1.68 g of phosphotungstic acid in 5.5 ml of distilled water was prepared, and 6.72g of Zr(OH), prepared from hydrolyzed $ZrOCl_2 \cdot 8H_2O$, was impregnated with this solution, with constant mixing, to make a 20% loading of phosphotungstic acid by weight. The impregnated zirconium hydroxide, $PW_{12}/Zr(OH)_4$, was placed in a 100°C oven overnight and then calcined to 300°C for 3 hr.

"Niobic acid", actually hydrated niobium oxide ($Nb_2O_5 \cdot xH_2O$), was calcined at 200°C for 2 hr. A literature report indicates that high surface area and strong acidity are maintained only with low calcination temperatures such as this (42).

Recently, an iron and manganese doped sulfate-modified zirconia catalyst

($Fe/Mn/ZrO_2/SO_4^{2-}$) has been reported to possess stronger and more populous acid sites than ZrO_2/SO_4^{2-} (43). This catalyst was also reported to be many times more active for the low temperature isomerization of butane.

The $Fe/Mn/ZrO_2/SO_4^{2-}$ catalyst was prepared according to the method described in Ref. 31. This involved first dissolving 73 g of $ZrOCl_2 \cdot 8H_2O$ in *ca.* 100 ml of distilled water. About 700 ml of aqueous ammonia was added, and the solution was stirred for 2 hr. The $Zr(OH)_4$ formed was filtered and washed with distilled water until free of chloride ion. This solid was put in an oven at 100°C overnight to dry. The solution used to impregnate the $Zr(OH)_4$ consisted of 1.133 g $(NH_4)_2SO_4$, 2.234 g of $Fe(NO_3)_3 \cdot 9H_2O$, and 0.658 g of a 51 wt% solution of $Mn(NO_3)_2$. These salts were dissolved in distilled water to make 26.5 ml of a solution that was used to impregnate 25 g of $Zr(OH)_4$. The impregnated catalyst was dried in a 110°C oven overnight followed by calcination at 620°C for 3 hr. The catalyst preparation was designed to give 1.5% Fe, 0.5% Mn, and 4.0% SO_4^{2-} by weight supported on ZrO_2.

Catalytic Testing Results

The samples were diluted with Pyrex beads, charged to the reactor, and tested using the following reaction conditions:

Temperature	90, 125, 150, 175°C, (also 200 and 225°C)
Pressure	0.1 MPa
Methanol feed	1.72 mol/kg catalyst/hr
Isobutanol feed	1.72 mol/kg catalyst/hr
He + N_2 flow	16.0 mol/kg catalyst/hr
Catalyst weight	5.0 g

The results, presented as the space time yields of the major products as a function of reaction temperature, are given in Figures 29 and 30 for the catalysts prepared at the 100 and 200°C calcination temperatures of PW_{12}/SiO_2. The results are identical for the two

Figure 29. Space time yields of products over the PW_{12}/SiO_2 catalyst calcined at 100°C from methanol/isobutanol = 1/1 reactant at 0.1 MPa as a function of temperature.

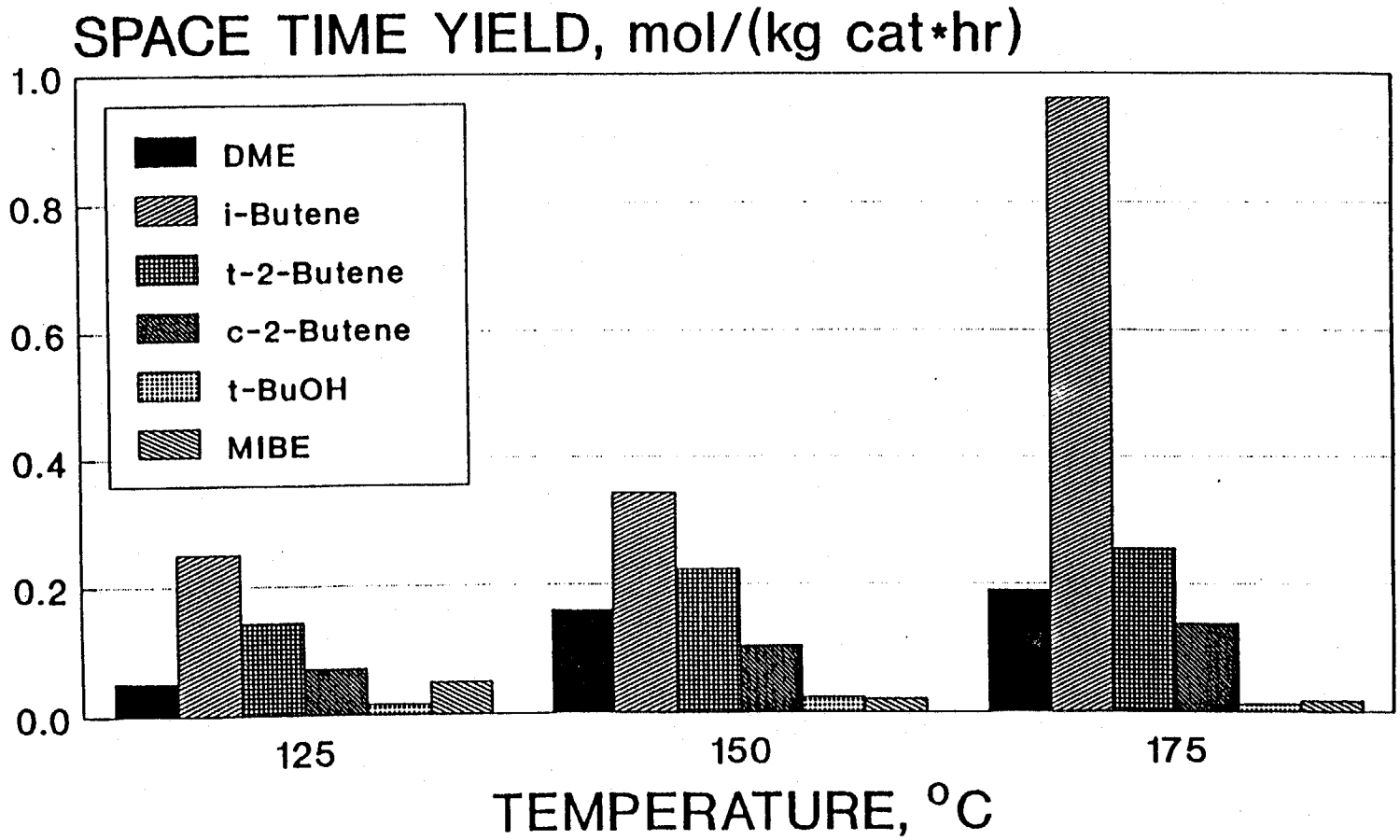

Figure 30. Space time yields of products over the PW_{12}/SiO_2 catalyst calcined at 200°C from methanol/isobutanol = 1/1 reactant at 0.1 MPa as a function of temperature.

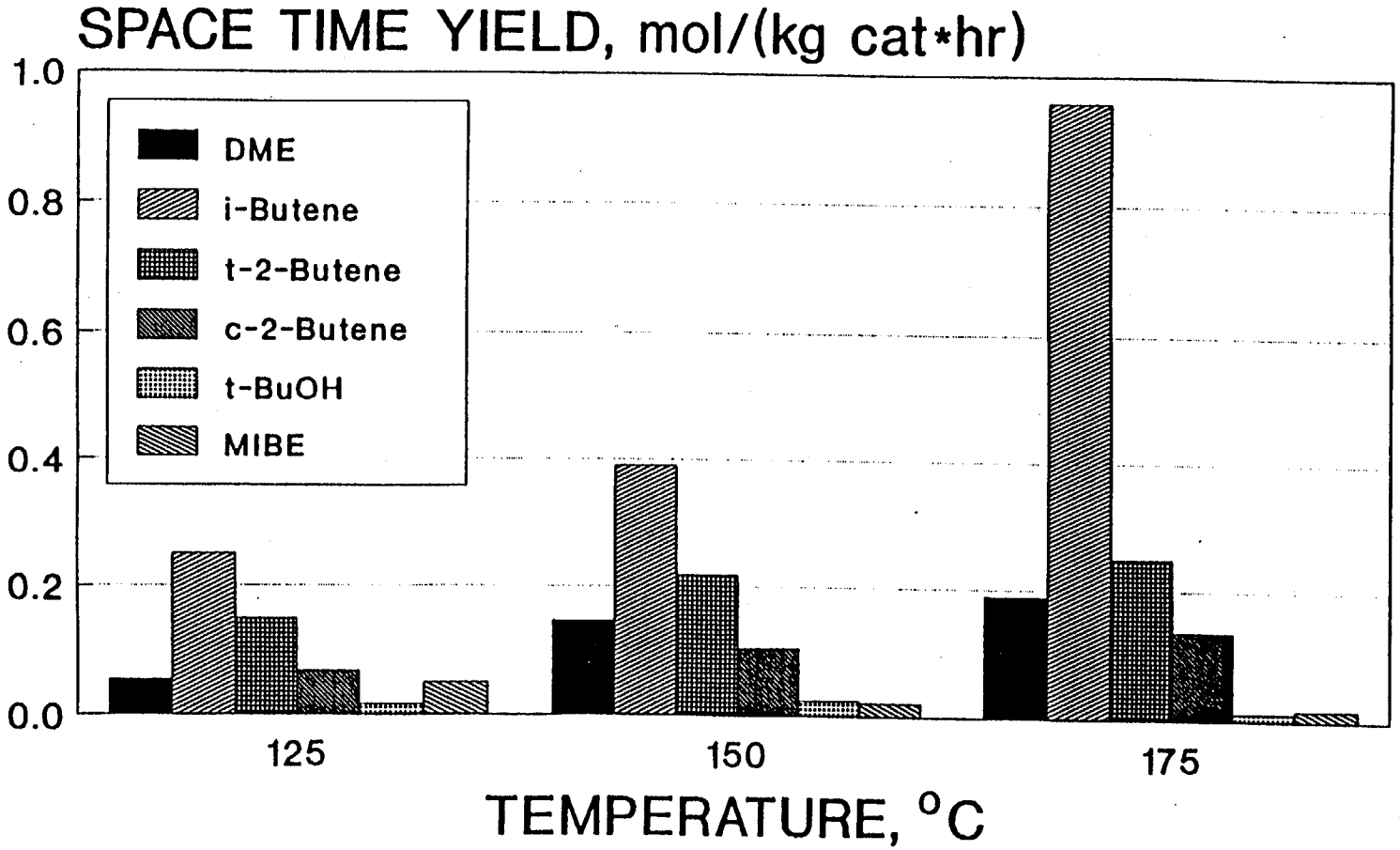

catalyst samples. No activity was found at a reaction temperature of 90°C. The activity and selectivity of PW_{12}/SiO_2 was comparable with the silica-alumina catalyst tested previously, with isobutene being the most selective product at 175°C. However, the ZrO_2/SO_4^{2-} catalyst remains as the most active and selective of all catalysts in the standard test screenings for the reaction of the MeOH/i-BuOH mixture. The presence of t-BuOH (cf. Figures 29 and 30) indicates that some of the isobutene product had been hydrated over this catalyst.

The zirconia-supported heteropolyacid catalyst, PW_{12}/ZrO_2, exhibited low activity and poor selectivity, as indicated in Figures 31-33, relative to other catalysts tested previously. This is especially true with respect to the SO_4^{2-}/ZrO_2-based catalyst. As shown in Figure 31, isobutene is the principal product formed with a space time yield of 0.254 $mol*kg^{-1}*hr^{-1}$, while the rate of production of DME was 0.147 $mol*kg^{-1}*hr^{-1}$. This means that more methanol was converted to DME than the quantity of isobutanol that was converted to isobutene. However, based on the quantities of products formed, the molar selectivities were 29.2% DME, 50.5% isobutene, 8.5% *trans*-2-butene, 8.0% *cis*-2-butene, and 3.8% MIBE.

The overall conversions at 175°C corresponded to 20.7 mol% conversion of isobutanol to products and 18.2 mol% of methanol to products. The %yields are shown in Figure 32, and these are based on the conversion levels of the reactants. For comparison purposes, the %yields are shown in Figure 33 on the basis of product molar composition, where the only difference between Figures 32 and 33 are in the values of DME since DME contains two methyl groups, as already discussed. Earlier, it had been found that pure ZrO_2 was totally inactive for these reactions. Therefore, the activity of the PW_{12}/ZrO_2 catalyst can be attributed to the presence of the phosphotungstic acid ($H_3PW_{12}O_{40}$).

Figure 31. Space time yields of products over the PW_{12}/ZrO_2 catalyst from methanol/isobutanol = 1/1 reactant at 0.1 MPa as a function of temperature.

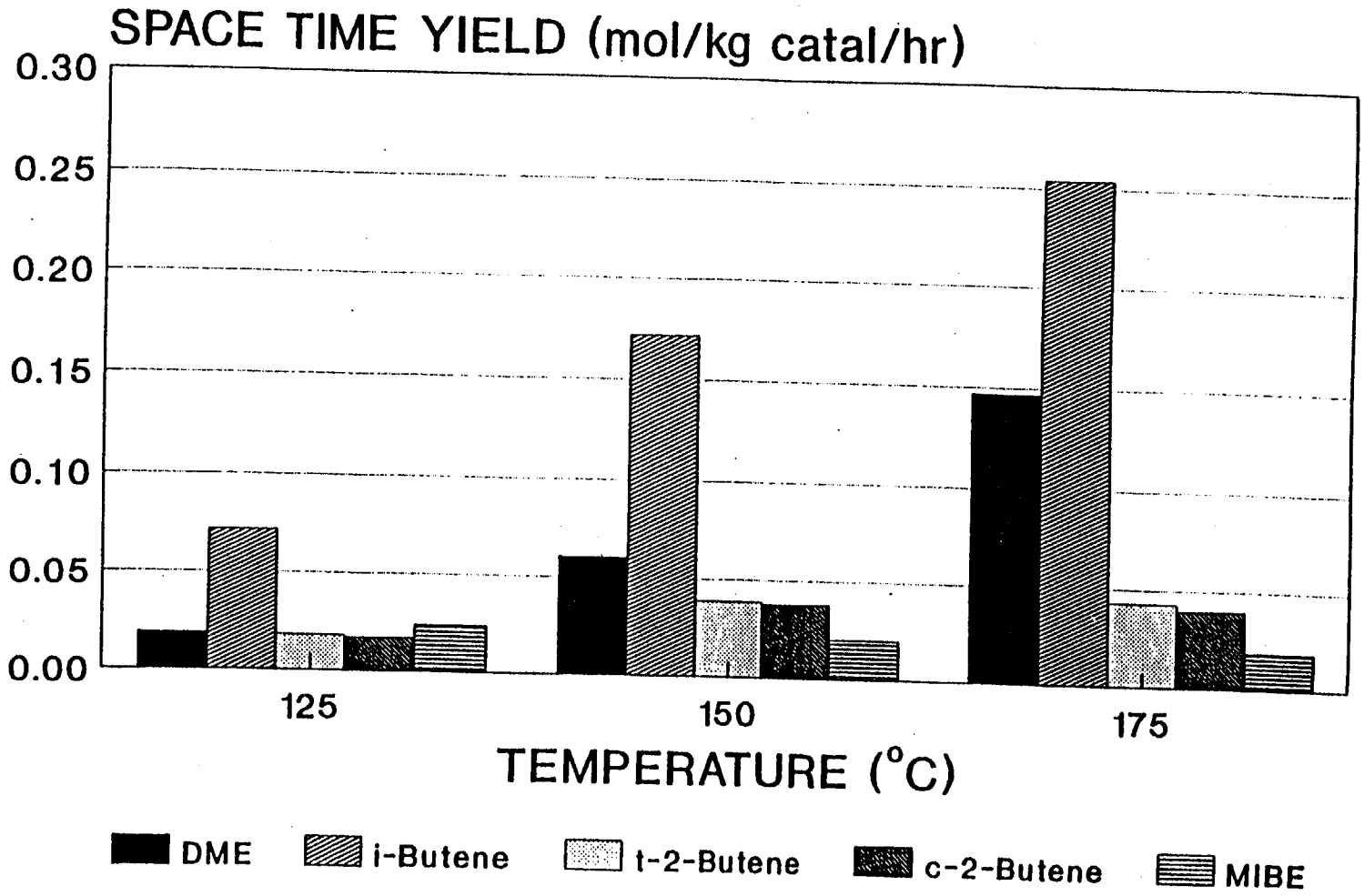

Figure 32. Percent yields of products (based on reactant conversions) over the PW_{12}/ZrO_2 catalyst from methanol/isobutanol = 1/1 reactant at 0.1 MPa as a function of temperature.

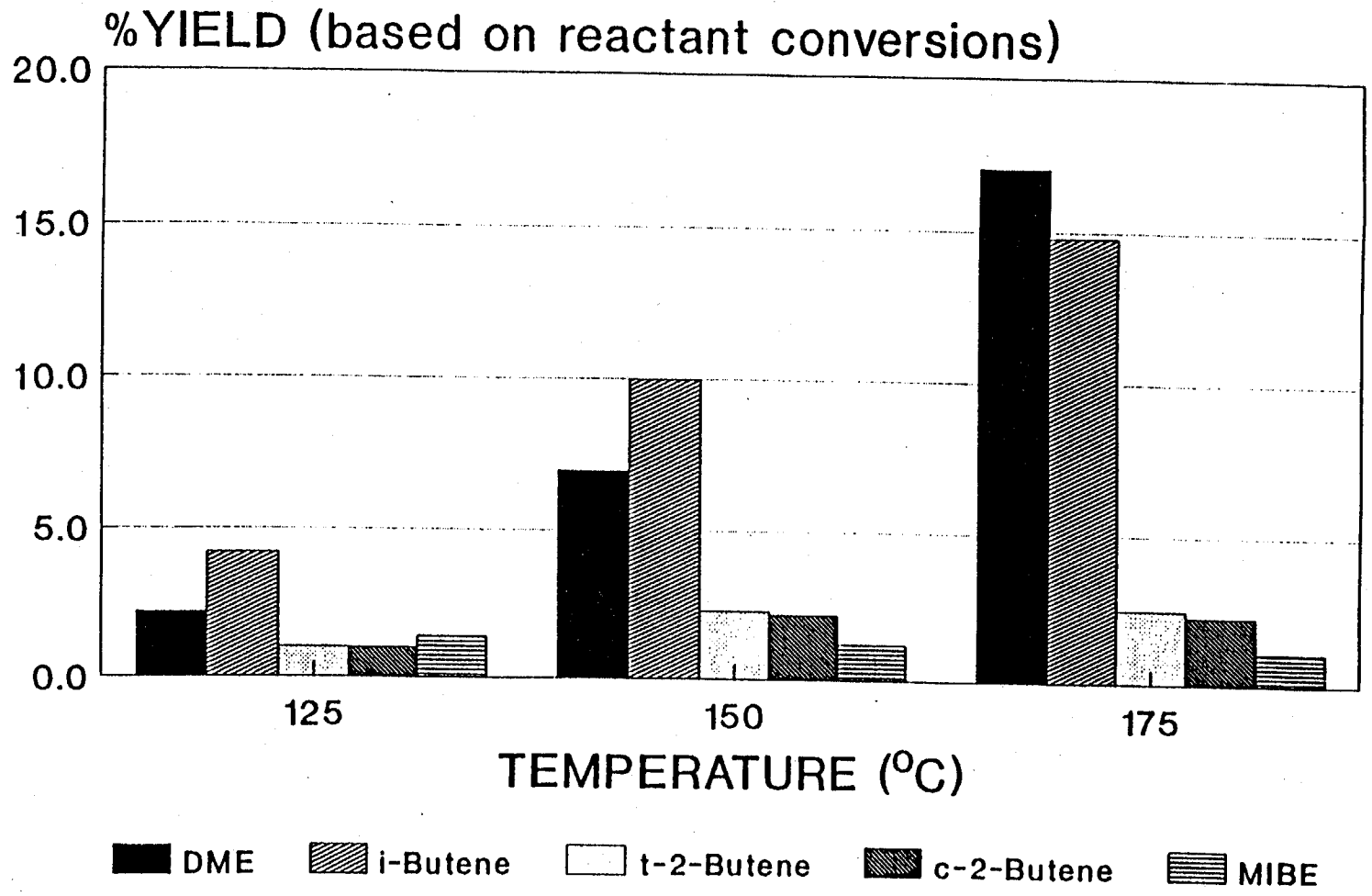

Figure 33. Percent yields of products over the PW_{12}/ZrO_2 catalyst from methanol/isobutanol = 1/1 reactant at 0.1 MPa as a function of temperature.

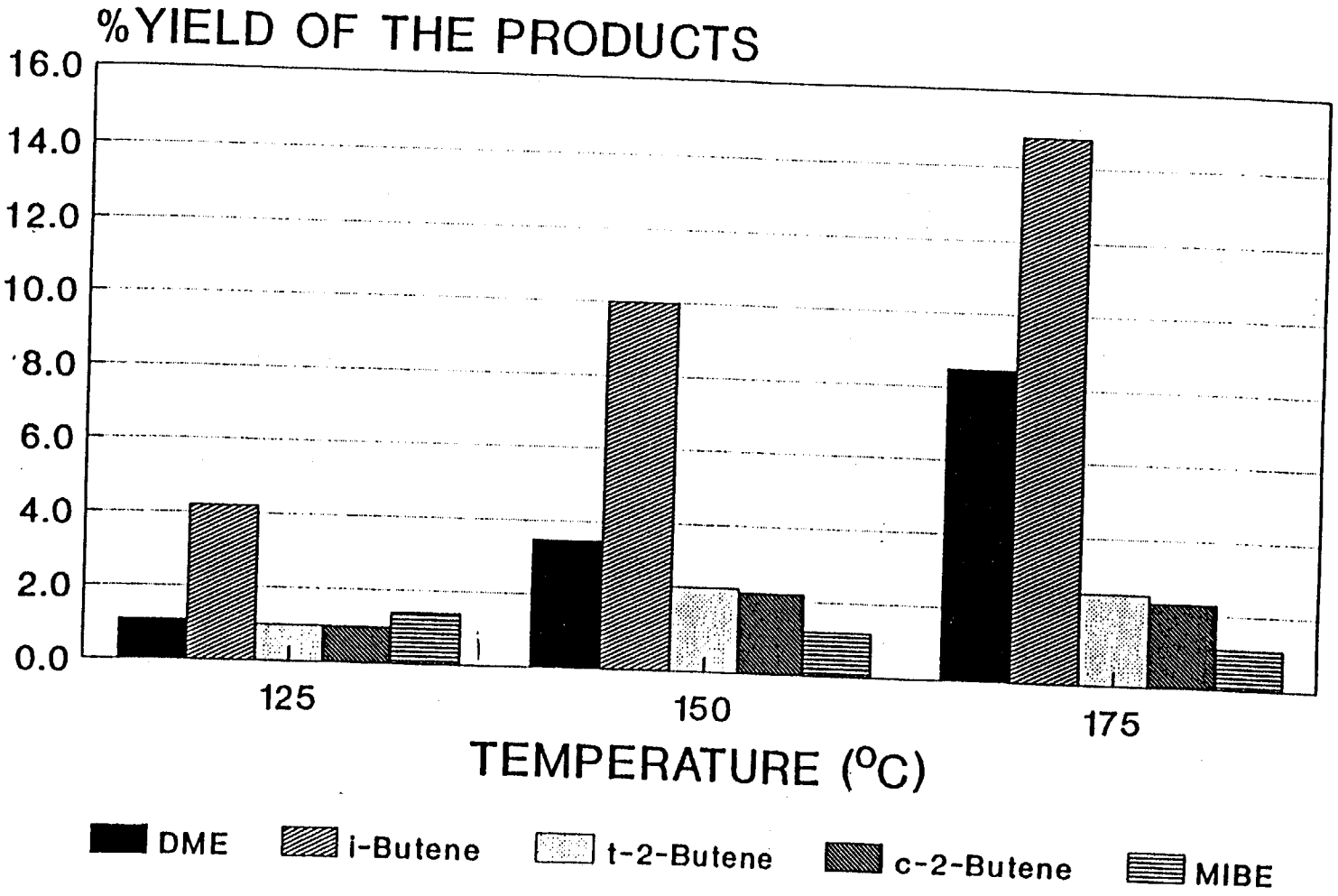

The niobic acid catalyst was essentially inactive at and below 175°C, as shown in Figures 34 and 35. At 200°C, the methanol and isobutanol conversions levels were 9.3 and 10.5%, respectively. When higher temperatures were used, most notably at 225°C, the activity and selectivity approached that seen for the best catalyst tested so far, the ZrO_2/SO_4^{2-} catalyst. At 225°C, as shown in Figure 34, this niobic acid catalyst produced 1.0 $mol*kg^{-1}*hr^{-1}$ of isobutene and only 0.13 $mol*kg^{-1}*hr^{-1}$ of DME. In comparison, the ZrO_2/SO_4^{2-} catalyst produced 1.1 $mol*kg^{-1}*hr^{-1}$ of isobutene and only 0.10 $mol*kg^{-1}*hr^{-1}$ of DME, which was achieved at the lower temperature of 175°C. With the Nb_2O_5 catalyst at 225°C, the reactant conversions were 70.2% isobutanol and 19.6% methanol to products, and Figure 35 shows that the %yields of isobutanol to isobutene and of methanol to DME were 58.7 and 15.5 %, respectively.

The catalytic results for the $Fe/Mn/ZrO_2/SO_4^{2-}$ catalyst were similar at the higher reaction temperatures employed to those of the ZrO_2/SO_4^{2-} catalyst. At 175°C, the Fe- and Mn-doped catalyst produced 0.91 $mol*kg^{-1}*hr^{-1}$ of isobutene and 0.03 $mol*kg^{-1}*hr^{-1}$ of DME, as shown in Figure 36. However, at lower temperature, the $Fe/Mn/ZrO_2/SO_4^{2-}$ catalyst as prepared here was considerably less active than the ZrO_2/SO_4^{2-} catalyst. For example, at 150°C the yield of isobutene was only 0.24 $mol*kg^{-1}*hr^{-1}$ for $Fe/Mn/ZrO_2/SO_4^{2-}$ compared to 0.61 $mol*kg^{-1}*hr^{-1}$ for ZrO_2/SO_4^{2-}.

This $Fe/Mn/ZrO_2/SO_4^{2-}$ catalyst exhibited a greater selectivity in activating isobutanol relative to methanol than the PW_{12}/ZrO_2 catalyst and the $Nb_2O_5 \cdot H_2O$ catalyst. The overall conversion levels for the $Fe/Mn/ZrO_2/SO_4^{2-}$ catalyst at 175°C were 61.3% isobutanol to products and 6.2% methanol to products. The %yields for this catalyst are shown in Figure 37. Figures 36 and 37 demonstrate that this catalyst was quite selective for the dehydration of isobutanol to isobutene, specifically 86.6 mol% of the C_4-containing

Figure 34. Space time yields of products over the $Nb_2O_3 \cdot H_2O$ catalyst from methanol/isobutanol = 1/1 reactant at 0.1 MPa as a function of temperature.

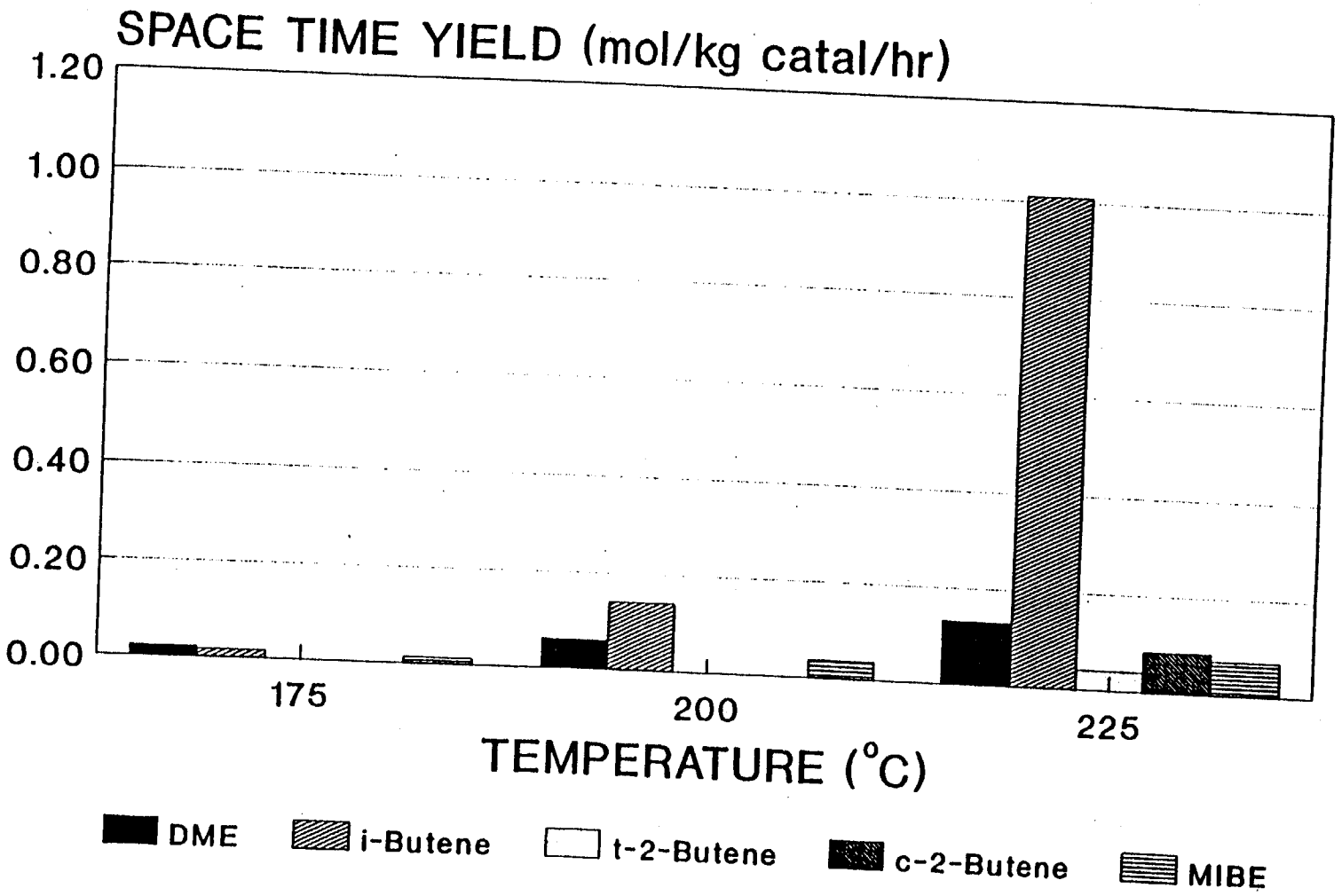

Figure 35. Percent yields of products (based on reactant conversions) over the $Nb_2O_3 \cdot H_2O$ catalyst from methanol/isobutanol = 1/1 reactant at 0.1 MPa as a function of temperature.

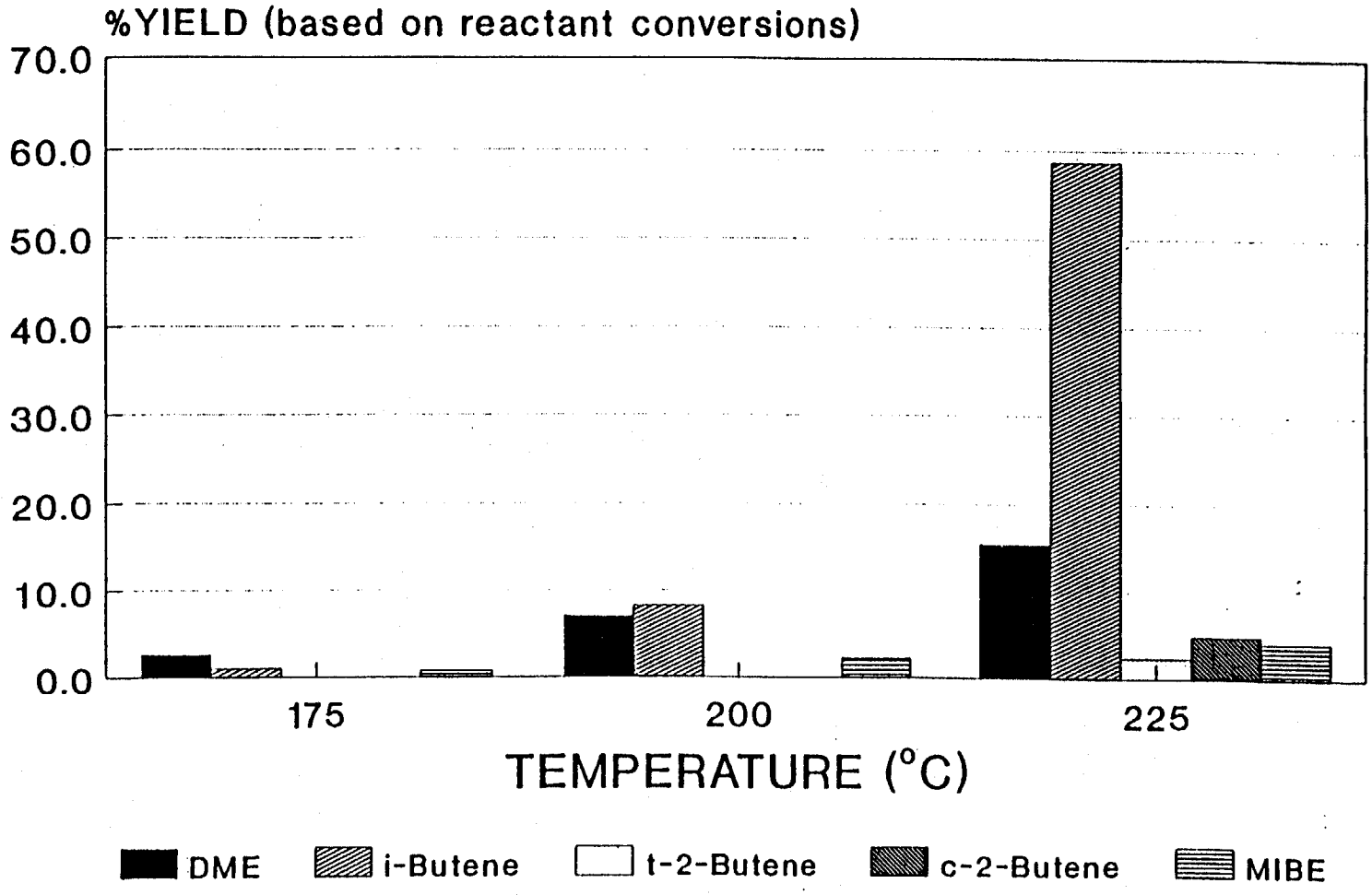

Figure 36. Space time yields of products over the $Fe/Mn/ZrO_2/SO_4^{2-}$ catalyst calcined at 620°C from methanol/isobutanol = 1/1 reactant at 0.1 MPa as a function of temperature.

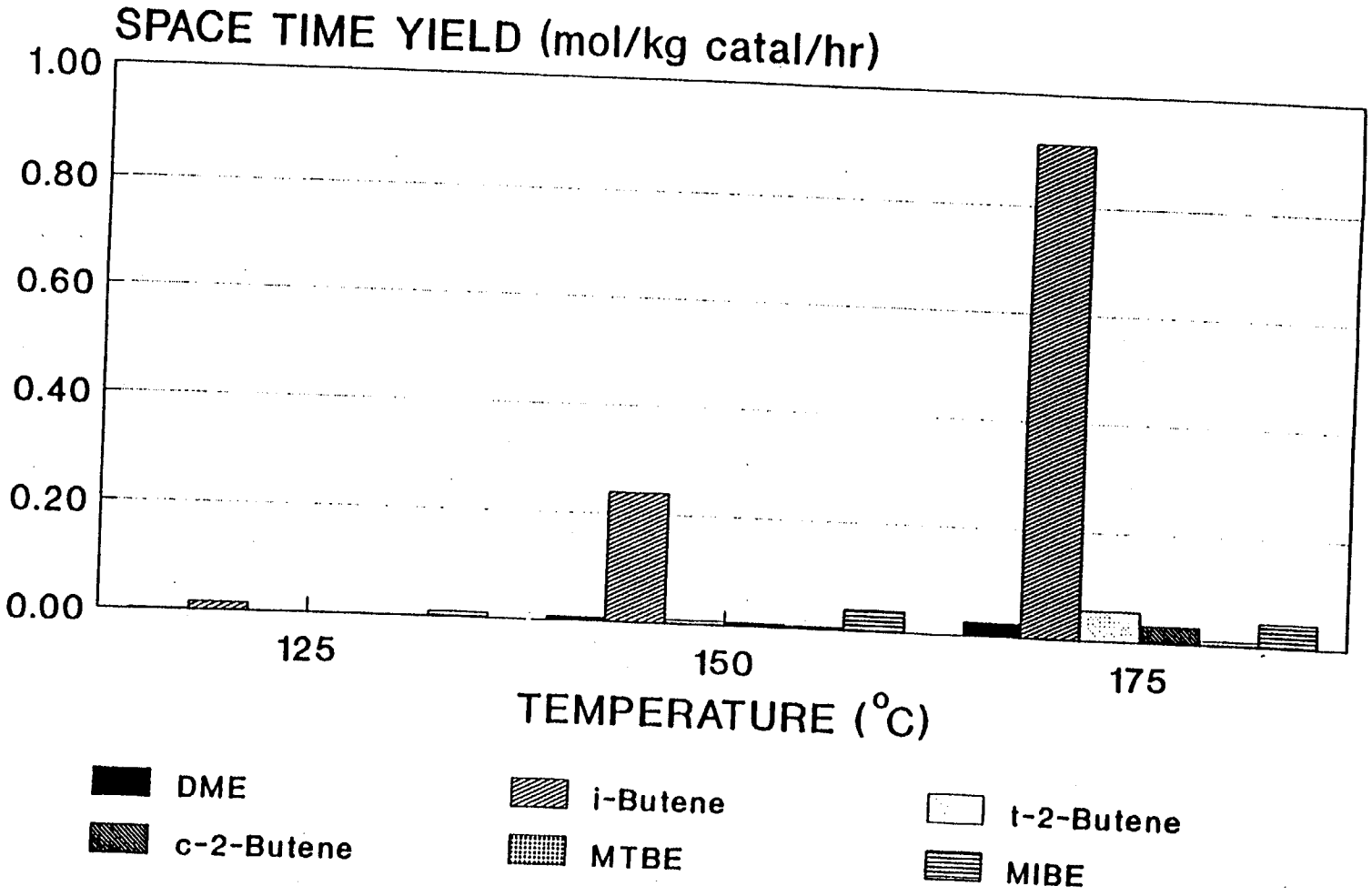

Figure 37. Percent yields of products (based on reactant conversions) over the $Fe/Mn/ZrO_2/SO_4^{2-}$ catalyst calcined at 620°C from methanol/isobutanol = 1/1 reactant at 0.1 MPa as a function of temperature.

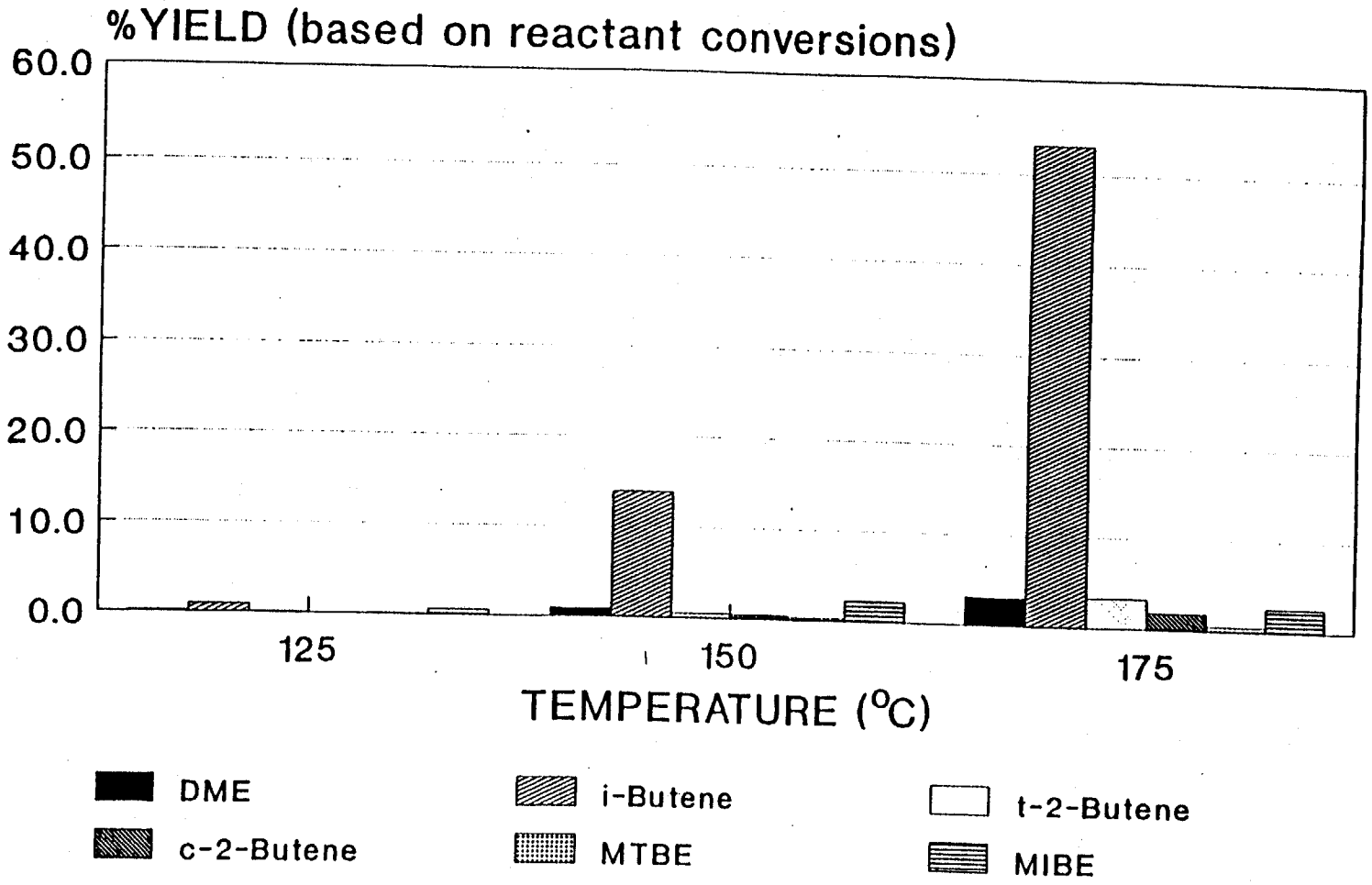

products was isobutene and 84.4 mol% of all significant products, not including water, was isobutene.

The $Fe/Mn/ZrO_2/SO_4^{2-}$ catalyst sample that was tested as described above was calcined at 620°C, although recent literature indicates that a higher calcination temperature might be beneficial for strong acid catalyzed reactions such as isomerization (43,44). Thus, a portion of the impregnated catalyst (prepared by simultaneous aqueous impregnation of $Zr(OH)_4$ with SO_4^{2-}, Mn^{2+}, and Fe^{3+}) that had been dried in a 110°C oven overnight was calcined at 720°C for 3 hr and then tested. As noted previously, the catalyst preparation was designed to give 1.5% Fe, 0.5% Mn, and 4.0% SO_4^{2-} by weight supported on ZrO_2.

The catalytic results are presented in Figure 38 in terms of %yield of the products. Again, it is evident that the predominant product was isobutene and that little of the methanol reactant was converted to products.

The productivity of this catalyst, as expressed in terms of space time yield, is shown in Figure 39 for the reaction temperatures of 125, 150, and 175°C. Low conversion levels are observed at 125 and 150°C, where the mol% conversions of methanol were 0.4 and 2.2%, respectively, while those of isobutanol were 0.7 and 8.9%, respectively. At 175°C, 55.9% of the isobutanol was converted to products, with a selectivity toward isobutene of 88%. In comparison, only 5.0% of the methanol was converted to products at this temperature. These conversions and selectivity were similar to those observed previously for the $Fe/Mn/ZrO_2/SO_4^{2-}$ catalyst calcined to 620°C. Therefore, the temperature of calcination in the range utilized in these studies did not produce a significant effect on the observed activity and selectivity of the catalyst.

Surface areas have been determined for samples of $Fe/Mn/ZrO_2/SO_4^{2-}$, and compairsons were made with niobic acid ($Nb_2O_5.xH_2O$), as well as the 12-phosphotungstic

Figure 38. Percent yields of products (based on reactant conversions) over the $Fe/Mn/ZrO_2/SO_4^{2-}$ catalyst calcined at 720°C from methanol/isobutanol = 1/1 reactant at 0.1 MPa as a function of temperature.

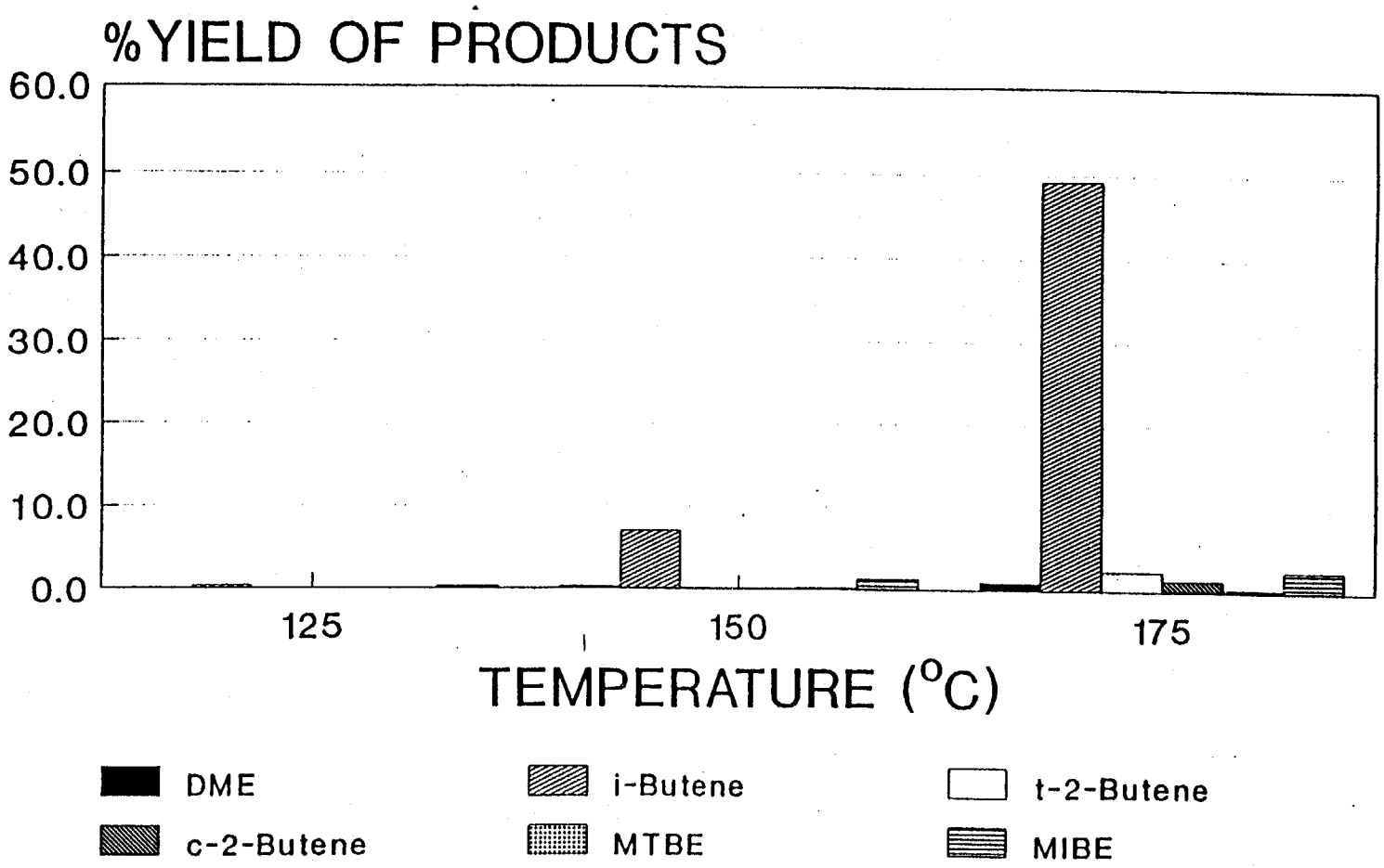

Figure 39. Space time yields of products over the $Fe/Mn/ZrO_2/SO_4^{2-}$ catalyst calcined at 720°C from methanol/isobutanol = 1/1 reactant at 0.1 MPa as a function of temperature.

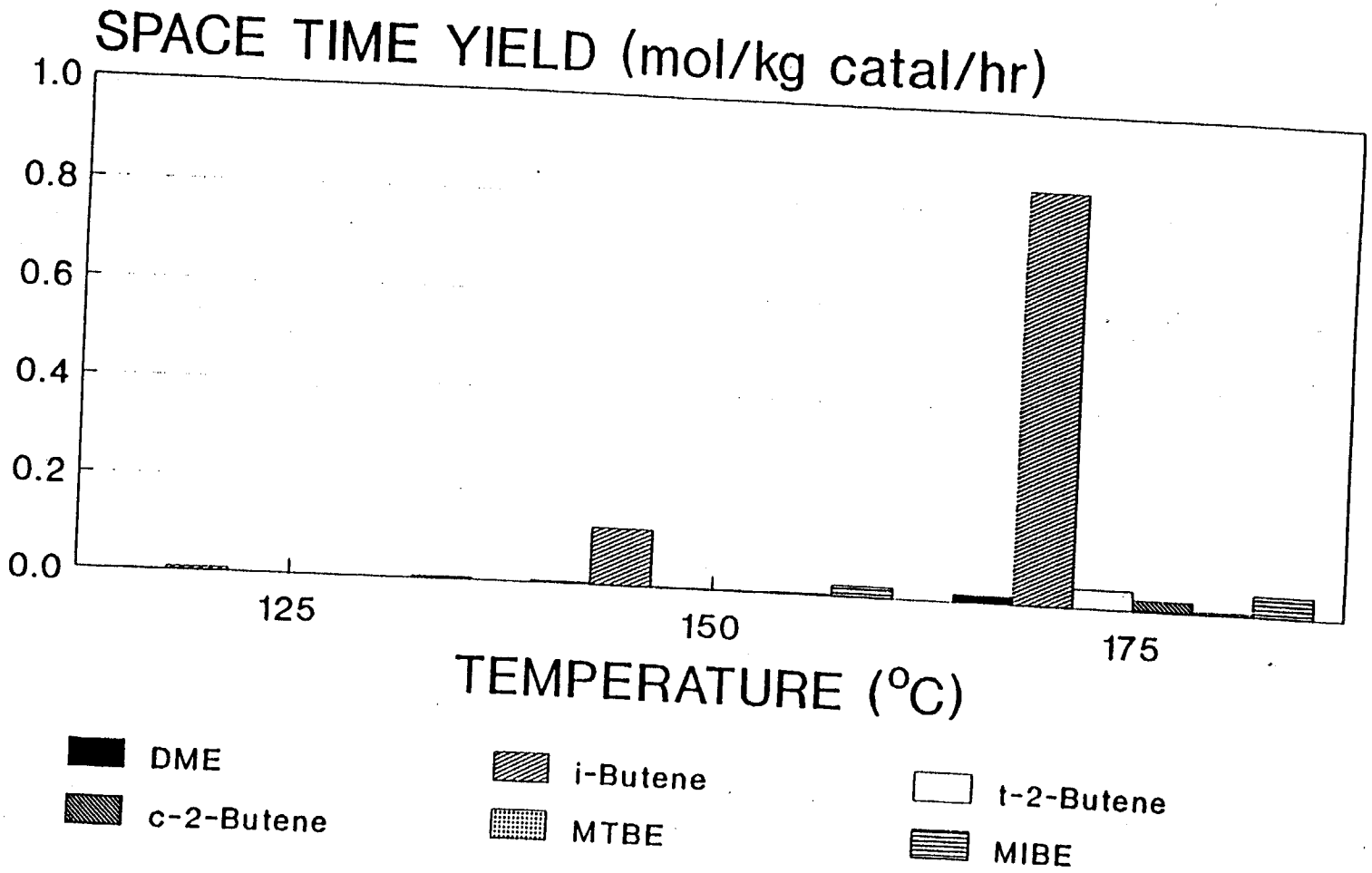

acid on silica catalyst (PW_{12}/SiO_2) that was prepared and tested. Particular surface areas were determined for $Fe/Mn/ZrO_2/SO_4^{2-}$ samples dried at 100°C and after calcination at 620°C. The uncalcined sample of $Fe/Mn/ZrO_2/SO_4^{2-}$ was degassed at 120°C prior to exposure to N_2 at -196°C, whereas the calcined $Fe/Mn/ZrO_2/SO_4^{2-}$, niobic acid, and phosphotungstic acid on silica (PW_{12}/SiO_2) catalysts were degassed at 300°C. The measured surface areas are given in Table 16. The surface area determined for the calcined $Fe/Mn/ZrO_2/SO_4^{2-}$ sample was in good agreement with the value of 97 m^2/g reported by others (14).

Table 16. Surface Areas

Catalyst	Surface Area (m^2/g)
$Fe/Mn/ZrO_2/SO_4^{2-}$ dried to 100°C	219
$Fe/Mn/ZrO_2/SO_4^{2-}$ calcined to 620°C	83
Niobic Acid	118
(PW_{12}/SiO_2)	218

D. Dehydration of Isobutanol Over H-Mordenite

Dehydration of a methanol and isobutanol mixture gave primarily DME over H-mordenite between 90 and 150°C, as shown in Table 15. The preferential dehydration of methanol was explained in terms of shape selectivity. To investigate if H-mordenite exclusively can dehydrate methanol, a test with only isobutanol as the feed was conducted.

The experiment was carried out at 0.1 MPa at the reaction temperatures of 90, 125, 150, 175, and 185°C, and then the reaction temperature was returned back to 150°C. The isobutanol feed rate was 1.72 mol/kg cat/hr and the He + N_2 flow was maintained at 16.9 mol/kg cat/hr. H-Mordenite was calcined at 400°C for 3 hr, and then a 2.5 g portion was

loaded into the reactor for the catalytic test.

As can be seen from Figure 40, the butene product was primarily composed of isobutene, which was also the case for other catalysts such as sulfated zirconia, silica-alumina and montmorillonite, e.g. about one-third of the total quantity of the synthesized butenes consisted of linear butenes. The productivity of butenes was very low at 90°C and at 125°C, which is comparable to the same experiment in the presence of methanol. The dehydration reaction of isobutanol to butenes was facilitated by an increase of the temperature, i.e. higher temperature was needed to activate isobutanol for dehydration. After reaction at 185°C, the system was brought back to 150°C to measure any deactivation of the catalyst. The conversion of isobutanol to butenes decreased from 8.8 to 5.9% over the course of this study.

Figure 40 also indicates methanol as a product in this reaction. Methanol was not present in the alcohol feed. The catalyst was not at any point exposed to methanol. In addition to a methanol peak, a new peak was seen in the chromatogram. The new peak has not been unambiguously identified, but comparisons of retention times indicate the possibility of assigning this peak to 1-propanol. The origin of methanol is not known, but the possibility exists that isobutanol or the butenes may crack to C_1 and C_3 fragments giving rise to methanol and propanol following hydration.

E. X-Ray Powder Diffraction of H-Mordenite and H-ZSM-5 Zeolites

Objective

The objective of this experiment was to evaluate the crystallinity of H-ZSM-5 zeolite and H-mordenite before and after the alcohol coupling reaction was carried out to determine if these zeolites were structurally stable under the reaction conditions employed.

Figure 40. The dehydration behavior of isobutanol only over the H-mordenite catalyst as a function of reaction temperature.

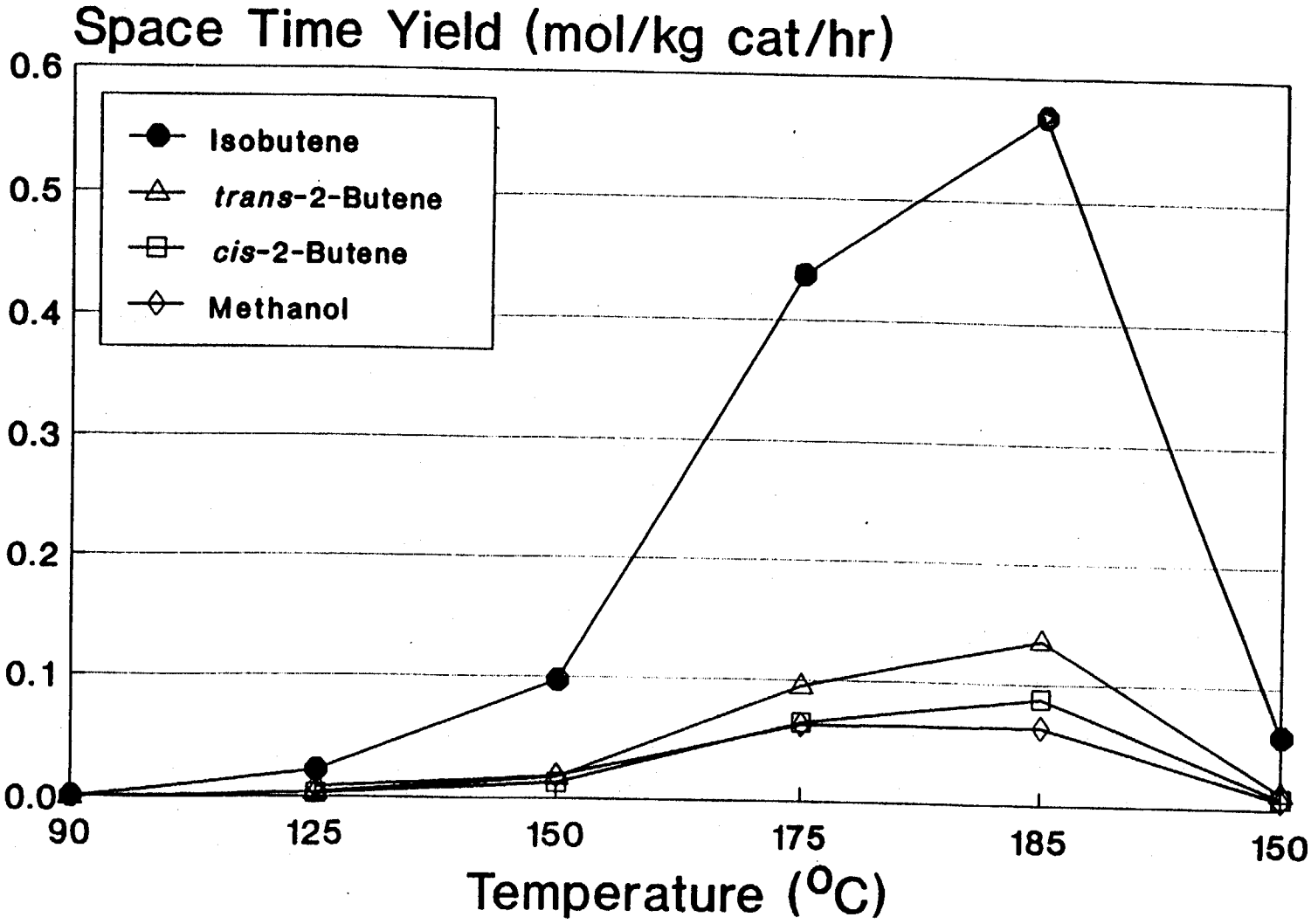

The activities and selectivities observed for testing in a tubular downflow reactor with a methanol/isobutanol = 1/1 reactant mixture at ambient pressure and a sequence of temperatures have been previously presented and discussed.

Experimental

The X-ray powder diffraction (XRD) patterns for the two zeolites were obtained on a Phillips APD 3720 Automated X-Ray Powder Diffractometer. Cu K_α radiation with a wavelength of 1.5418 Å was used to obtain the diffraction patterns using the instrument that is located in the Earth and Environmental Sciences Department at Lehigh University. Data were collected in the 2θ scan range from 1 to 60 degrees with a scan rate of 1 degree/min and an angle increment of 0.02 degree. The powdered samples were analyzed in a dry state.

Results

The XRD patterns were obtained for four samples consisting of H-mordenite fresh and after catalytic testing and of H-ZSM-5 zeolite fresh and after catalytic testing. Figure 41 shows the XRD pattern of fresh H-mordenite, and Figure 42 shows the XRD pattern of H-mordenite after reaction. A few of the more intense peaks have been indexed by using ASTM reference cards and tables of data given by Breck (34). Less intense peaks also correspond to the diffraction pattern expected for mordenite. The peaks in Figure 41 are more intense than in Figure 42, which might indicate some amorphous species sorbed on the surface of the used H-mordenite catalyst. This phenomenon is commonly exhibited (45) when analyzing used catalyst samples such as mordenite. As shown in Figure 42, the XRD peaks were in the same positions as those for the fresh catalyst (Figure 41), and all of the peaks were retained after catalytic testing. In addition, no extra peaks are observed in Figure 42 as compared to Figure 41. The crystallite size of the catalyst particles can be determined by using the Sherrer equation for diffraction line broadening (45). The main

Figure 41. XRD pattern of H-mordenite prior to catalytic testing.

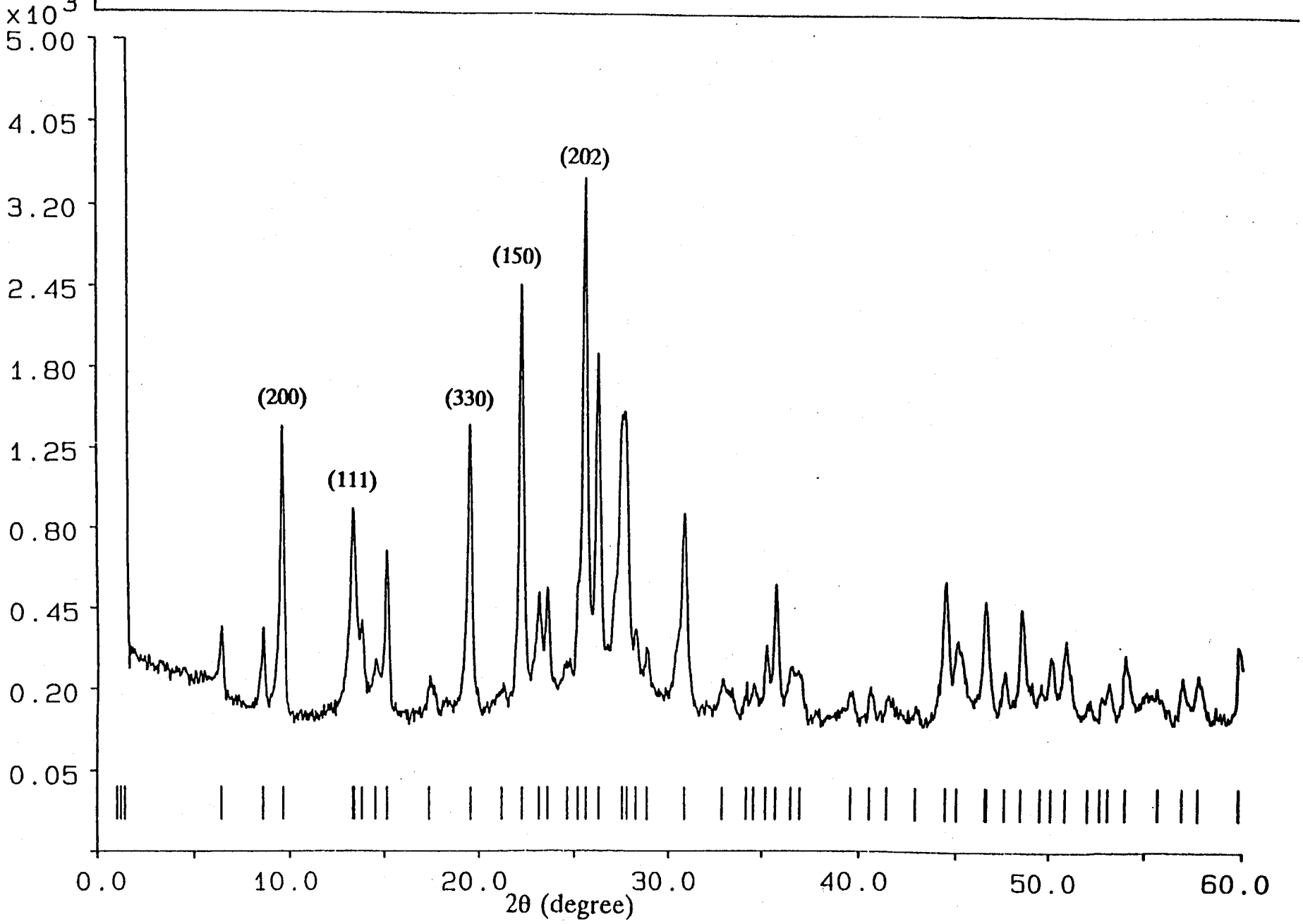

Figure 42. XRD pattern of H-mordenite after catalytic testing.

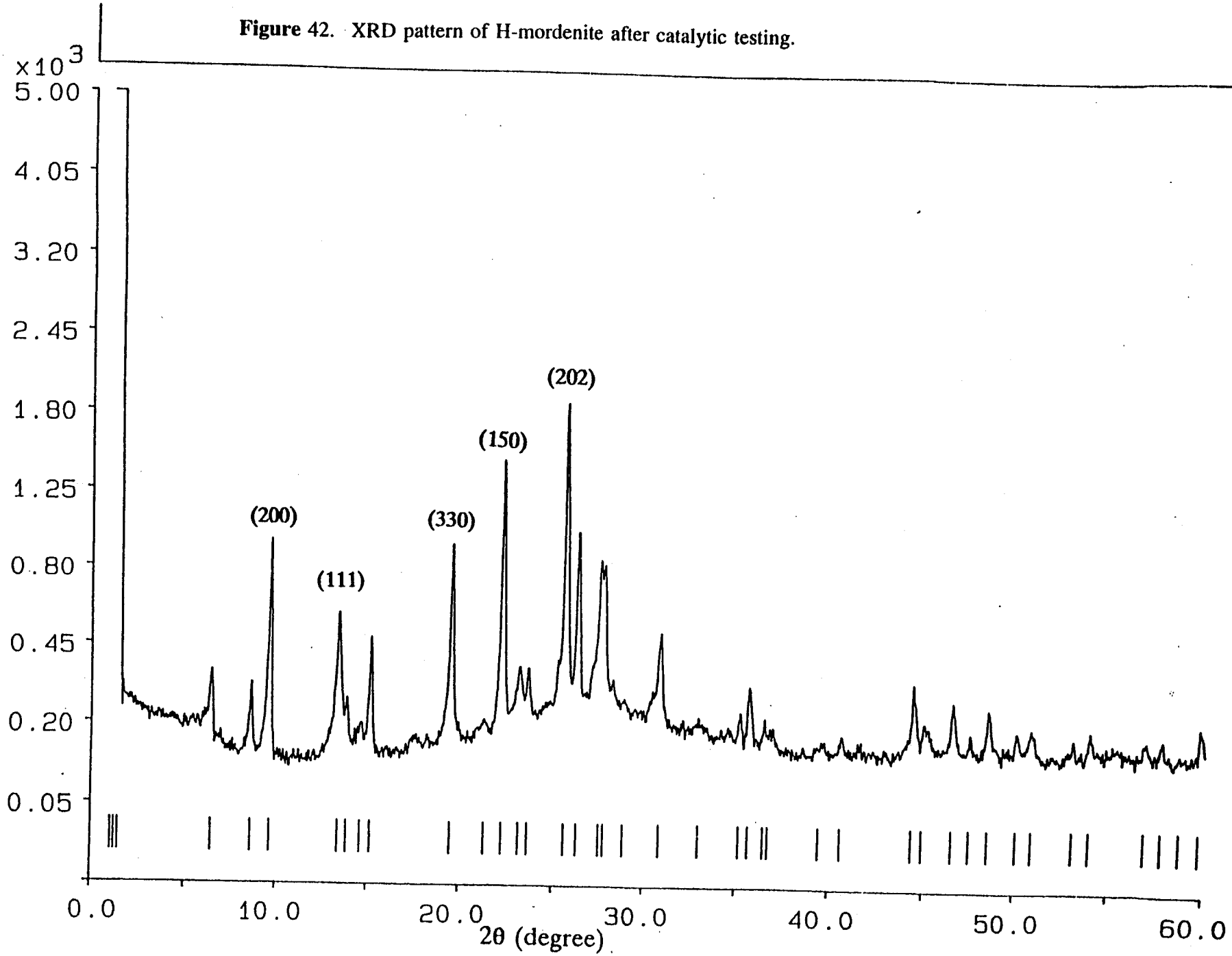

dimensional parameter extracted from the diffraction peaks is the full width at half of the maximum peak height (FWHM). It is evident from Figures 41 and 42 that there is no significant difference in FWHM, which indicates that the crystallite size of the mordenite had not changed significantly due to the catalytic testing. Absolute values have not yet been obtained for the crystallite sizes because of the uncertainty in the instrumental contribution to the linewidth.

Figures 43 and 44 show the XRD patterns of H-ZSM-5 zeolite before and after carrying out the catalytic alcohol coupling testing, respectively. The main diffraction peaks have been assigned according to data presented by Breck (34). The peaks were present in the same positions in both diffraction patterns, and there was no significant differences in the measured FWHM values. The intensity of the XRD pattern for the used H-ZSM-5 zeolite catalyst (Figure 44) was lower than for the fresh sample (Figure 43), again as expected if the used sample had some adsorbed amorphous material on the surface of the particles. These data indicate that profound changes in the zeolite structure had not occurred in terms of particle size or crystallinity due to the catalytic testing at elevated temperatures.

F. Scanning Electron Microscopy of H-Mordenite and H-ZSM-5 Zeolite

Objective

The objective of these analyses was to obtain information in regard to the sample morphology of the zeolite particles before and after the alcohol coupling reaction was carried out in the reactor system.

Experimental

Portions of the same catalysts that were utilized for the XRD analyses were used for

Figure 43. XRD pattern of H-ZSM-5 zeolite prior to catalytic testing.

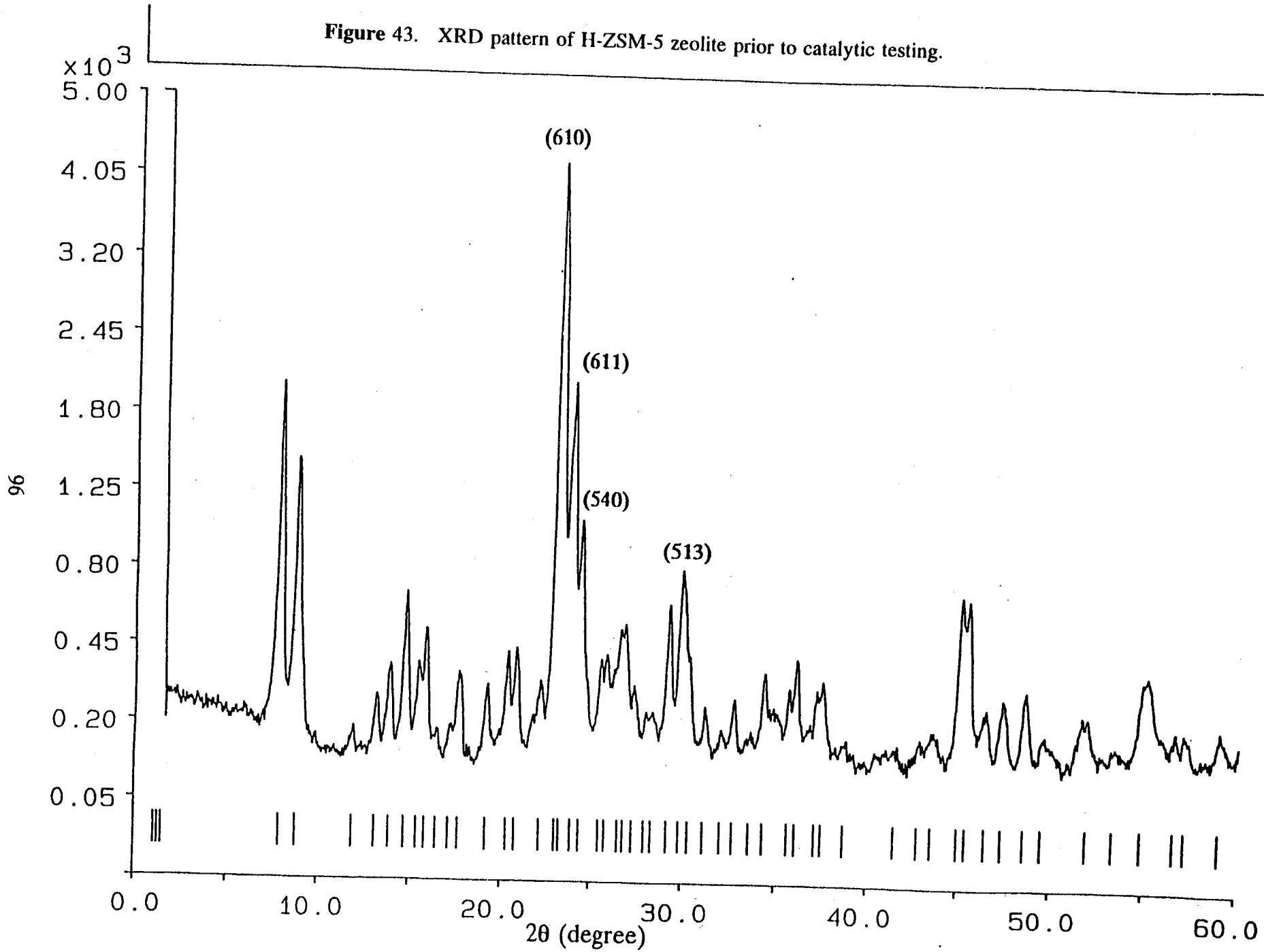

Figure 44. XRD pattern of H-ZSM-5 zeolite after catalytic testing.

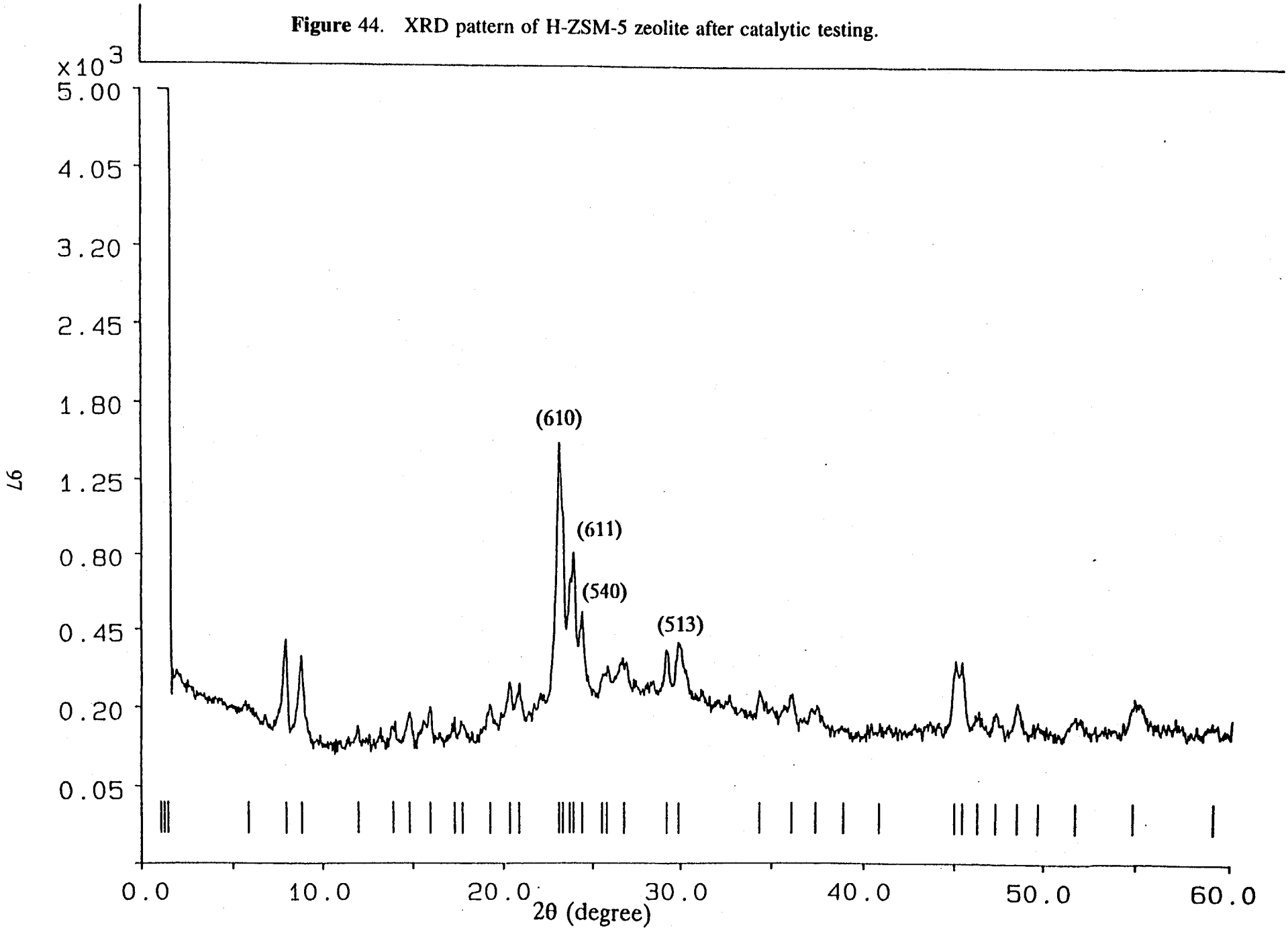

these microscopy studies. The instrument used was a Jeol JSM-6300F Scanning Microscope equipped with a field emission source. The vacuum in the sample chamber was kept at about $4 \cdot 10^{-7}$ torr.

Results

Figures 45a and 45b show electron micrographs of the H-mordenite catalyst before and after catalytic testing, respectively. It can be seen that there are small particles (≤ 1 μm), as well as larger agglomerates forming oval shaped beads. The catalytic testing at temperatures up to 150°C does not appear to have altered the particle size nor the distribution.

Figures 46a and 46b show the electron micrographs obtained with the H-ZSM-5 zeolite catalyst before and after reaction, respectively. The H-ZSM-5 zeolite exhibited a rather narrow particle size distribution compared to the H-mordenite catalyst. The catalytic testing at temperatures up to 175°C does not appear to have an effect on the H-ZSM-5 zeolite catalyst in terms of particle size or particle size distribution.

Figure 45a. Scanning electron micrograph of H-mordenite prior to catalytic testing. The magnification is 1,000 X and 10 mm equals 10 μm.

Figure 45b. Scanning electron micrograph of H-mordenite after catalytic testing. The magnification is 1,000 X and 10 mm equals 10 μm.

Figure 46a. Scanning electron micrograph of H-ZSM-5 zeolite prior to catalytic testing. The magnification is 1,000 X and 10 mm equals 10 μm.

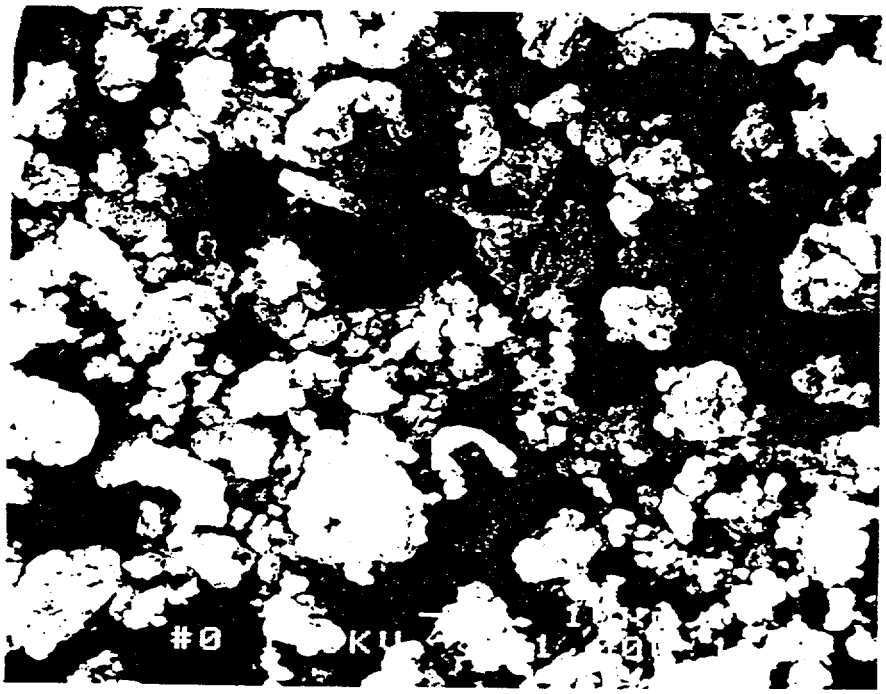

Figure 46b. Scanning electron micrograph of H-ZSM-5 zeolite after catalytic testing. The magnification is 1,000 X and 10 mm equals 10 μm.

G. Molecular Modelling of Alcohol Reactions in H-Mordenite

It has been shown in this report, e.g. see Tables 15 and 17, that mordenite, unique with respect to all other catalysts studied during this research project, was able to exclusively dehydrate methanol to dimethylether (DME), while leaving the isobutanol in the methanol/isobutanol = 1/1 reactant mixture unconverted at all but the highest temperature studied. At 150°C, 96.5% of the methanol was converted to dimethylether, while only 4.4% of the isobutanol was converted to butenes and dibutylethers.

The selective synthesis of DME was unexpected because H-mordenite is considered to be a large pore zeolite with channels of about 7 Å, while H-ZSM-5 is a medium pore zeolite with pores about 5.5 Å in diameter. The H-ZSM-5 zeolite, however, was found to be nonselective in this reaction and converted both methanol and isobutanol to many products at all temperatures studied, shown in Table 17. The extreme selectivity of H-mordenite in the reaction of the methanol/isobutanol mixture has been explored further *via* molecular modelling.

Table 17. Space Time Yields of the Products (mol/kg cat/hr) Formed Over H-Mordenite and H-ZSM-5 Zeolite from Methanol = Isobutanol = 1.72 mol/kg cat/hr Reactants in He/N_2 Carrier Gas at 0.1 MPa as a Function of Temperature.

	$T_{Reaction}$	DME	Butenes	MIBE	MTBE	C8 Ethers
H-Mordenite	90°C	0.060	------	------	------	------
	125°C	0.660	------	------	------	------
	150°C	0.830	0.068	------	------	0.004
H-ZSM-5 Zeolite	90°C	0.005	0.001	0.012	------	------
	125°C	0.071	0.169	0.350	0.004	0.003
	150°C	0.261	0.339	0.134	0.003	0.003
	175°C	0.185	1.086	0.131	0.005	0.002

H-ZSM-5 is a medium pore zeolite with interconnecting channels of the dimensions

5.3 × 5.6 Å and 5.1 × 5.5 Å. H-Mordenite is also a porous zeolite and has elliptical 7.0 x 6.5 Å channels (12-rings with openings crystallographical running in the c-direction). However, mordenite also has a system of small channels running perpendicular to the large channels (and running in the b-direction). These small channels are sometime said to consist of 3.7 x 4.8 Å channels because they have entrances of 8-ring openings (windows) of these dimensions. However, because of the mordenite structure, about 8 Å into each small pore there is a zig-zag Y-branching of the pore structure due to twisted 8-rings. This results in a distorted window to each side of the Y-branching of some 2.6 x 5.7 Å. This is a considerable restriction in the free diameter of the small channel pores through which reactant molecules can move, i.e. be transported to reactive sites in the small pores with subsequent diffusion of product molecules out of the small pores and the zeolite. The net result is that the mordenite structure is more realistically viewed as large channels having two rows of side *pockets*.

The main channels in H-mordenite are large and are accessible to isobutanol, which has a van der Waals diameter along the line joining the two methyl groups of 4.9 Å. The smaller interconnecting channel system of ZSM-5 zeolite is also accessible to isobutanol, but this oxygenate molecule is excluded from the smaller channel system of mordenite. Methanol, with a van der Waals diameter of 3.8 Å for the methyl group, has access to all channels to which isobutanol is accessible, as well as to the side pockets of mordenite.

Of interest here is the distribution of the active, strongly acidic protons in the H-mordenite. Using crystallography as a guide, it was found that the alkali ions (8 cations/unit cell) in dehydrated Na-mordenite (33) and Cs-mordenite (46) were the following: 1.5-2 in the large channels (designated as Type I), 2-3 in the 8-ring window openings to the small channel system (designated as Type II), and 3-4 inside the small channels (designated as

Types III). A ^{133}Cs NMR investigation located the Cs^+ ions at locations that were consistent with this crystallography (47). It may be assumed that the proton distribution in dry H-mordenite will be similar to those of the alkali cations, except for a shift of the protons to proximal oxygens to form OH species. The small channel protons can be located in the pocket pores on the side of the channels.

As pointed out previously, these pockets consist of an entrance 8-ring, a second parallel 8-ring at the distance of 3.5 Å from the first, and two fused oxygen 8-rings that form the bottom of the pocket. The pocket is 3.7 x 4.8 Å wide and ca. 8 Å deep, and two offset antiparallel pocket systems are wedged into each other, resulting in the ca. 2.6 Å constriction at the bottom of each pocket, to form the backbone structure surrounding the large channels. The cations located deepest in the pocket are symmetrically placed on the two sides of the bottom center oxygen of the pocket and are shared by pockets meeting at their bottoms from opposite sides. The pocket shape in mordenite resembles that of a chalice, or cup, from which the name of organic calixarenes of similar shape is derived. As the mordenite structure is made of channels surrounded by the fused cups, it could perhaps be appropriate to characterize this structure as inorganic crystalline polycalixarene.

The observed reaction selectivity whereby no isobutanol reacts in H-mordenite below 150°C, as shown in Table 17, indicates that the Type I acid sites located in the large channels are rendered unreactive. It is proposed that this poisoning of the most exposed acid sites occurs by the formation of a very strong complex between the Type I protons and isobutanol or its decomposition products. If these strong acid protons react with isobutanol to produce irreversibly bonded esters or carbenium ions or oligomeric species, they will be inaccessible for further steady state reactions with both alcohols, and only the protons located in the side pockets, which are accessible only to methanol, will be able to function

as active catalytic centers. No coke formation was observed at the reaction temperatures employed. It appears that at 150°C, the Type I acid sites begin to be regenerated, as indicated by the appearance of isobutene and C_8 ether.

The high selectivity of H-mordenite to DME at low temperatures appears to be due to a combination of selective poisoning of the large channel Type I protons by isobutanol and a size exclusion of isobutanol in reactions catalyzed by the Type III protons located in the side pockets. The role of Type II protons depends on their location. Functionally, they will act as Type I if located in the large channels and as Type III if placed inside the small channel pockets. Computer graphics have been used to model:

a. the entrance of methanol and isobutanol into the large channels and of methanol into the small channels and pockets,

b. formation of oxonium $CH_3OH_2^{\oplus}$ by reaction of methanol with the strongly acidic Type III protons,

c. S_N2 attack on this oxonium by a second methanol molecule to form DME, and

d. the exit of the DME from the small channels of the zeolite.

The cartesian coordinates of H-mordenite were obtained from the crystallographic literature (33,46). Utilizing the symmetry elements of the Cmcm space group, a large section of the zeolite was built from a limited data set. The Spartan software program from Wavefunction Inc. running on an IBM RISC 6000-based computer was used as a visualization program into which the calculated structure of H-mordenite was entered. With this implementation, the accessibilities of methanol and isobutanol molecules to potential acidic sites in the zeolite could be determined, including all of the geometries mentioned above.

In particular, it was found that methanol molecules had access to all possible proton sites in H-mordenite, especially the preferred sites in the side-pockets, Figure 47a, while these pocket sites were inaccessible to isobutanol molecules. The preferred orientation of

isobutanol in the large main channels of the zeolite is with its longest dimension parallel to those channels. Because the access to the side pockets is in a perpendicular direction to the main channels, isobutanol would have to rotate 90° in order to react with protonated methanol protruding from the side pocket Figure 47b. The computer models have shown this particular spatial configuration of the reactant molecules to be significantly strained with respect to van der Waals radii contact between isobutanol and the channel walls. This type of shape selectivity could be classified as restricted transition state selectivity. If this steric constraint were overcome and a molecule of MIBE were formed, there exists the additional larger spatial constraint of the larger MIBE molecule reorienting to its preferred trajectory through the main channels. Due to their much smaller sizes, the reactant methanol and product DME molecules do not have these impediments to reactions involving side pocket protons. It is proposed that the steric factors that the computer graphics model illustrated are important contributors to the absence of MIBE observed in the synthesis products, as well as the general lack of reactivity of isobutanol over H-mordenite.

The self-poisoning of Type I acid sites for isobutanol reactions at temperatures below 150°C occurs even in the absence of methanol, as demonstrated by separate experiments carried out here. At temperatures above 150°C, the reaction products that are formed from isobutanol in the presence and absence of methanol are the same except for DME and MIBE that contain methyl groups originating from methanol. The conversion rates of isobutanol are slightly higher in the absence of methanol as compared with methanol present, but the difference is small enough to permit the conclusion that the poisoning of Type I acid sites in the large channels is due to isobutanol only and not to preferential adsorption or reactions of methanol. This is consistent with the greater basicity of isobutanol as compared with methanol with which it competes for acid sites (16,17).

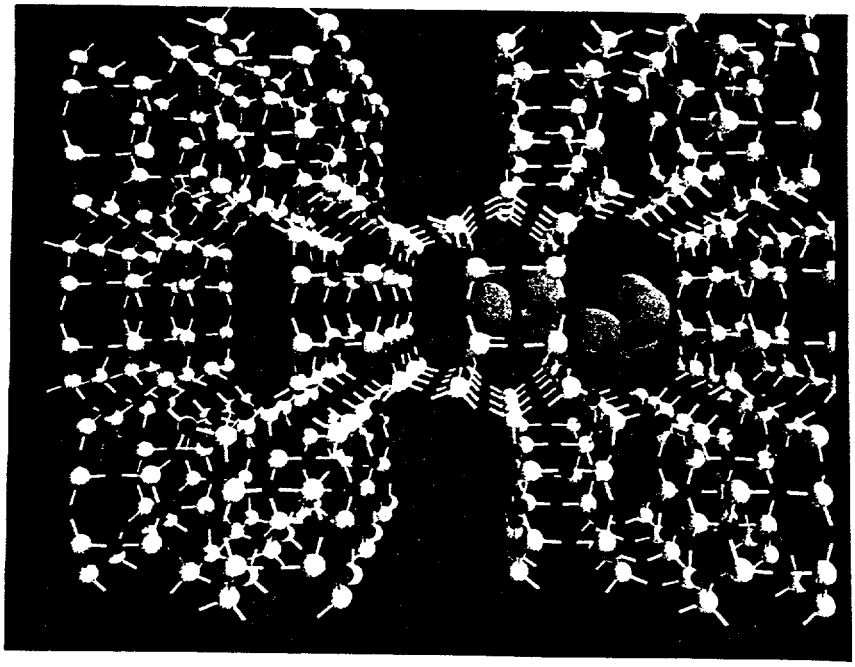

Figure 47a. Visualization of a methanol molecule in the main channel reacting with methoxonium ion in the side-pocket of H-mordenite.

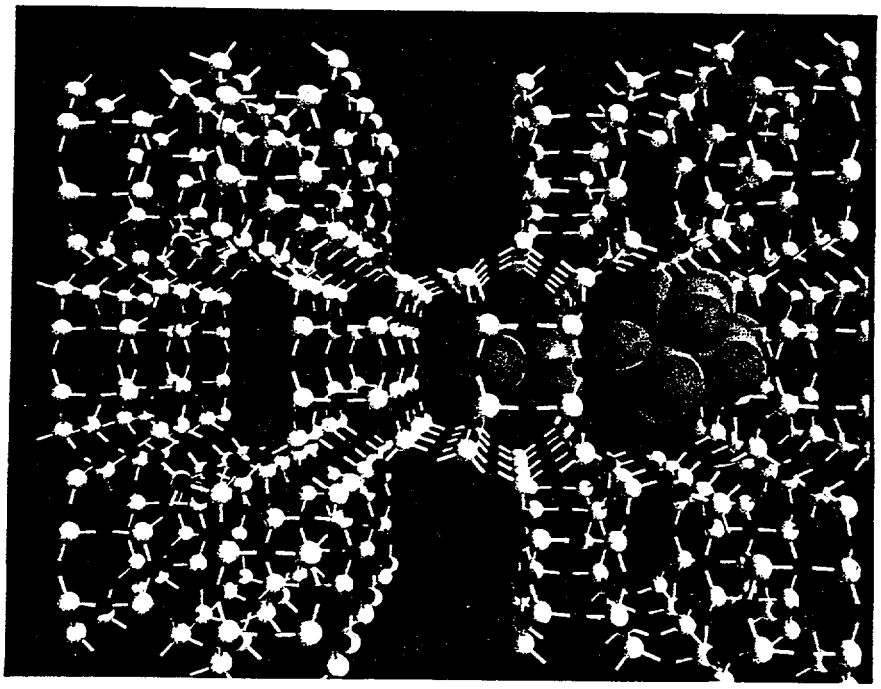

Figure 47b. Visualization of an isobutanol molecule in the main channel reacting with methoxonium ion in the side-pocket of H-mordenite. Note the size limitations of this orientation.

V. Extended Reactivity Studies Over the ZrO_2/SO_4^{2-} Catalyst

A. Alcohol Pressure Dependence on Product Selectivity

The effect of reactant pressure on the activity and selectivity of the dehydration of a 2:1 molar methanol and isobutanol mixture to butenes and ethers was studied. Nunan et al. had previously studied this reaction over Nafion-H (17). The reaction conditions chosen in the present study using ZrO_2/SO_4^{2-} as catalyst are similar to those of Nunan et al (17). To allow for kinetic analysis, the conversions were kept below 10%. The ZrO_2/SO_4^{2-} catalyst has very low activity at 116°C, and a very low space velocity was needed to induce appreciable conversion. The catalyst has high activity at 157°C and the space velocity was adjusted accordingly.

The following experimental conditions were used for the two reaction temperatures:

Temperature	116°C
Pressure (total)	0.1-7.1 MPa (1-70 atm)
Methanol feed	1.18 mol/kg catalyst/hr
Isobutanol feed	0.59 mol/kg catalyst/hr
He (+ N_2 trace) flow	20.94 mol/kg catalyst/hr
Catalyst weight	5.0 g
Temperature	157°C
Pressure (total)	0.1-6.3 MPa (1-62 atm)
Methanol feed	42.2 mol/kg catalyst/hr
Isobutanol feed	21.1 mol/kg catalyst/hr
He (+ N_2 trace) flow	756 mol/kg catalyst/hr
Catalyst weight	2.0 g

Figures 48 and 49 show the space time yields of the major products under the conditions given above as a function of total alcohol partial pressure, which was increased stepwise by sequentially increasing the reactor pressure. The results at 116°C exhibit more scatter than those at 157°C, but the trends seen are the same. It is evident that isobutene production was strongly pressure dependent, decreasing with increasing alcohol pressure. Ether production was only moderately pressure dependent, increasing somewhat with

Figure 48. Effect of alcohol partial presssure on product productivities for the reaction of methanol/isobutanol = 1/1 over the ZrO_2/SO_4^{2-} catalyst at 116°C.

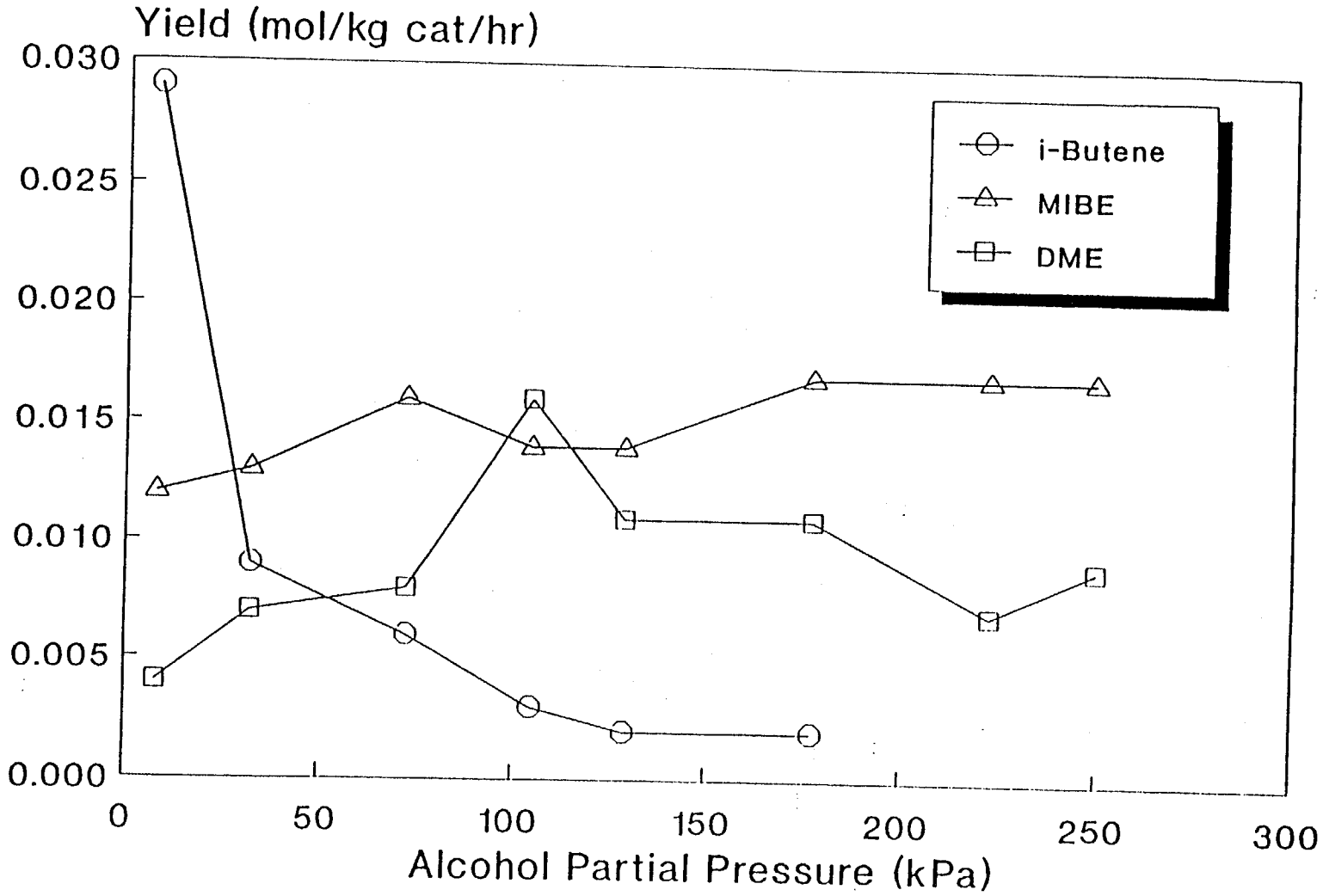

Figure 49. Effect of alcohol partial presssure on product productivities for the reaction of methanol/isobutanol = 1/1 over the ZrO_2/SO_4^{2-} catalyst at 157°C.

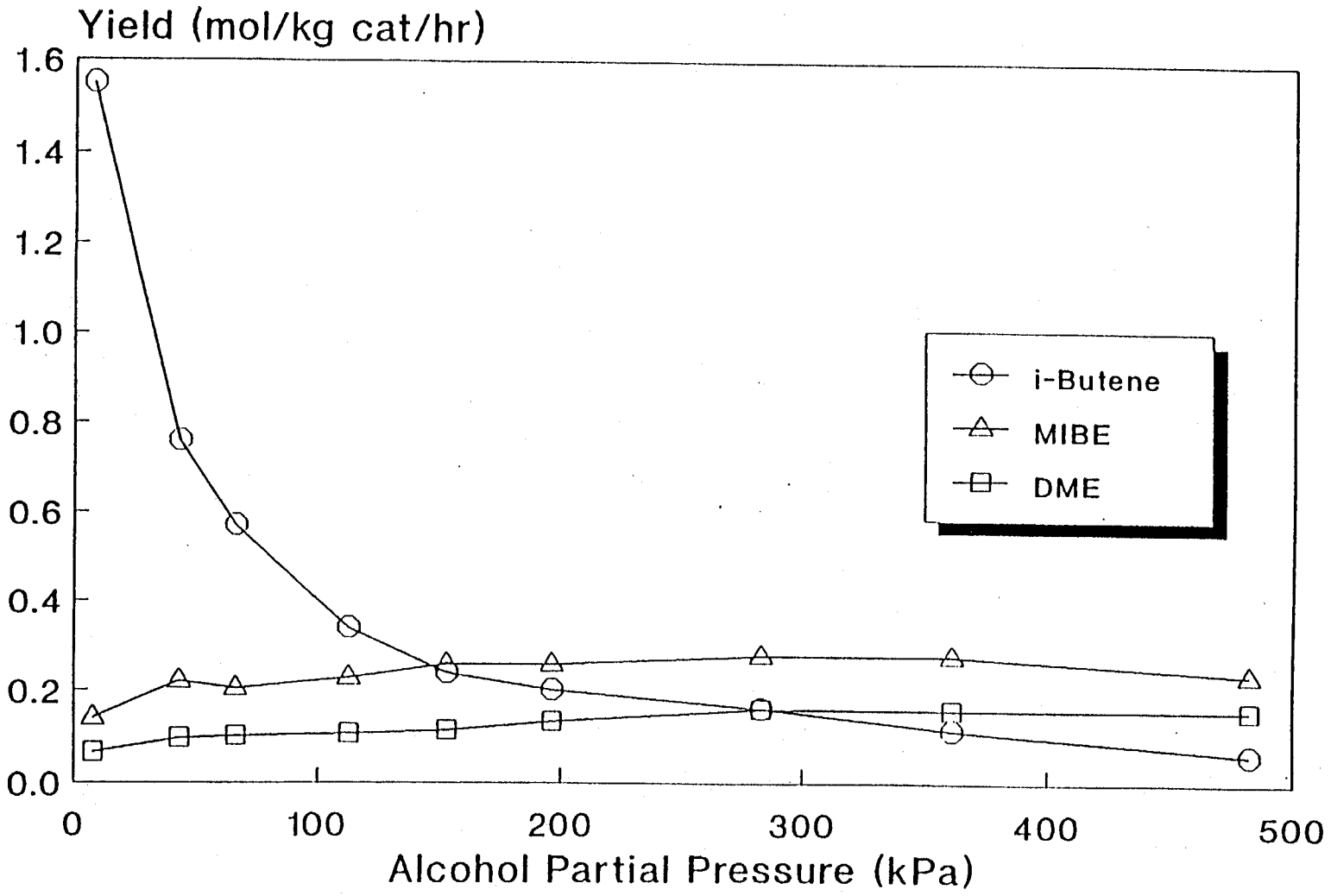

increasing alcohol pressure. Both the isobutene decrease and ether increase appear to level off to steady values. These results are similar to those observed with the Nafion-H resin catalyst (17). This suggests that the same catalytic functions and properties exist for the reaction over ZrO_2/SO_4^{2-} as was observed over Nafion-H. This pressure effect was found to be reversible in a separate experiment using fresh catalyst, i.e. when the alcohol pressure was decreased to its original value, isobutene production increased and ether production decreased to their original rates. This work also showed that the selectivity toward isobutene, which was seen previously with a 1/1 methanol/isobutanol mixture, also holds for the 2/1 methanol/isobutanol mixture used in this study at low pressures.

It is apparent from Figures 48 and 49 that low pressures are needed to maximize the selective dehydration of isobutanol to isobutene while leaving the methanol relatively unconverted. The reaction was kept far from equilibrium, and thus the effect of increasing pr essure on the reaction rate was purely a kinetic effect and not a thermodynamic one. It is also evident from Figure 50 that low temperatures are needed when pathways exist (*via* carbenium ion chemistry with Brönsted acids) for the formation of linear butenes in order to minimize the linear butenes and maximize the proportion of isobutene in the product stream. Figure 50 shows that below 150°C, i.e. the temperature range of interest, the equilibrium yield of 1-butene would be small compared to the 2-butenes.

B. Reaction of Methanol/Isobutanol Mixture over ZrO_2/SO_4^{2-} *vs* Contact Time

The kinetic studies of the methanol/isobutanol reaction over the ZrO_2/SO_4^{2-} catalyst presented above are complemented here with a study investigating the effect of contact time on the conversion and selectivity of the major reactions. The following conditions were used in these studies:

Figure 50. Equilibrium distribution of Butene isomers.

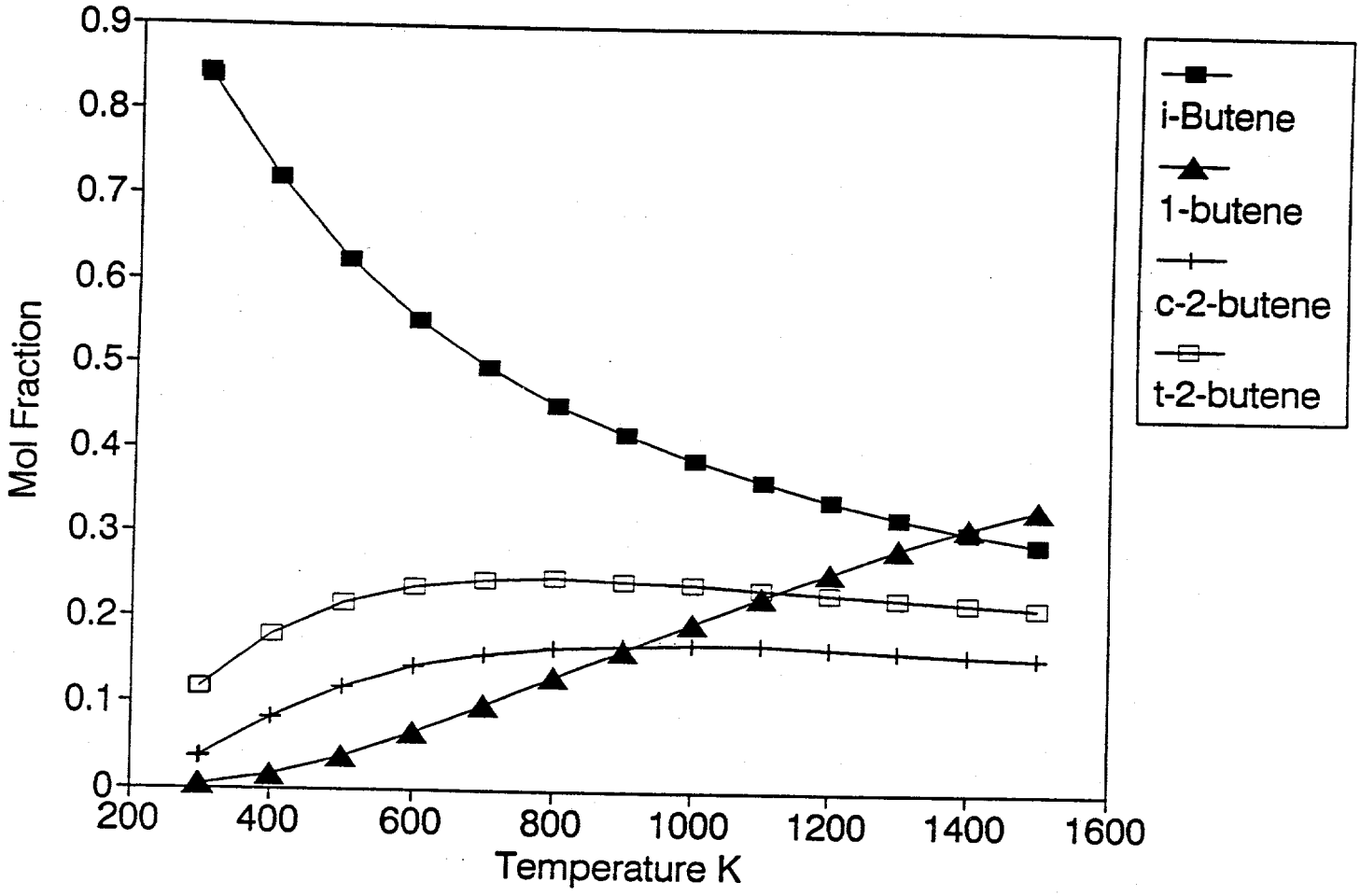

Temperature	157°C
Pressure (total)	0.1 MPa
Methanol feed	13.8-123.3 mol/kg catalyst/hr
Isobutanol feed	6.92-61.6 mol/kg catalyst/hr
He (+ N_2 trace) flow	245.2-2,207 mol/kg catalyst/hr
Zr_2/SO_4^{2-} weight	0.25 g.

The reactant mixture was a 2/1 molar MeOH/i-BuOH mixture, and the partial pressure of the alcohols was kept constant throughout the experiment by altering the space velocity of the inert gas feed (containing N_2 as an internal standard) proportionally to that of the alcohols. In the usual manner, a fresh ZrO_2/SO_4^{2-} sample calcined to 620°C was charged into the reactor, the gas flow rates were adjusted, and the reactor was brought to the reaction temperature. The experiment started with the highest space velocities, which were sequentially lowered. Product analysis at each space velocity was the average of multiple sampling at each point. The contact times were defined as 1/GHSV. The space velocity has been converted from mol reactant/(kg cat. hr) to STP liter of reactant gas/(liter catalyst × min) *via* the ideal gas equation and assuming that the volume of 1 kg catalyst = 1 liter.

Figure 51 shows the percent conversion of isobutanol *vs* the contact time. A linear relationship existed over the entire range tested, indicating that reaction studies within this range of contact times were within the kinetic regime. The kinetic data lie well within the bounds of the kinetic regime, thus establishing that kinetic interpretation of the data is valid.

The butene product selectivity as a function of contact time is presented in Figure 52. It is clear that isobutene was the predominant butene formed, and it was produced at a higher percentage, i.e. 86-88 mol%, than that calculated for thermodynamic equilibrium, ca. 70%, at the reaction temperature of 157°C, Figure 50. It is also interesting to note that the selectivity of *cis*-2-butene is now comparable to, or even greater than, that of the *trans*-2-

Figure 51. Contact time dependence of the reaction of methanol/isobutanol = 2/1 over the ZrO_2/SO_4^{2-} catalyst at 157°C.

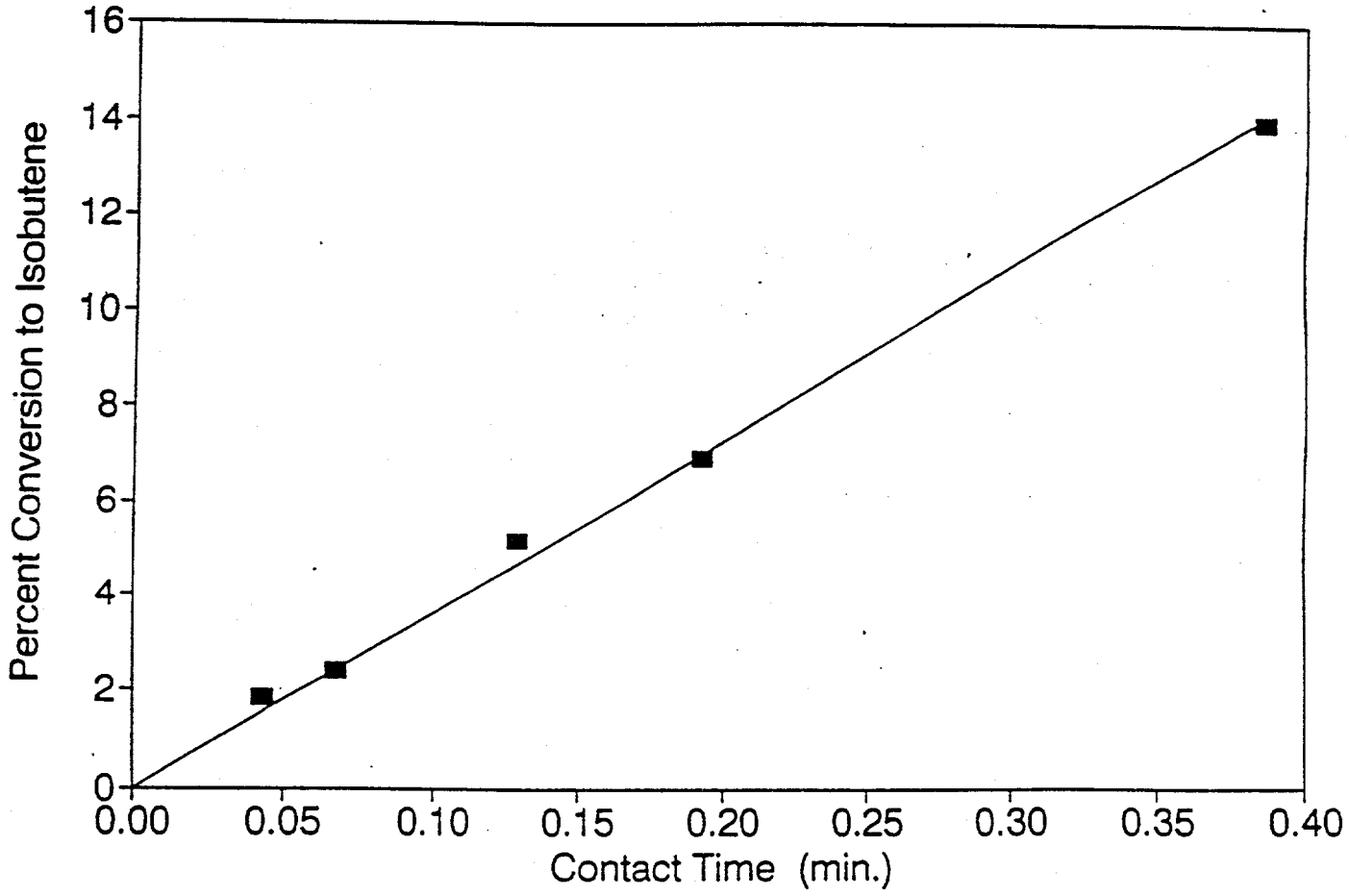

Figure 52. Butene product selectivity of the reaction of methanol/isobutanol = 2/1 over the ZrO_2/SO_4^{2-} catalyst at 157°C.

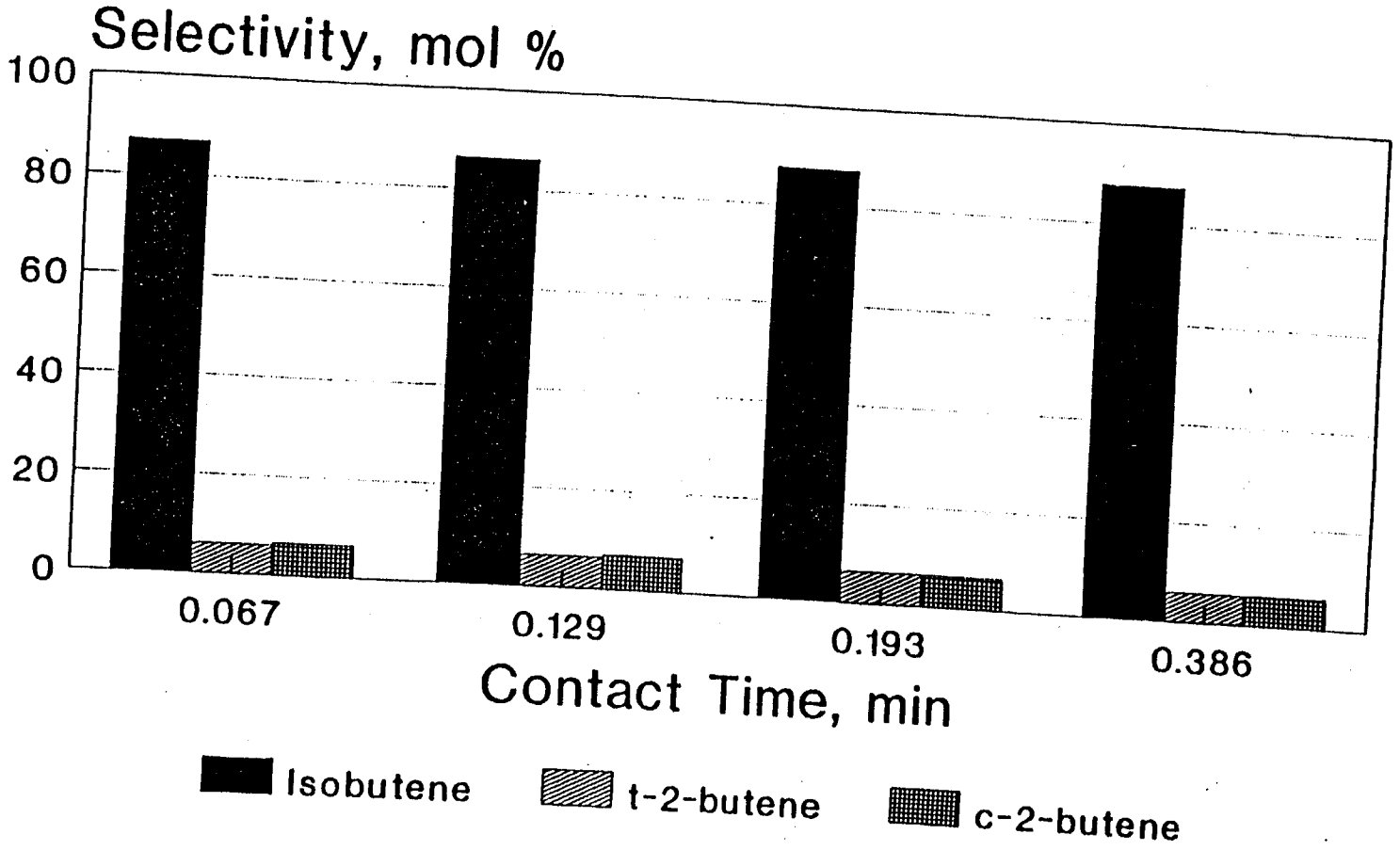

butene product, in contrast to the relative yields expected from equilibrium considerations (48). In addition, the composition of butenes with respect to selectivity remains constant over the range of contact times, and thus conversion levels of isobutanol, studied. This indicates that the linear butenes are also primary products and not the result of secondary isomerization of the isobutene produced in the reaction, in accordance with other studies (49).

C. Effect of Isobutanol Pressure on Mixed Alcohol Dehydration

The effect of increasing isobutanol pressure while maintaining the methanol partial pressure constant was investigated. Each alcohol flow was controlled with separate pumps. The following experimental conditions were used:

Temperature	157°C
Pressure (total)	0.1 MPa
Methanol feed	42.5 mol/kg catalyst/hr
Isobutanol feed	5.41-216.4 mol/kg catalyst/hr
He (+ N_2 trace) flow	778.3 mol/kg catalyst/hr
Zr_2/SO_4^{2-} weight	0.40 g

Figure 53 presents the space time yields of the major products of the mixed alcohol dehydration. As the pressure of isobutanol was increased, the production of isobutene and MIBE initially increased, but at higher isobutanol pressures they tended to decrease. DME tended to decrease consistently as the isobutanol pressure increased.

D. Pressure Dependence of Methanol Dehydration

To complete the alcohol pressure dependence study on sulfate-modified zirconia, methanol was utilized as the reactant in the absence of isobutanol. The following experimental conditions were used:

Figure 53. Space time yields of products as a function of isobutanol pressure over the ZrO_2/SO_4^{2-} catalyst at 157°C and 0.1 MPa total pressure.

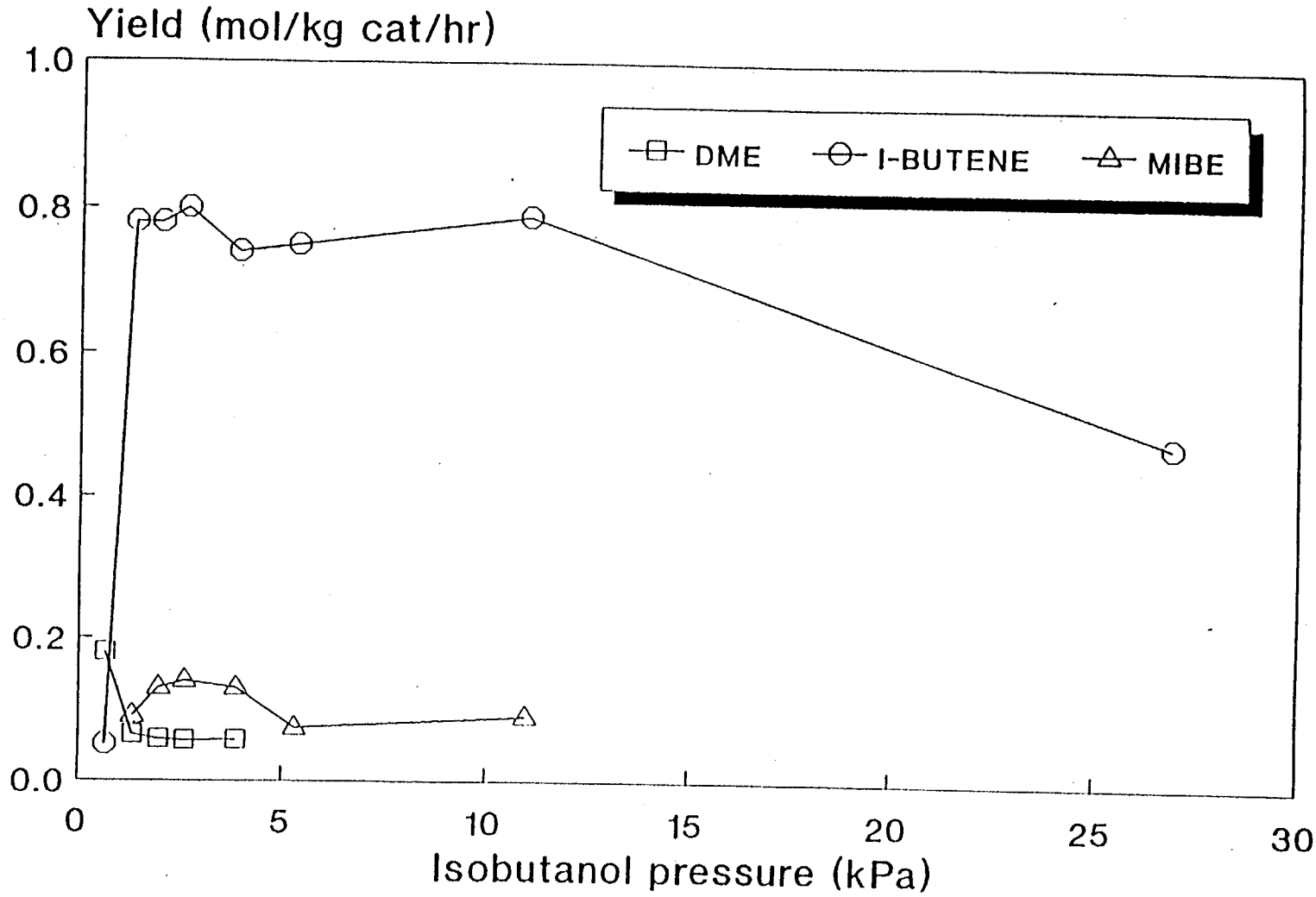

Temperature	157°C
Pressure (total)	1-7 MPa
Methanol feed	42.2 mol/kg cat/hr
He (+N_2 trace)	776.4 mol/kg cat/hr
Zr_2/SO_4^{2-} weight	0.40 g

Figure 54 presents the space time yield of dimethyl ether (DME). It is clear that increasing the methanol pressure favored an increase in the dimethylether (DME) formation rate. The productivity of DME was in general higher when no competition with isobutanol was present. Upon returning to the original partial pressure of methanol, only minor deactivation of the catalyst was seen.

E. Pressure Dependence of Isobutanol Dehydration

The effect of pressure on the dehydration of isobutanol over ZrO_2/SO_4^{2-} in the absence of methanol was investigated. The following experimental conditions were used:

Temperature	157°C
Pressure (total)	0.1-3.04 MPa (1-30 atm)
Isobutanol feed	21.1 mol/kg catalyst/hr
He (+ N_2 trace) flow	800.7 mol/kg catalyst/hr
Catalyst weight	0.40 g

Figure 55 presents the space time yields of the major products of isobutanol dehydration, mostly isobutene and some *cis*- and *trans*-2-butene, as a function of isobutanol pressure. It is apparent that the isobutene production was strongly dependent on isobutanol pressure. As in the case of the dehydration reaction in the presence of methanol above, the formation of isobutene decreased with increasing alcohol pressure.

F. Dehydration of Isobutanol Only Over ZrO_2/SO_4^{2-}

The activity and selectivity of dehydrating isobutanol over the ZrO_2/SO_4^{2-} catalyst in the absence of methanol was investigated further. The activity and selectivity of the

Figure 54. Space time yields of products as a function of methanol pressure over the ZrO_2/SO_4^{2-} catalyst at 157°C, in the absence of isobutanol.

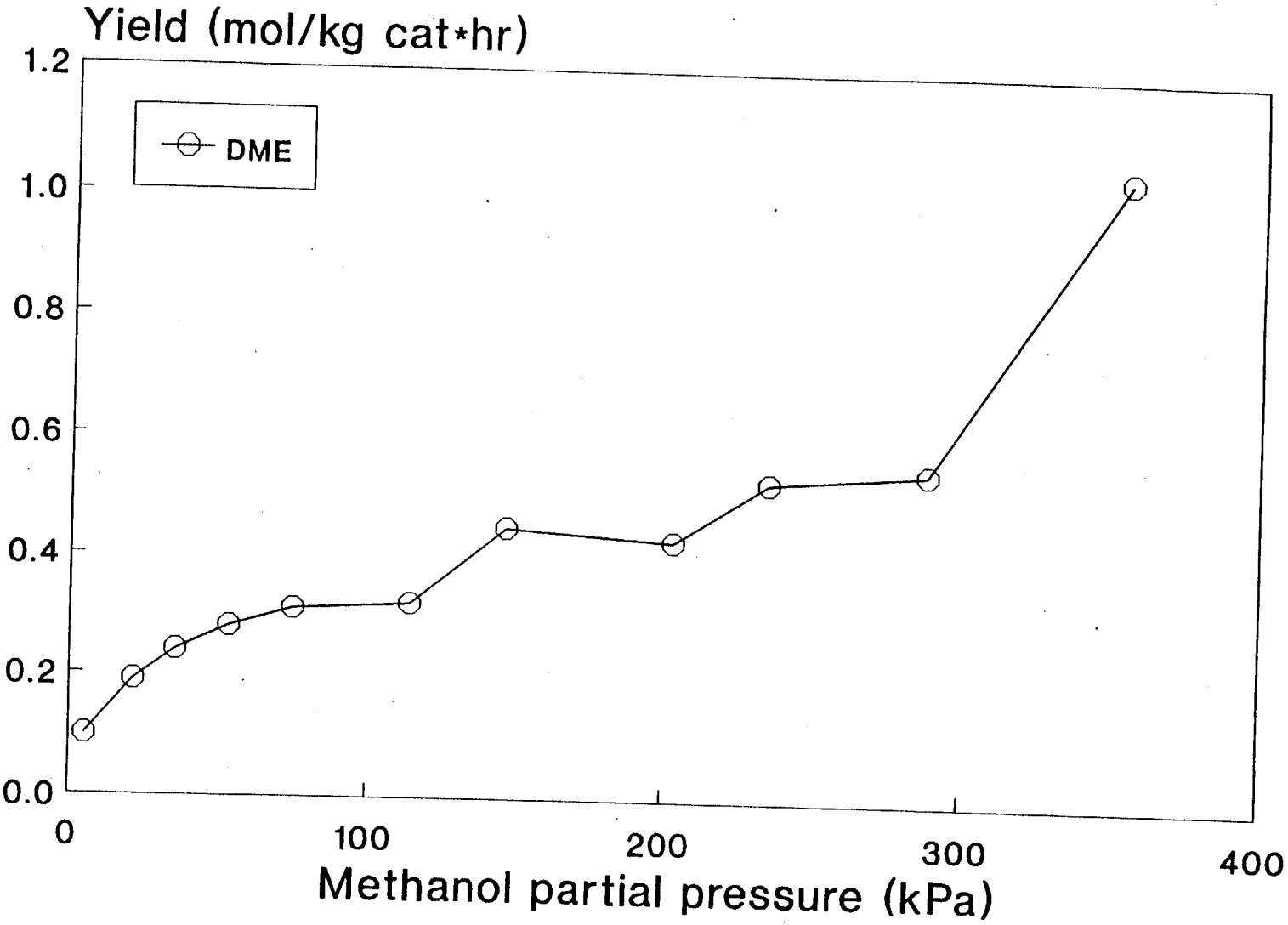

Figure 55. Space time yields of products as a function of isobutanol pressure over the ZrO_2/SO_4^{2-} catalyst at 157°C at 0.1-3.04 MPa, in the absence of isobutanol.

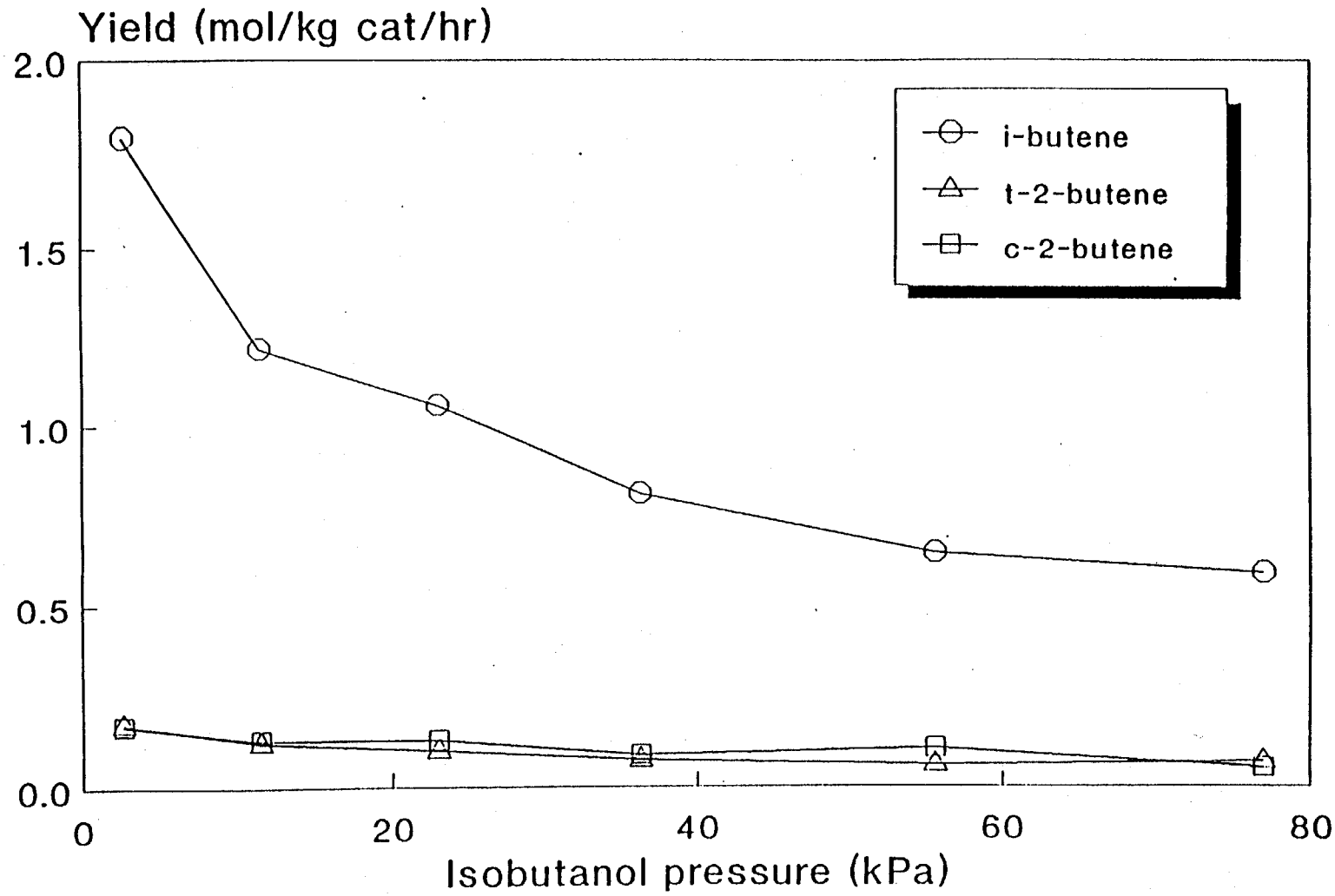

catalysts for isobutanol dehydration were obtained with respect to reaction temperature and reactant space velocity.

The ZrO_2/SO_4^{2-} catalyst calcined to 620°C was placed in the reactor and the following reaction conditions were utilized during the course of the investigation:

Temperature	125, 135, 150, 175, 200, 225°C
Pressure	0.1 MPa
Isobutanol feed	1.69-20.28 mol/kg catalyst/hr
He + N_2 flow	18.78 mol/kg catalyst/hr
Catalyst weight	5.0 g.

The isobutanol space velocity of 1.69 mol/(kg cat. hr) was used in an initial temperature dependence study from 125 to 175°C. At the temperature of 200°C, the isobutanol flow rate was raised sequentially to 6.76, 13.52, and 20.28 mol/(kg cat. hr). A final test was performed at 225°C using 20.28 mol/(kg cat. hr) of isobutanol. Testing was carried out for several hours at each point of temperature and space velocity. The only major products observed with the on-line GC analysis were isobutene, *trans*-2-butene, and *cis*-2-butene, while trace amounts of octenes and C_8 ethers were seen. At higher reaction temperatures, methanol and other products believed to be cracking products of isobutanol were seen, as was also observed for isobutanol dehydration over H-mordenite.

The yields of the major products under these conditions are presented in Figures 56A-56C. It can be seen that the predominant product was isobutene in each case and that high activity was achieved at 175°C while maintaining the high selectivity to isobutene (Figure 56A). As the temperature was increased from 125°C to 175°C, the total isobutanol conversion progressively increased from 13 to 85 mol% while the isobutene selectivity varied from 86 to 79 mol%. Increasing the space velocity of the isobutanol (Figure 56B) increased the yield of isobutene while also maintaining the isobutene selectivity at 80-81 mol%. The highest productivity of isobutene of 11.35 mol/(kg cat. hr) was obtained at 225°C and a flow

Figure 56a. Space time yields of products for the dehydration of isobutanol only over the ZrO_2/SO_4^{2-} catalyst as a function of temperature.

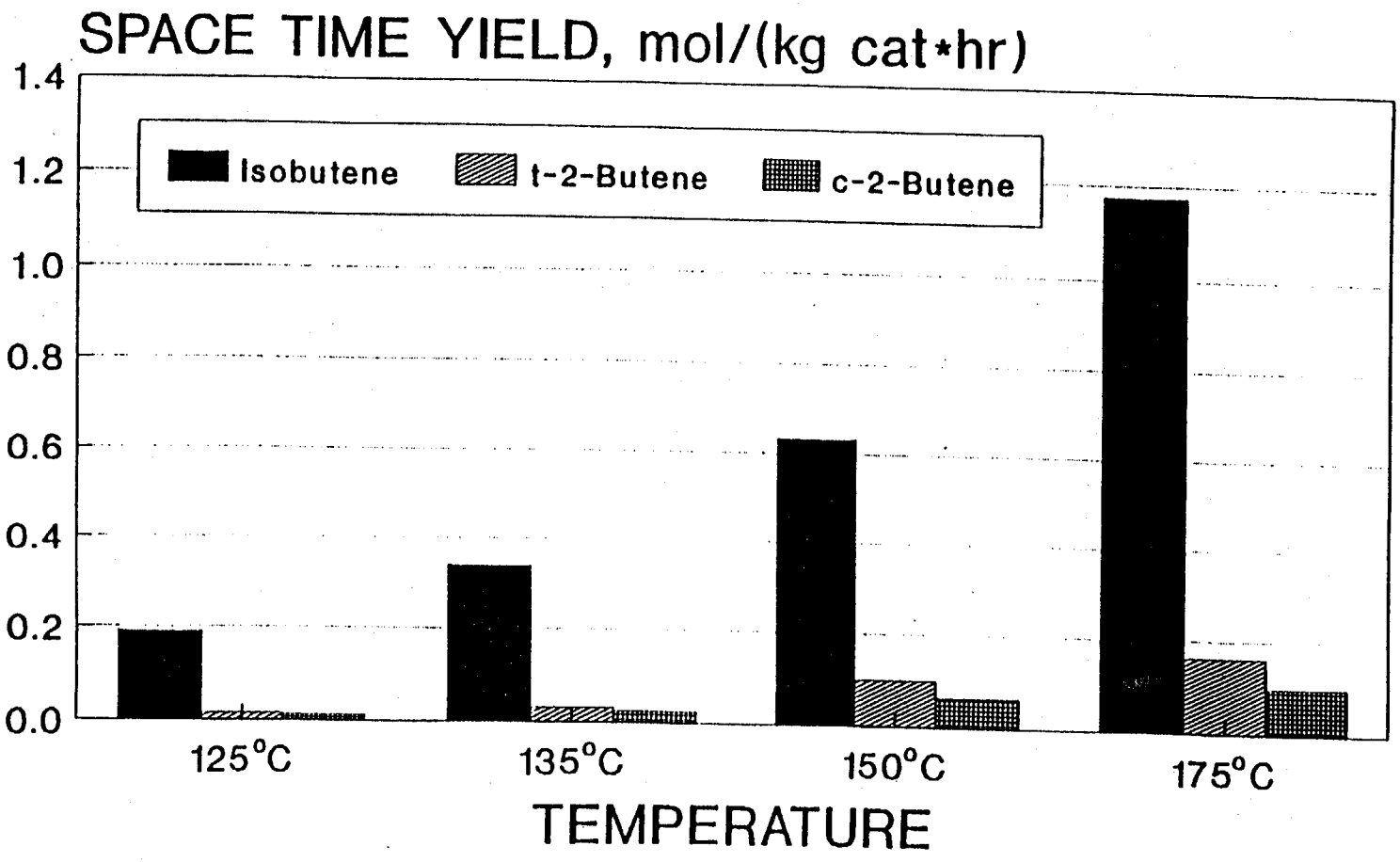

Figure 56b. Space time yields of products for the dehydration of isobutanol only over the ZrO_2/SO_4^{2-} catalyst as a function of gas hourly space velocity at 200°C.

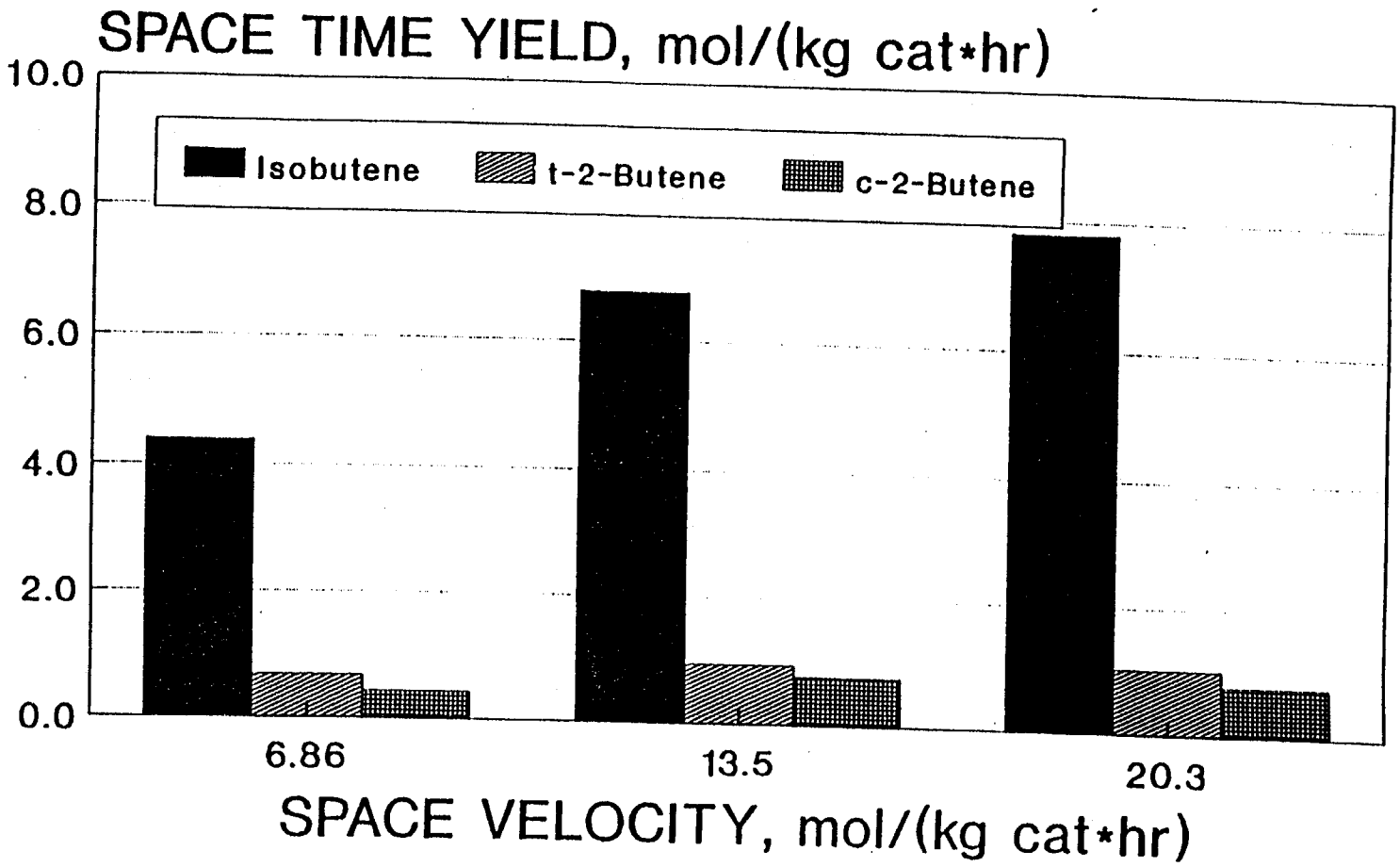

Figure 56c. Space time yields of products for the dehydration of isobutanol only over the ZrO_2/SO_4^{2-} catalyst at 200°C; isobutanol feed = 20.69 mol/kg cat/hr.

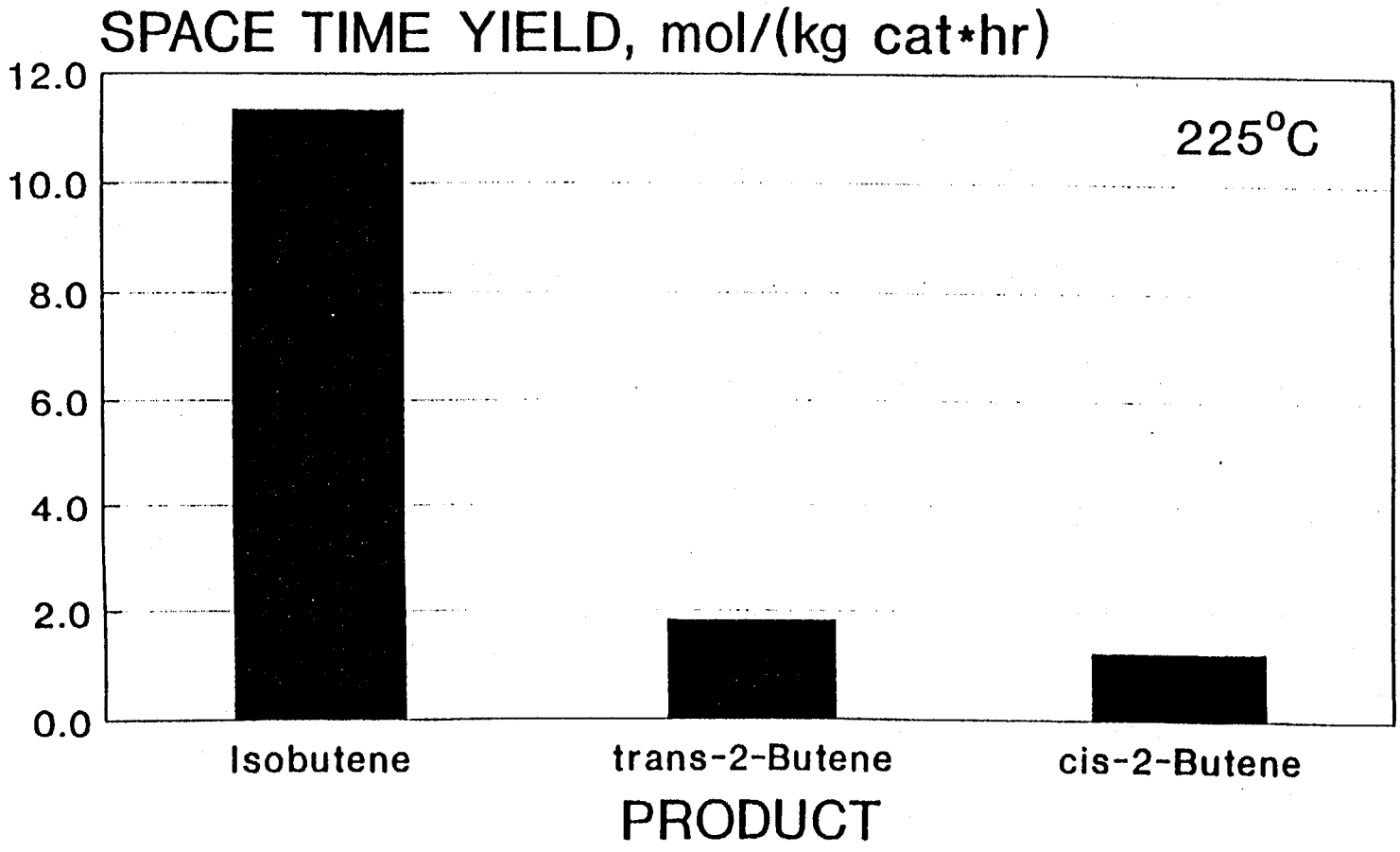

rate of 20.28 mol isobutanol/(kg cat. hr), as shown in Figure 56C. In this case, the selectivity of isobutene among the butenes at this high productivity was 79%. This space time yield can be compared with the highest reported value of isobutanol production from synthesis gas, which is claimed to be 10 mol/(kg cat. hr) (50). Thus, the dehydration of isobutanol to isobutene would not be a limiting step in an overall process of converting synthesis gas to MTBE.

G. Dehydration of Primary Alcohols Over the ZrO_2/SO_4^{2-} Catalyst

In order to compare the ability of the 1% SO_4^{2-}/ZrO_2 catalyst to dehydrate linear alcohols with the dehydration of isobutanol to isobutene, a series of alcohols was individually passed over the catalyst under the usual standard reaction conditions that include an alcohol feed rate of 1.72 mol/kg catal/hr. In this series, the dehydration behavior of isobutanol can be compared with those of the linear primary C_2-C_4 alcohols, i.e. ethanol, n-propanol, and n-butanol. The conversion levels obtained at 157°C are shown in Figure 57. It is evident that the highest activity was shown by the isobutanol reactant and that an appreciably greater quantity of isobutanol was converted to isobutene than observed for the conversion of n-butanol to 1-butene. These results indicate that with a mixture of alcohols over this catalyst, the predominant initial reaction will be dehydration of isobutanol to isobutene, which then could subsequently couple with the other alcohols in the reactant mixture.

H. The Effect of Water on Reaction of MeOH/i-BuOH Over ZrO_2/SO_4^{2-}

A major product of any conversion of the methanol/isobutanol mixture over solid acid catalysts is water. The presence of water can influence the type of acid sites present, e.g. it can in principle convert Lewis acid sites into Brönsted acid sites. In addition, water may also retard the reaction, as was reported for alumina earlier in this report. This latter

Figure 57. Conversion of primary alcohols over the ZrO_2/SO_4^{2-} catalyst at 157°C, alcohol feed rate = 1.72 mol/kg cat/hr.

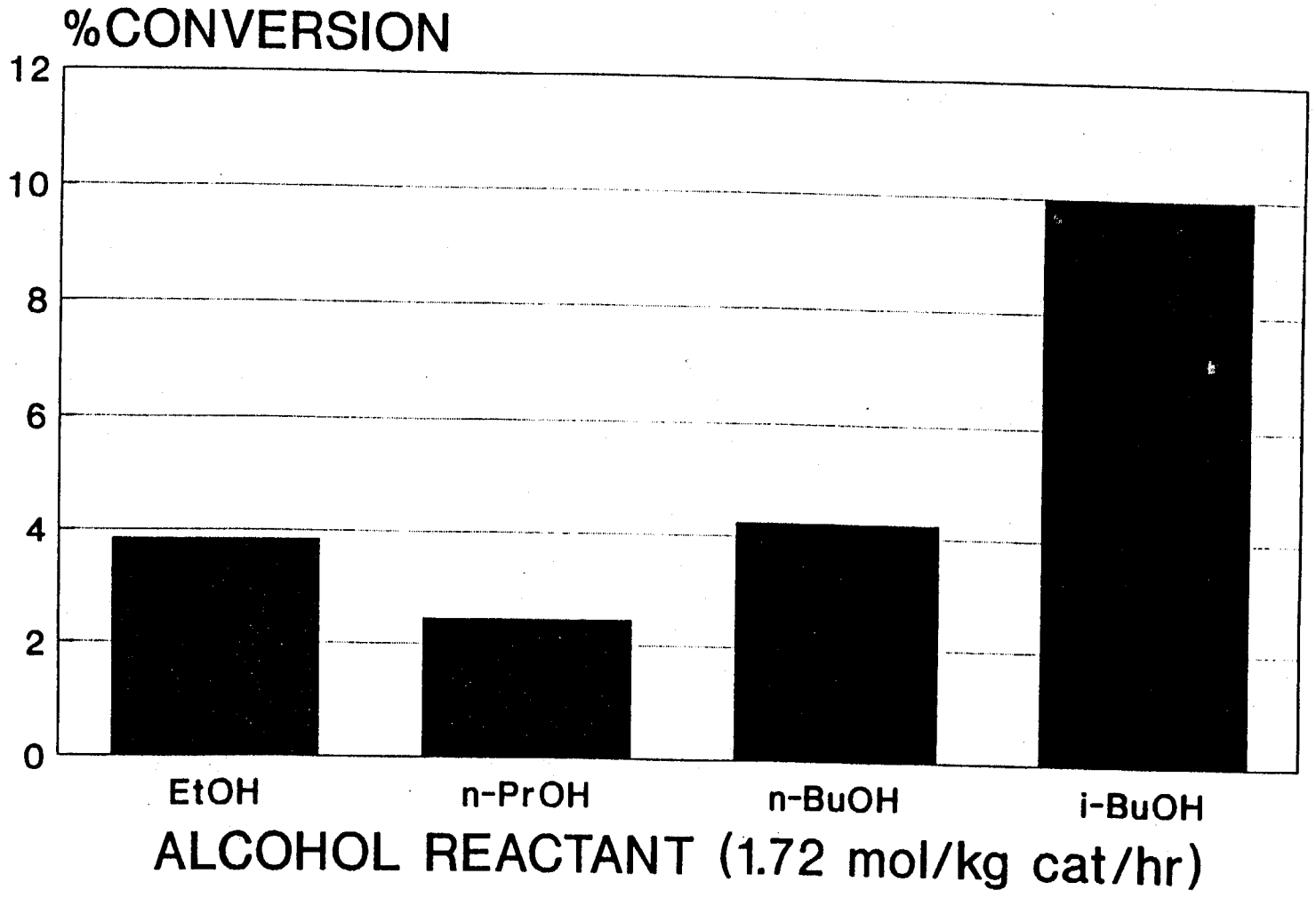

effect may arise from competitive adsorption of water and partial blockage of active sites. In the present experiment, reaction conditions were chosen where a 2/1 mixture of MeOH/i-BuOH was reacted over a 1% SO_4^{2-}/ZrO_2 catalyst at 157°C and 0.1 MPa within the differential regime as described previously. Specifically, the conditions were:

Temperature	157°C
Pressure	0.1 MPa
Water feed	0, 1.08, 2.16 mol/kg catalyst/hr
Methanol feed	43.3 mol/kg catalyst/hr
Isobutanol feed	21.6 mol/kg catalyst/hr
He + N_2 flow	762 mol/kg catalyst/hr
Catalyst weight	0.4 g

The catalyst was first exposed to the dry 2/1 MeOH/i-BuOH mixture, then to a MeOH/i-BuOH/H_2O = 2/1/0.05 mixture, followed by a 2/1/0.1 mixture. The feed was again switched to the dry 2/1 mixture and then back to the 2/1/0.1 MeOH/i-BuOH/H_2O mixture. The results of this experiment are shown in Figure 58. The high gas hourly space velocity (GHSV) of the carrier gas ensured low conversion levels of the reactants, e.g. at 100 hr on stream the conversion of isobutanol to products was about 4 mol% (≈3.7 %yield of isobutene). It can be seen from Figure 58 that the catalyst gradually and steadily deactivated with time on stream. However, the presence or absence of water in the feed under the reaction conditions employed did not affect the productiviry or selectivity of the products, which consisted mainly of isobutene.

Another experiment with a fresh catalyst was carried out wherein the catalyst was first exposed to the water-containing reactant mixture and then to the dry alcohol reactant mixture. No difference in the lack of a water-induced effect from the previous experiment was observed. These results differ from those observed earlier for alumina, where a strong inhibition, *ca.* 30%, in the production of DME, MIBE, and isobutene was noted. Those

Figure 58. Effect of water feed on reaction of methanol/isobutanol = 2/1 over the ZrO_2/SO_4^{2-} catalyst at 157°C and a total pressure of 0.1 MPa.

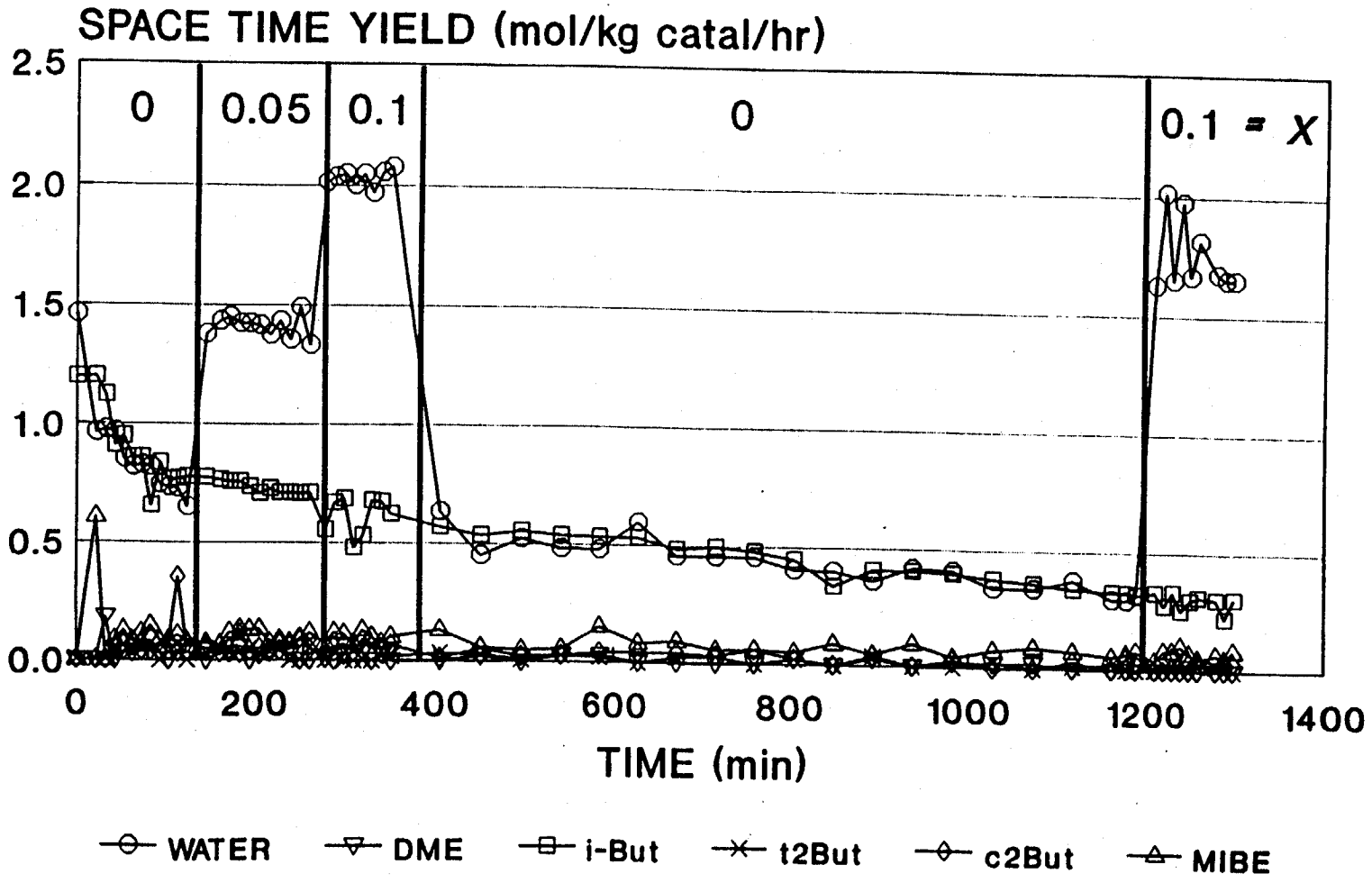

MeOH/i-BuOH/H_2O = *2/1/x* molar ratio

results with alumina were explained with the knowledge that alumina is known to possess strong acidity only in the form of Lewis acid sites that depend in number and strength on the degree of hydration of the surface. In the case of ZrO_2/SO_4^{2-}, however, Arata (51) has proposed that Lewis acid sites can be converted to strong Brönsted acid sites upon exposure to low partial pressures of water, e.g. 5 torr. In the present investigation, in the "dry" runs where the only water present was that formed as a product of the reaction, the partial pressure of water was less than 1 torr. In the "wet" runs, the partial pressure of water was about 3 torr. Under high conversion conditions, however, the water produced during reaction can reach rather high levels. This test showed that water did not suppress activity nor did it increase activity by creating additional Brönsted sites in the reaction environment utilized in this experiment.

VI. Characterization of the ZrO_2/SO_4^{2-} Catalyst

A. Surface Area of the ZrO_2/SO_4^{2-} Catalyst

The surface areas of the samples were determined by applying the BET/method of analysis at $p/p_o = 0.3$, where p = equilibrium pressure and p_o = the vapor pressure of N_2 at the temperature of the experiment (-196°C). First, the samples were degassed in a helium flow at 250°C, which in general took 30-45 min, depending on the sample size, where the sample weight ranged from 0.03 to 0.3 g. After the degassing procedure was completed, a helium/nitrogen gas mixture was allowed to pass over the sample. Adsorption of nitrogen occurred when the sample container was immersed in liquid nitrogen. The amount of N_2 adsorbed was monitored by measuring the decrease of nitrogen in the helium/nitrogen mixture, as determined by a thermal conductivity detector (TCD). After the adsorption of nitrogen was completed, the liquid nitrogen used for cooling was removed. Upon removal of the coolant, the adsorbed nitrogen started to desorb from the sample. The amount desorbed was also monitored by a TCD.

Calibration of the TCD was performed by injecting a known amount of pure nitrogen gas. It should be noted that this procedure is a single point determination which is not as good as a multipoint determination but usually gives a good approximation of the surface area.

Surface area was determined for non-sulfated zirconia calcined at 620°C and for sulfated zirconia calcined at 100 and 620°C, the results are given in Table 18. The addition of sulfate groups to zirconia dramatically increased the surface area. However, the surface area for sulfated zirconia was strongly dependent on the calcination temperature. Sulfated zirconia has been reported to have a surface area of 65-85 m^2/g (1). Our result, 60.2 m^2/g, is in good agreement. Tanabe et al. also reported that if ammonium sulfate were used as

the sulfate source instead of sulfuric acid, a higher surface area (e. g. ~120 m^2/g) can be obtained (1). The preparation procedure is, however, more complex when ammonium sulfate is used as the sulfate source.

Table 18. Surface Areas Determined by Nitrogen Absorption/Desorption

Catalyst	Surface Area (m^2/g)
ZrO_2 (620°C)	<10
ZrO_2/SO_4^{2-} (620°C)	55
ZrO_2/SO_4^{2-} (100°C)	11

The effect of calcination temperature on the surface area of sulfated zirconia was also investigated. It was found that the surface area of the sulfate-modified zirconia decreased as the calcination temperature increased, as shown in Table 19. The reduction in surface area can be attributed to sintering of the catalyst by agglomeration of small particles to form larger particles. The agreement between the BET single point and multipoint methods of analysis is very good. However, the reasons for the much higher values determined by the Langmuir method of data analysis are unknown at this time. The effect of surface area on the catalytic properties of these catalysts, as well as stability of the catalysts under reaction conditions, will be investigated in the successor to this project.

Table 19. Surface Area of the Sulfated Zirconia *vs* Calcination Temperature

Calcination Temp. (°C)	Langmuir (m^2/g)	BET Single Point (m^2/g)	BET Multipoint (m^2/g)
350	379	225	232
455	334	200	205
551	248	146	150
620	181	105	108
720	58	36	37

B. Calculation of the Amount of Sulfur on Sulfated Zirconia

The amount of sulfur on the surface of sulfate modified zirconia has been calculated from data obtained from elemental analysis. The elemental analyses were performed by Galbraith Laboratories, Inc. The results from the two samples that were analyzed were in good agreement, as shown in Table 20. The analytical data from sample number 1 were used to calculate the surface coverage of sulfur on zirconia. Assuming that the zirconia has a body-centered tetragonal structure and that the (100) plane is the surface plane, there would be 5.2×10^{18} ZrO_2/m^2. Assuming that all of the sulfate is on the surface, the amount of sulfur corresponds to 0.55 monolayer.

Table 20. Result of elemental analysis

Sample number	Zirconium (weight %)	Sulfur (weight %)
1	71.33	0.84
2	69.97	0.96

C. Determination of Acidity *via* Aqueous Titration of ZrO_2/SO_4^{2-}

Characterization of the ZrO_2/SO_4^{2-} catalyst included an attempt to determine the number of accessible acid sites in terms of milliequivelents per gram of catalyst, i.e. meq/g. The concentration of sulfur was determined, *via* elemental analysis, to be 0.26 and 0.30 mmol/g for two separate preparations, samples 1 and 2 above. Calcined ZrO_2/SO_4^{2-} is known to possess both Lewis and Brönsted acidic sites. In this study, a suspension of ZrO_2/SO_4^{2-} in water, as well as a Na^+ ion-exchanged sample, were titrated with standard solutions of NaOH to determine the acid content of the catalyst.

A Markson model 88 pH meter was used for determination of pH during the titration

experiments. The NaOH solutions were standardized against known amounts of potassium hydrogen phthalate from Aldrich. In the first experiment, a 2.3095 g sample of ZrO_2/SO_4^{2-} previously calcined to 620°C and containing 0.30/mmol S/g was suspended in *ca.* 40 ml of distilled water. The electrode of the calibrated pH meter was immersed in the aqueous suspension to be titrated. Small volumetric additions from a buret containing 0.07965 N NaOH solution were added to the suspension while recording both the volume of NaOH solution added and the resultant pH of the aqueous suspension. It was noticed that long equilibration times were necessary following NaOH additions, i.e. 1-2 hr. When the titration was close to the neutralization point, i.e. pH of 7, the beaker containing the suspension was covered tightly with parafilm and stirred for three days to equilibrate. Following this period, the titration was continued. In total, 8.17 ml of 0.07965 N NaOH solution were needed to neutralize the suspension with the 2.3095 g sample of ZrO_2/SO_4^{2-}. The following calculation determined the number of acid sites titrated in the experiment:

$$8.17 \text{ ml} \times (0.07965 \text{ meq/ml}) \times (1/2.3095 \text{ g}) = 0.28 \text{ meq/g}.$$

In light of the extensive equilibration times necessary to achieve stable pH readings in the above experiment, an alternative method of acid site determination was utilized. Forni described the method of adding excess NaCl to exchange with H^+ on the surface of catalysts in cases of long equilibration titrations (53). The HCl solution thus formed is easily titrated with base. Approximately 30 ml of a 5% NaCl solution by weight was added to 2.3036 g of ZrO_2/SO_4^{2-}, and this was allowed to stir overnight. The solution was then titrated with 0.1051 N NaOH solution while measuring its pH with the meter. With this method, equilibration was fast, within about a minute at each point. The total volume of 0.1051 N NaOH needed to neutralize the HCl solution was 6.3 ml. The acidity of the ZrO_2/SO_4^{2-} was determined to be:

$$6.30 \text{ ml} \times (0.1051 \text{ meq/ml}) \times (1/2.3036 \text{ g}) = 0.29 \text{ meq/g}.$$

This was approximately the same value as that found for the direct titration of the aqueous suspension. As the concentration of sulfur, existing as SO_4^{2-}, was 0.3o/mmol/g, it appears that there is one Brönsted acid site, under wet conditions, for each sulfate group on the surface. This result indicated that sulfuric acid, which would have two Brönsted protons per sulfate, is not reformed by the addition of water to the catalyst.

D. Catalyst Characterization using X-Ray Photoelectron Spectroscopy (XPS)

Nafion-H was exchanged to its potassium form, designated Nafion-K. To achieve the ion exchange, 10 g of Nafion-H was immersed in 75 ml of 1 M potassium nitrate (KNO_3) and stirred for approximately 45 min. The solution was strongly acidic due to the exchange of H^+ for K^+. A new portion of potassium nitrate was added after the previous was decanted and the catalyst was washed with distilled water. The procedure was repeated until full exchange was reached, as determined by testing the pH of the exchange solution. Four portions of KNO_3 were needed for total exchange of the Nafion-H. Amberlyst-15 was exchanged in the same manner, except ten portions of KNO_3 was required. The higher exchange capacity per weight of Amberlyst-15 *vs.* Nafion-H explains this requirement. Finally, the Nafion-K and K-exchanged Amberlyst-15 were washed in distilled water and allowed to dry overnight at 90°C. XPS measurement of Amberlyst-15, Nafion-H and sulfated zirconia have been conducted to investigate the oxidation state of elements, as well as their relative concentration.

Amberlyst-15 and potassium exchanged Amberlyst-15 were ground to fine powders that were placed on pieces of silver foil mounted on sample holders. Sulfated zirconia was used as prepared and placed on silver foil as described above. Neither Nafion-H nor

potassium exchanged Nafion-H could be prepared using this technique. Instead, each resin was placed on a piece of aluminum foil covered with silver paint and pressed using a pressure of 18-20 tons for 15 min. to give a smooth continuous surface to analyze.

Amberlyst-15 is a poly(styrene-divinylbenzene) polymer that has been sulfonated with sulfuric acid. The only oxygen atoms present in this copolymer are in the sulfonyl group. XPS data showed that indeed the ratio of oxygen to sulfur was about 3:1 as calculated by using the intensity and sensitivity factors for the elements. Sensitivity factors used for O 1s and S 2p were 2.85 and 1.679, respectively. The potassium exchanged Amberlyst-15 showed a ratio of sulfur to potassium of about 1/1, which confirmed that the resin was 100% exchanged and no acid sites were present. The K 2p lines were used for potassium and the sensitivity factor used was 3.97.

Nafion-H has additional oxygen atoms in ether linkages to the fluorocarbon backbone, and the ratio of oxygen to sulfur was experimentally found to be about 7/1. Potassium exchanged Nafion-H has no catalytic activity as mentioned earlier in this report. The lack of acid sites was confirmed by a ratio of sulfur to potassium of 1/1. It was also determined that the different oxygen atoms in Nafion-H can be distinguished from one another by a slight shift in binding energy.

Sulfated zirconia has at least two different "types" of oxygen, which is demonstrated in Figure 59 as a shoulder on the main oxygen peak. The two maxima within the oxygen peak are about 2 eV apart; although this peak is very broad this follows the pattern described by Arata (51), where the shoulder refers to oxygen in the sulfate group and the peak at lower binding energy corresponds to oxygen of the zirconia. Sulfur was reported to appear at 169.3 eV (51) and that is approximately where the sulfur peak in this sample was observed (Figure 60). This binding energy for sulfur corresponds very well with the binding

Figure 59. XPS of the oxygen 1s region of the ZrO_2/SO_4^{2-} catalyst.

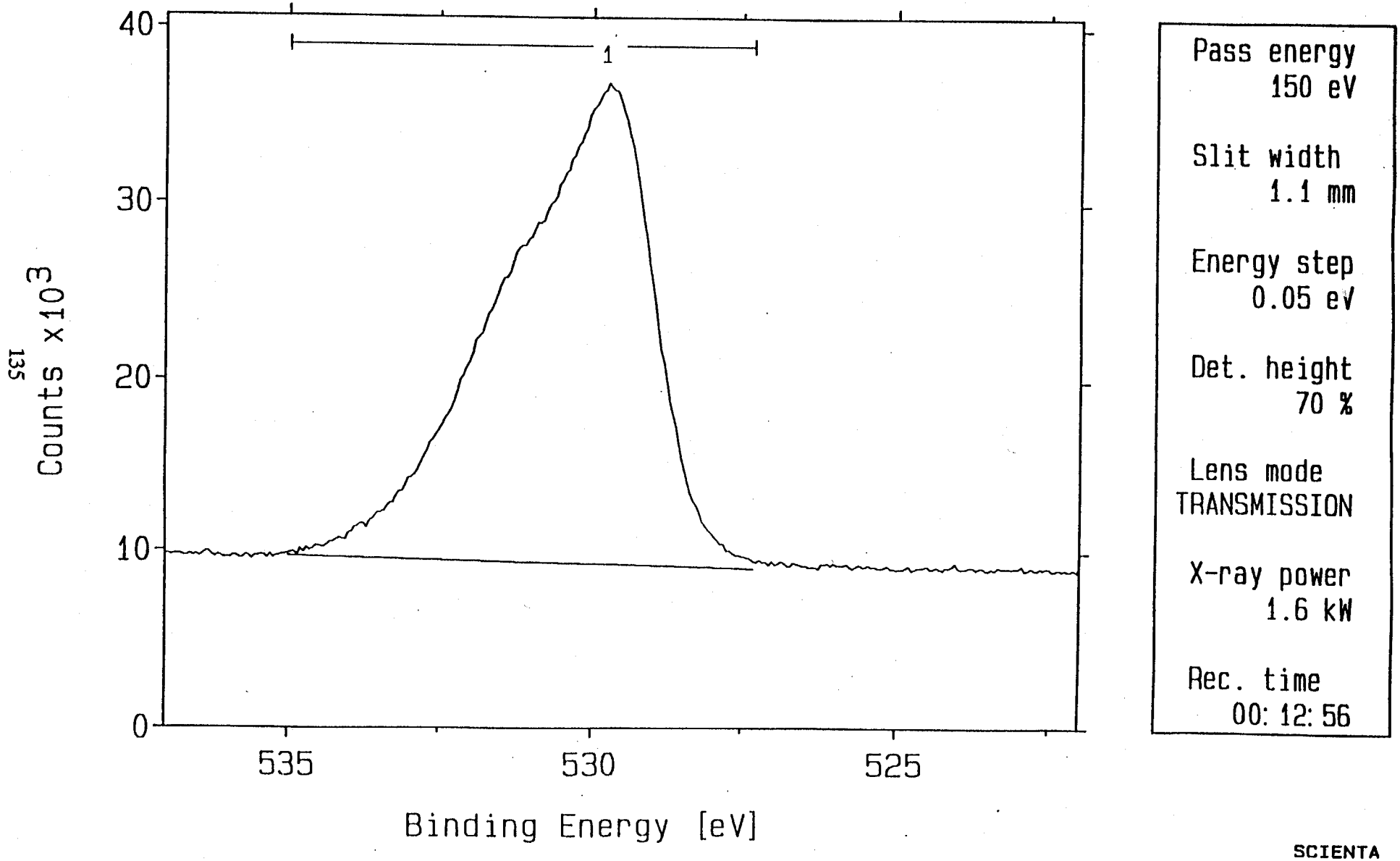

Figure 60. XPS of the sulfur 2p region of the ZrO_2/SO_4^{2-} catalyst.

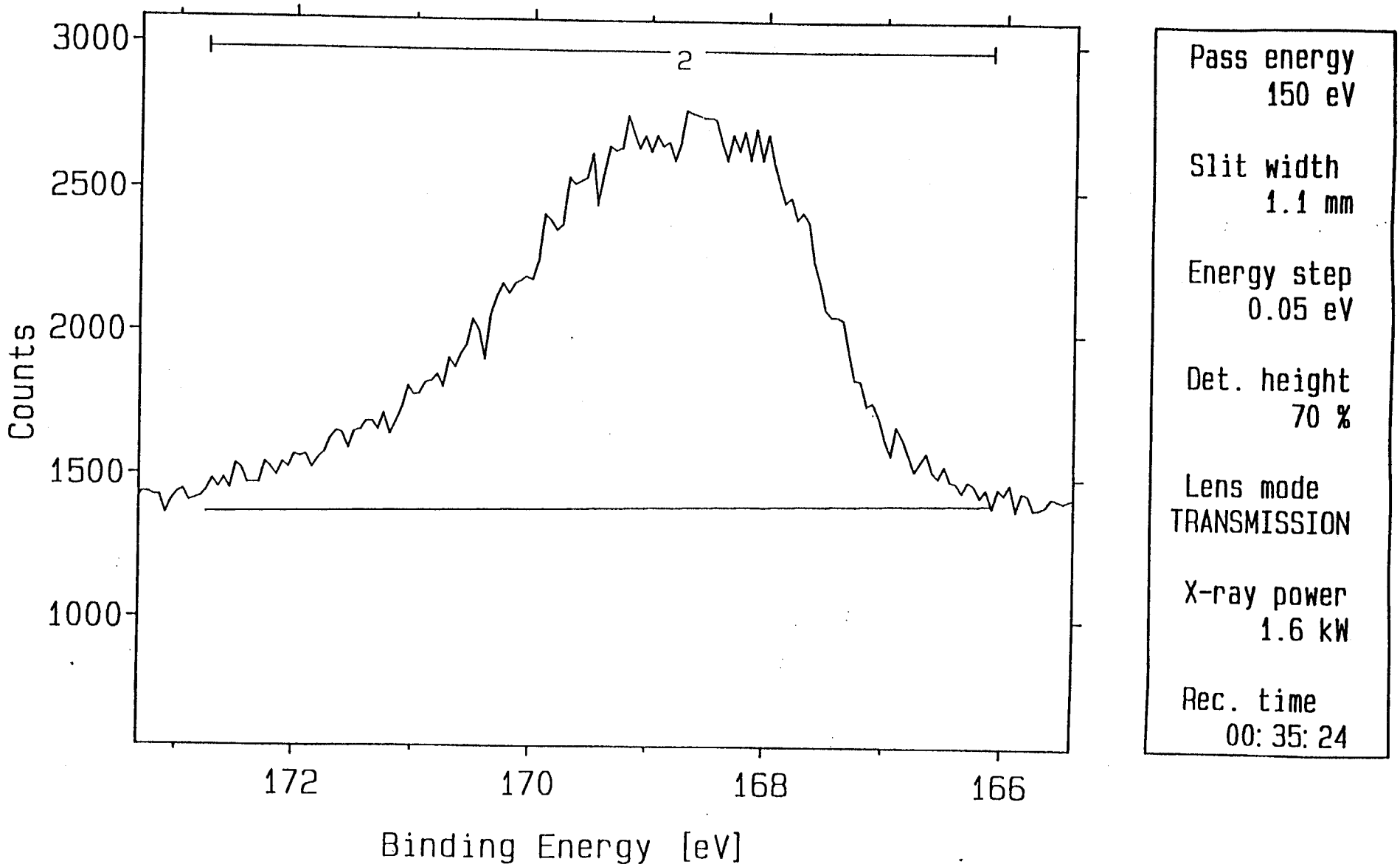

energy for sulfur in zirconium sulfate ($Zr(SO_4)_2$), as obtained by Arata (51). Figure 61 show the spectrum of the zirconium $3d_{3/2}$ and $3d_{5/2}$ core levels. The separation by approximately 2 eV also follows the results Arata presented. These results confirm that the utilized preparation procedure indeed gave sulfated zirconia. The peaks in the spectra presented are broad due to charging of the sample. This phenomenon will always occur when XPS is performed on non-conducting materials. Charge compensation using a flood gun was used to minimize the charging effect.

E. Probing the Acidity of Sulfate-Modified Zirconia by XPS

The objective of these experiments was to investigate the acidic properties of sulfate-modified zirconia. An understanding of the acid function induced by the sulfate dopant might provide for further improvement of this very active catalyst for the high temperature (175°C) dehydration of isobutanol to isobutene and the low temperature (125°C) coupling of methanol and isobutanol to ethers. By adsorbing nitrogen-containing bases such as pyridine, on the catalyst surface, the presence and type of acidic species can be monitored by XPS N 1s core level shifts. The observed shifts of the N 1s binding energy line can be related to the strength with which the nitrogen-containing base is adsorpbed onto the surface. By this means, Lewis and Brönsted acid sites on the surface of this catalyst were distinguished and quantified. Water is a reaction product formed over the catalyst during isobutanol dehydration, as well as during ether synthesis, and probe the correlation of partial pressure of water over the catalyst to the ratio of Lewis to Brönsted sites, a water adsorption experiment was also carried out prior to adsorption of the pyridine adsorbate.

A new glass vacuum system was designed and constructed in our laboratory for the pretreatment of the sulfate-modified zirconia samples. The system was able to attain a

Figure 61. XPS of the zirconium 3d region of the ZrO_2/SO_4^{2-} catalyst.

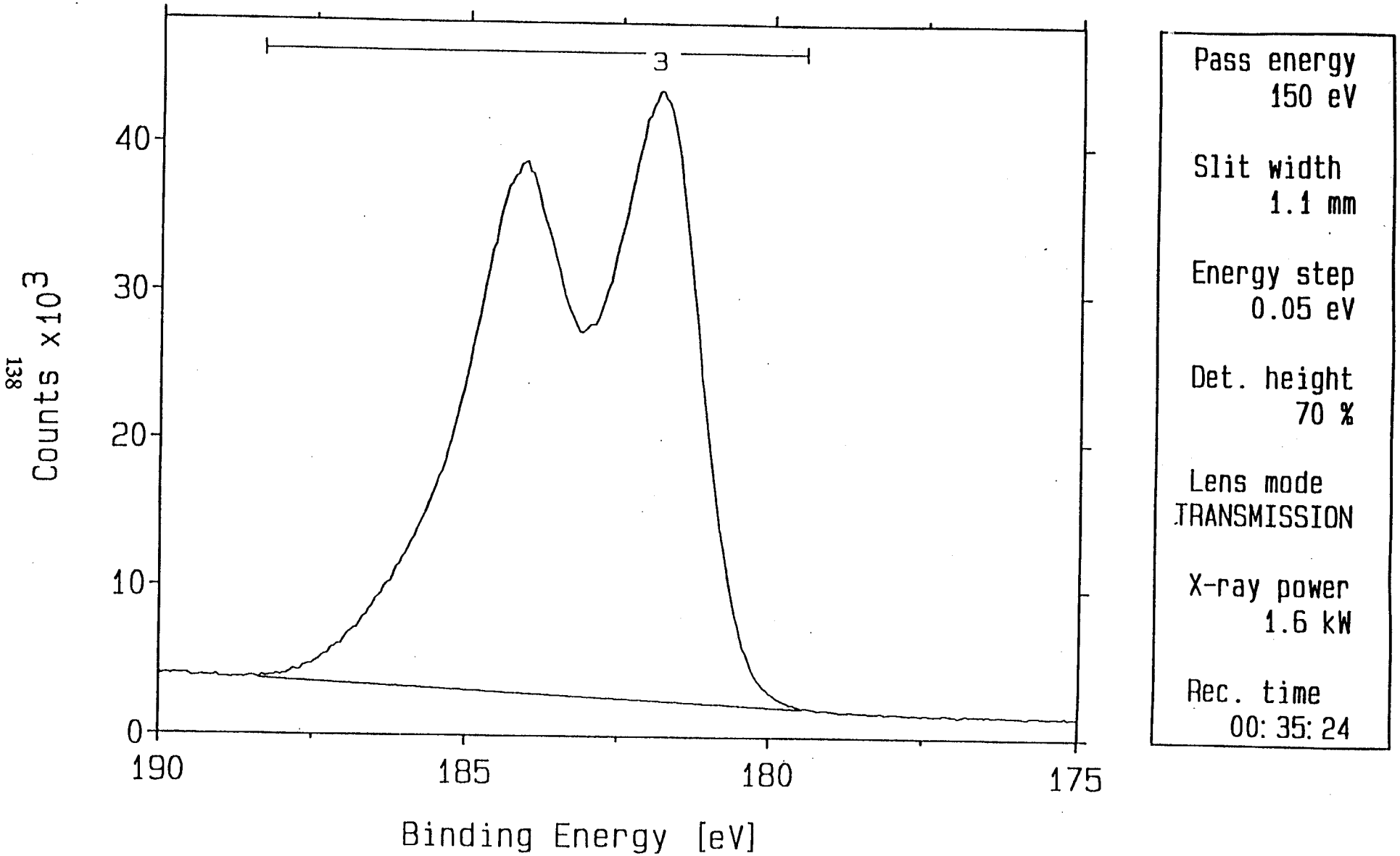

vacuum of 10^{-5}-10^{-6} torr. A schematic of the vacuum system is shown in Figure 62. External ovens were used to heat the sample as well as the adsorbates so that a constant designated vapor pressure of the individual adsorbates could be maintained. A new high precision digital pressure manometer was purchased to monitor the pressure of gas in the sample pretreatment, as well as to measure the uptake of pyridine during the experiments. The model 572 Barocel pressure sensor with a model 1174 electronic manometer from Edwards High Vacuum Int. can measure pressures from 0.001 torr to 1000 torr with 0.001 torr resolution.

The procedure used for the pretreatment of the catalyst prior to XPS analysis was as follows:

1. The sulfate-modified zirconia was freshly calcined at 620°C for 3 hr.
2. The sample was introduced into one of the glass tubes on the vacuum system under ambient conditions.
3. The sample was evacuated at 415°C for 1 hr.
4. The catalyst was then exposed to 15 torr of pyridine for 0.5 hr at 25°C.
5. Finally, the sulfate-modified zirconia was evacuated at 150°C for 1 hr to desorb excess physisorbed pyridine not chemisorbed to Brönsted or Lewis acid sites.

For the water-adsorption experiment, the following two steps were carried out after Step 3, but before Step 4, given above:

3a. Water vapor at 75 torr was allowed to adsorb onto and equilibrate with the catalyst at 175°C for an exposure time of 0.5 hr.

3b. The sample was then evacuated at 175°C for 1 hr.

Sample tubes with the teflon stopcocks closed and still in place were removed from the vacuum manifold and put into a glovebag purged with dry nitrogen gas. The sample tubes were opened in the glovebag, and the catalyst sample was mounted onto a sample

Figure 62. Schematic of the new high vacuum system for pretreatment of samples for XPS analysis.

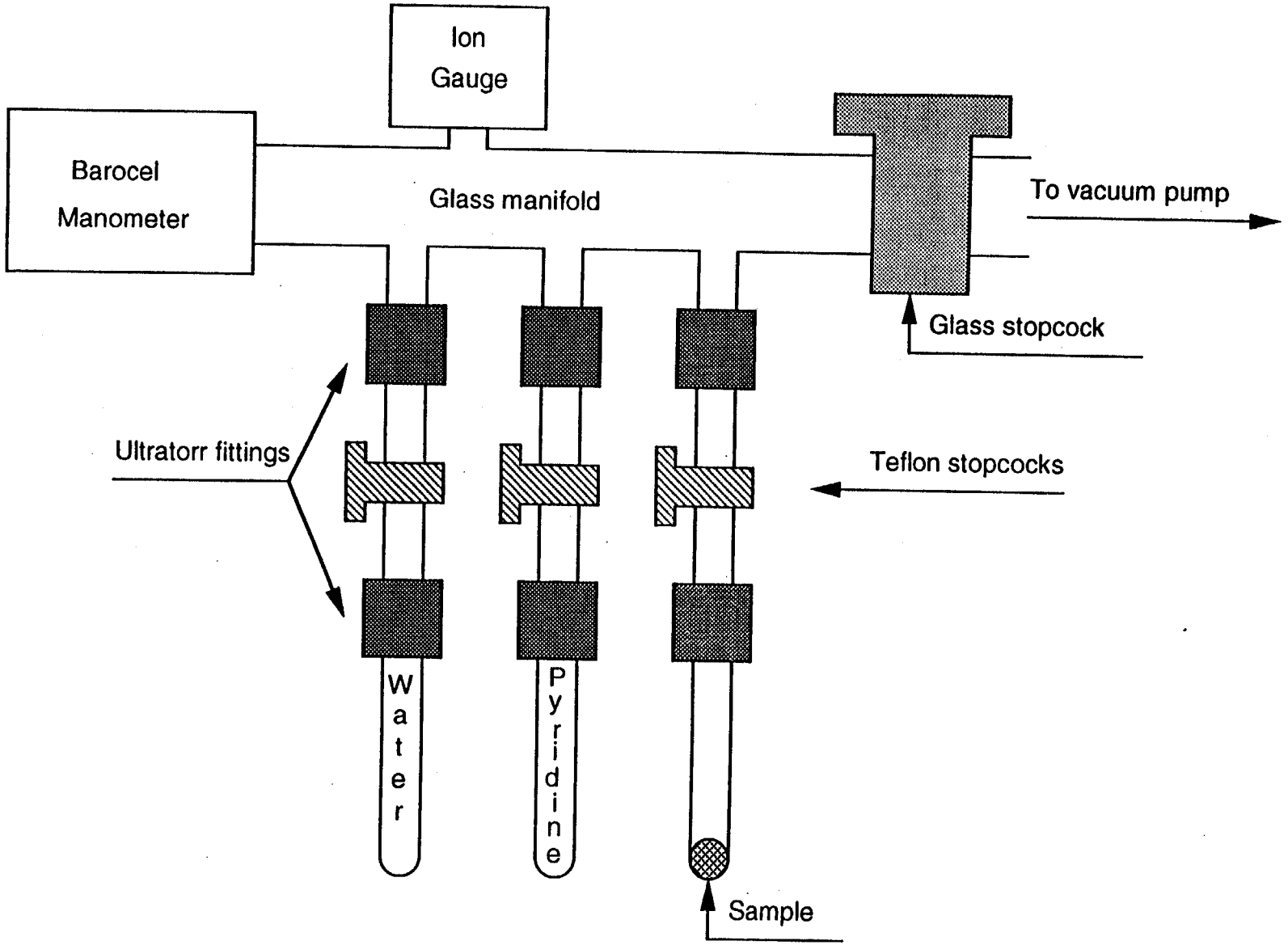

holder and introduced into the SCIENTA-300 ESCA instrument without exposure to air or moisture.

The nitrogen 1s binding energy is 398-400 eV for free pyridine compounds and pyridine coordinated to Lewis acid sites (54). The binding energy of N 1s increases to 400-402 eV for pyridinium compounds, such as pyridine protonated by a Brönsted acid (54).

The first sulfate-modified zirconia sample was pretreated according to Steps 1-5 given above. This sample is dry since no water was introduced. Figure 63 shows the N 1s XPS spectrum of pyridine adsorbed onto this dry SO_4^{2-}/ZrO_2 sample. There are two main peaks observed at 398.8 eV and 401.4 eV, and these correspond to pyridine coordinated to a Lewis acid site and to a Brönsted acid site, respectively. The line positions were referenced to Zr $3d_{5/2}$ = 182.3 eV, and a flood gun was used to reduce sample charging, which was minimized by manipulating the flood gun until the Zr 3d lines were as narrow as possible. The peak at 404.6 eV could be due to very strong Brönsted acid sites, but this has to be confirmed by further experiments. Pyridine as an aromatic compound could exibit final state effects, however when data of pyridine were taken on Nafion-H (see later Figure 66), the peak at very high binding energy was absent thus indicating that final state effects are only minor if present at all. If only the two peaks at lower binding energy are considered, the peak at 401.4 eV is 65% of the total peak area, whereas the peak at 398.8 eV makes up the remaining 35%. This means that for a dry sample, calcined to 620°C, the Brönsted acid sites are still the major contributor to the acidity of the sample. It should be noted that the pyridine used in this experiment was not exposed to moisture since it was packed and stored under nitrogen.

Following this experiment, a new SO_4^{2-}/ZeO_2 sample was pretreated and exposed to water vapor, as indicated by Steps 3a and 3b. Figure 64 shows the resultant N 1s XPS

Figure 63. XPS of the N 1s region of the dry ZrO_2/SO_4^{2-} catalyst with adsorbed pyridine.

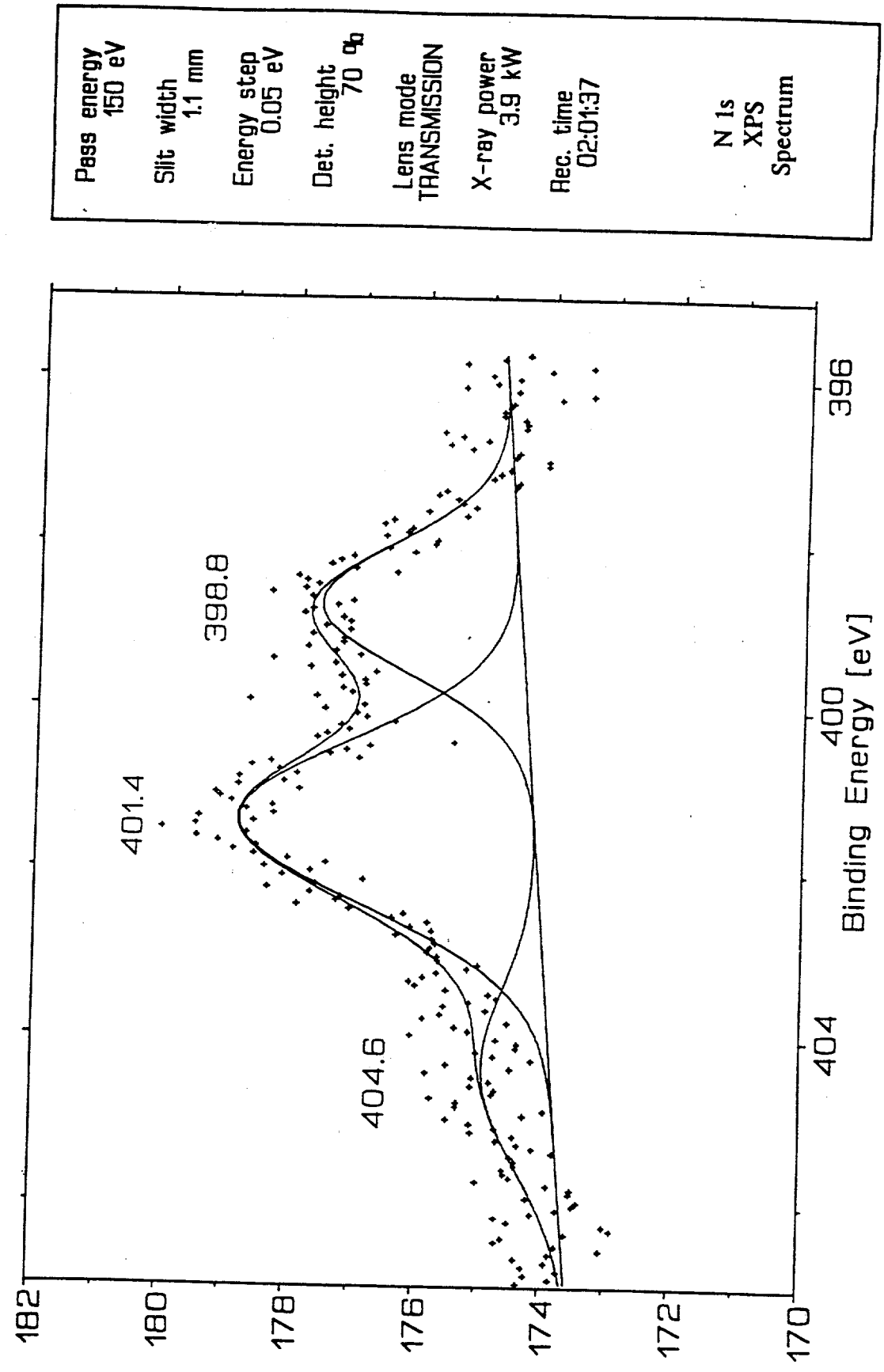

Figure 64. XPS of the N 1s region of the wet ZrO_2/SO_4^{2-} catalyst with adsorbed pyridine.

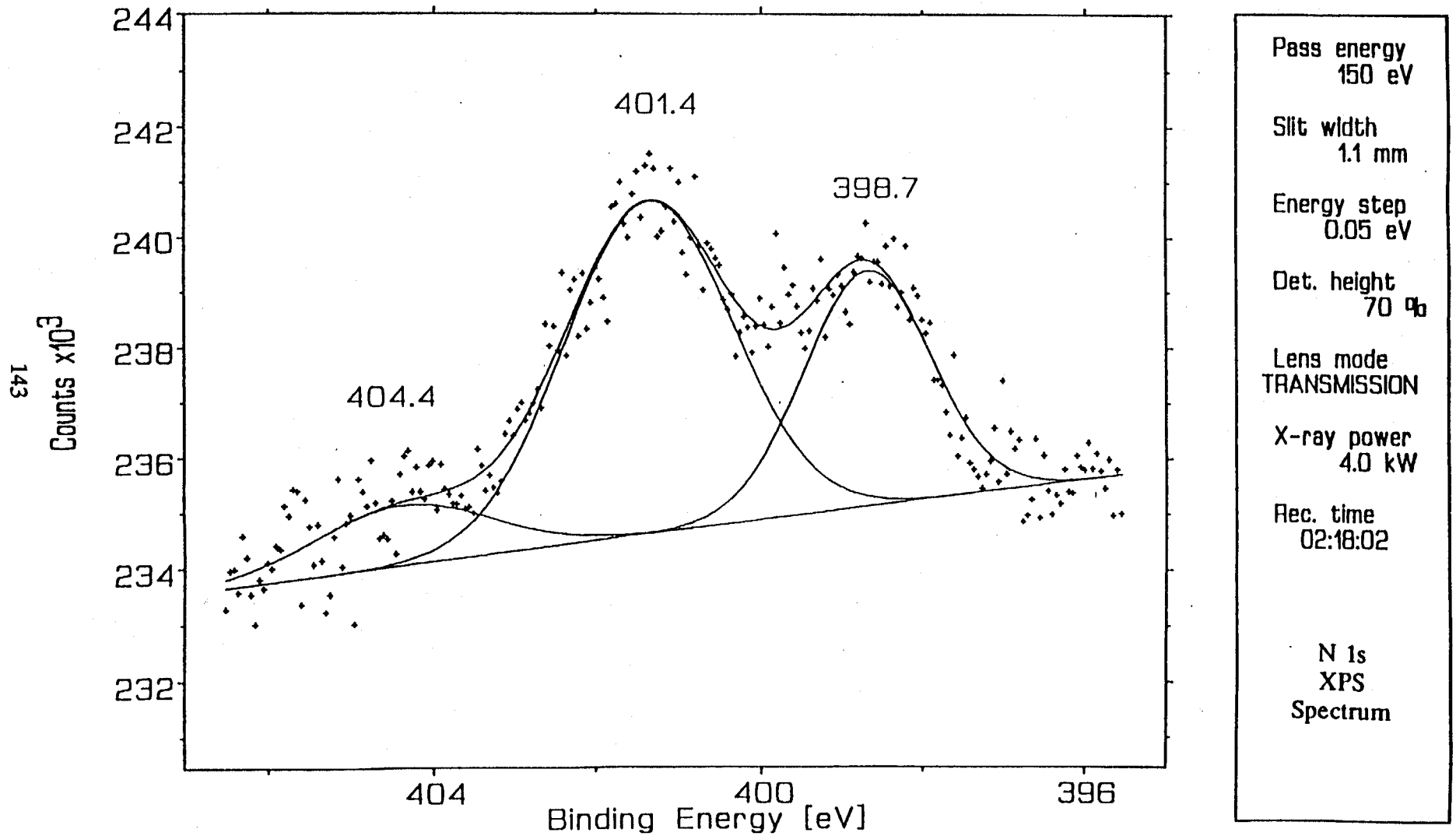

spectrum of this SO_4^{2-}/ZrO_2 sample. This sample is termed to be "wet" due to water admission prior to the pyridine adsorption. Again, the two main spectral peaks were observed at 398.7 eV and 401.4 eV, respectively. The same area percentages are seen for this wet sample as for the dry sample. The 401.4 eV peak corresponds to 64% of the total area, and the 398.7 eV peak is the remaining 36% provided that the peak at 404.4 eV is excluded as above.

These results indicate that even after calcination at 620°C for 3 hr, there is a significant quantity of Brönsted acid sites present on the catalyst surface. With the conditions used in this experiment, there is no evidence that Lewis acid sites convert to Brönsted acid sites upon introduction of a substantial amount of water (75 torr). Further experiments might reveal at what calcination temperature the surface becomes fully deprotonated so that only Lewis acid sites are present. The catalyst could then be investigated in terms of acid site conversion from Lewis to Brönsted acid sites. Improvements in the experimental technique such as more efficient charge compensation and use of pressed powder samples providing a smoother surface will enhance the quality of the data significantly in the future.

Two experiments were performed on other catalysts, i.e. γ-alumina and Nafion-H. These two samples were exposed to pyridine after being exposed to laboratory air. The samples were not evacuated at elevated temperature after pyridine adsorption, so more physisorbed pyridine is expected. Figure 65 shows the N 1s region for γ-alumina with adsorbed pyridine. The peak at a binding energy of 397.6 eV corresponds to pyridine coordinated to a Lewis acid site. No spectral peak is seen at higher binding energy, indicating that no Brönsted acid sites are present on this catalyst. This result agrees well with results of pyridine adsorption on γ-alumina obtained by IR-spectroscopy.

Figure 65. XPS of the N 1s region of the γ-alumina catalyst with adsorbed pyridine.

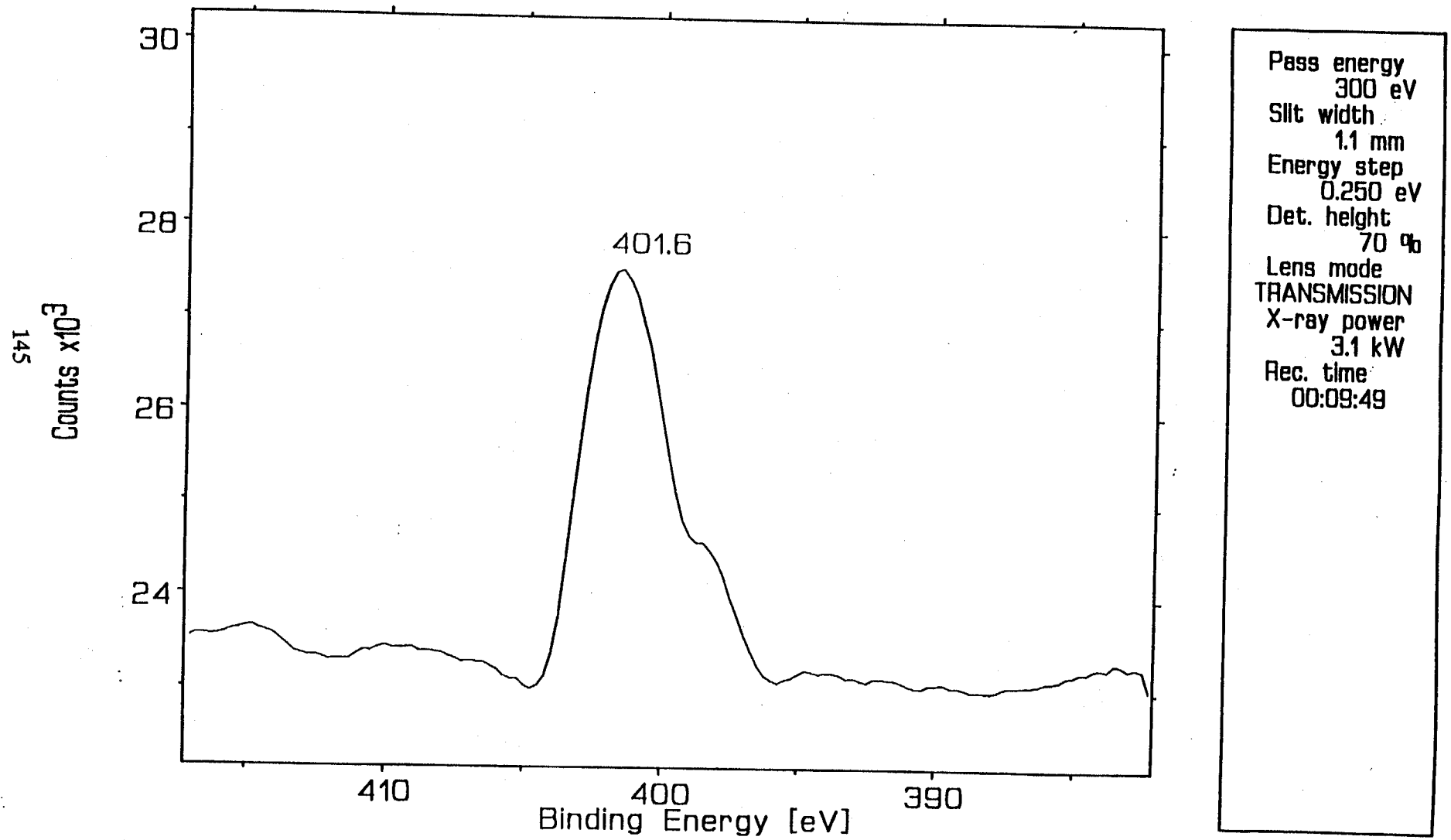

Figure 66 shows the N 1s binding energy region for Nafion-H with adsorbed pyridine. Nafion-H is a sulfonated polymer with a fluorocarbon backbone. Nafion-H is considered to be a Brönsted acid-containing material and is not expected to have any Lewis acid sites. In the XPS spectrum, the main peak is observed at 401.6 eV, which corresponds to a Brönsted acid site. A minor peak is evident in Figure 66 at 398.8 eV, and this is believed to be due to physisorbed pyridine. This peak would probably not be seen if the sample had been evacuated at elevated temperature prior to the analysis. The last two samples, γ-alumina and Nafion-H, indicate the validity of XPS as a method to distinguish and quantify Lewis and Brönsted acid sites.

F. Quantification of XPS Data: Amount of Sulfur on Sulfate-Modified Zirconia

The calculation of surface coverage has been performed such that it accounts for the mean free path of photoelectrons and instrumental constants. To determine the mean free path of the photoelectrons in the surface of the sample, the Chang equation (55) is used as given below.

Mean free path $(\lambda / = 0.2\ (E)^{0.5}\ t^0$

E = kinetic energy in eV

t^0 = monolayer thickness, which here is the spacing between the (100) layers of ZrO_2

The kinetic energy for Zr photoelectrons is 1304.4 eV and t^0 is 0.182 nm. Using these values yields a mean free path (escape depth) of 1.31 nm, which corresponds to about 7 layers. The mean free path and monolayer thickness values were used in the Dreiling equation (56), which gives a relationship between the measured photoelectron intensity and the atomic concentration on the surface. The equation considers attenuation effects due to surface overlayers of a certain thickness. The version of the Dreiling equation used for

Figure 66. XPS of the N 1s region of the Nafion-H catalyst with adsorbed pyridine.

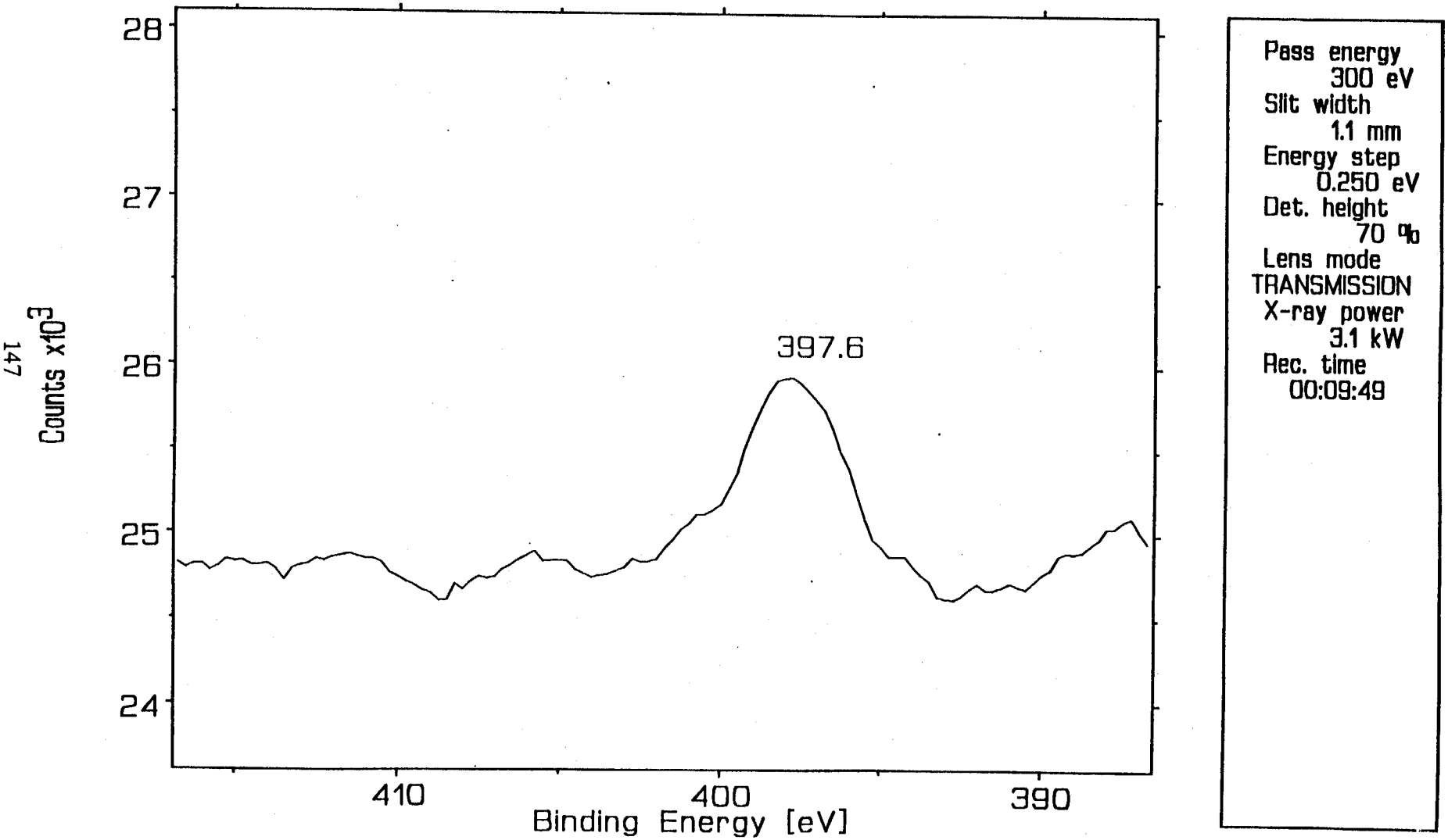

these calculations is the one utilized by Vedage et al. (57), as given below.

$$\frac{[S]}{[Zr]} = \frac{I_s}{I_{Zr}} \quad \frac{g\lambda_{Zr}}{t^0_{Zr}} \quad / \quad \left(\frac{\sigma_s}{\sigma_{Zr}} \frac{E_{Zr}}{E_S} + \frac{t^0_S}{t^0_{Zr}} \frac{I_S}{I_{Zr}} \right)$$

[S] = Concentration of sulfur on the surface
[Zr] = Concentration of zirconium on the surface
I = Measured photoelectron intensity
g = Escape angular factor for porous materials
λ = Mean free path
t^0_{Zr} = Monolayer thickness
t^0_S = Thermodynamic diameter of the sulfate anion (0.488 nm)
σ = Photoionization cross-section

The surface concentration ratio of [S]/[Zr] calculated with this method is 0.49. This value agrees very well with the value obtained with chemical elemental analysis, which resulted in a value of 0.55 assuming that all of the sulfur is on the surface of the sample. This provides confidence that the sulfate dopant is on the surface or associated with the outer-most surface layers and not with the bulk of the ZrO_2 catalyst.

Seah and Dench (58) have compiled values of measured mean free paths, as given in the literature, and have obtained an empirical equation for estimating the mean free path, $\lambda = B\,(E)^{1/2}$ for $E > 150$ eV and where B is a universal value for inorganic compounds (= 0.098). This gives a mean free path of 3.47 nm for zirconia. This general equation has an error of some 35%. Using this equation instead of the Chang equation for the mean free path yields a surface [S]/[Zr] ratio on the surface of 0.74, which is more sulfur than is available according to elemental analysis.

If a simple data treatment is used that does not account for screening processes due to the sulfate ion and to the angular factor, the surface [S]/[Zr] ratio will be higher than the available amount of sulfur. Therefore it appears that these considerations are important. The use of the Chang equation here is valid and will be used for all future experiments.

VII. Octane and Cetane Number Determination

A. Octane Number Determination

Octane number was determined for MIBE, MTBE, and a 50/50 by volume mixture of MIBE and MTBE. MIBE was produced by the Williamson ether synthesis. The preparation involves the formation of sodium butoxide from metallic sodium and isobutanol. Methyl iodide was added to form MIBE and sodium iodide. The product resulting from this synthesis was a 50/50 mixture of MIBE and isobutanol. For the purpose of octane number determination, this mixture was distilled under nitrogen to yield a >96% purity of MIBE, as determined by gas chromatography. The major impurity was isobutanol. MTBE was obtained from Aldrich Chem. Co. Determination of octane number was performed by Amoco Oil Company with ether samples found by us. The standard ASTM methods D-2699 and D-2700 were used for Research Octane Number and Motor Octane Number, respectively. The ether samples were tested for peroxides prior to octane determination. The peroxide level was <20 ppm for all three samples, which is considered to be acceptable. The ether samples were mixed with unleaded regular gasoline, where the amount of ether was 10% in the gasoline. The results obtained by Amoco Oil Co. are summarized in Table 21.

Table 21. Octane Numbers of MTBE and MIBE Gasoline Blends.

Sample	Research Octane Number	Motor Octane Number	Peroxide (ppm)
Unleaded Regular Gasoline (ULR)	92.1	82.3	-
10% MTBE in ULR	94.9	83.7	14
10% MTBE/MIBE in ULR	92.0	82.4	6
10% MIBE in ULR	88.8	80.8	17

MTBE increased the research octane number by 2.8 units and the motor octane number by 1.4 units, which is in good agreement with values obtained by Spindelbalker and Schmidt (59). MIBE, on the other hand, decreased the research octane number and motor octane number by 3.2 and 1.5 units, respectively. The gasoline/ether mixture containing the 1/1 by volume MIBE and MTBE had the same values as the base unleaded regular gasoline. In this case, an appreciable amount of oxygen was added to the ULR gasoline without altering its octane rating.

The blending octane numbers were calculated according to the following equation: Blending Research Number = RON (component A) × (percent component A) + RON (component B) × (percent component B). Table 22 lists the blending octane numbers for MIBE and MTBE. MTBE and MIBE are isomers, but it is clear from the results presented above that MTBE is superior to MIBE for octane enhancing purposes.

Table 22. Blending Research Octane Number (BRON) and Blending Motor Octane Number (BMON) of MTBE and MIBE in gasoline.

Sample	BRON	BMON
MTBE in ULR	120.1	96.3
MIBE in ULR	60.8	67.0

B. Cetane Number Determination

A 140 ml portion of MIBE was sent to Southwest Research Institute (SRI) for evaluation of the cetane number. The cetane number was reported to be 53. As commercial fuel in the U.S. is normally 40-45 cetane, MIBE shows promise as a high cetane additive should oxygenates be required in fuel as they are in gasoline fuels.

VIII. Experimental Methods

A. Calibration of Thermal Response Factors and GC Parameters

Thermal response factors (TRF) are necessary to quantitatively calculate amounts of products from the raw peak areas in gas chromatographic analysis when a thermal conductivity detector (TCD) is used. The raw peak area is divided by the thermal response factor to give the true response value.

Thermal response factors used in previous reports have not been determined in this laboratory, but literature values for reactants and products, as listed by Dietz (60), were utilized. However, it was found that the values from Dietz were not always satisfactory. New thermal response factors have been determined for methanol, isobutanol, methyl tert-butyl ether, dimethylether, and isobutene.

To avoid any interference from catalytic reactions, the reactor was filled with only 3 mm glass beads. Calibration was carried out at 123°C and ambient pressure. According to Dietz (60), thermal response factors are independent of temperature and flow rate. The flow of the internal standard, N_2, was carefully determined by several measurements using a bubble meter. Either dimethylether (DME) or isobutene was added and the total flow was measured. Liquid samples such as methanol (MeOH), isobutanol or methyl tert-butyl ether (MTBE) were introduced *via* a Gilson pump at a rate of 12.0 μl/min. Finally, helium, an inert carrier, was added to give a total flow of 5-6 l/hr.

Steady-state was reached within a 2 hr period and the calibration was allowed to run overnight to get a longtime average. Flows were very stable and the difference from injection to injection was kept to a minimum.

The new thermal response factors were determined in reference to the internal standard. This approach assumes that the thermal response factor for nitrogen is correct.

Nitrogen is a common internal standard in GC analysis, and therefore this assumption was accepted for this application. As can be seen from Table 23, the new thermal response factors were increased for isobutene and isobutanol by 13% and 19% respectively, while the thermal response factor for methanol decreased by 9%. The largest change was measured for dimethylether, which dropped 25%. The value for MTBE only changed by a difference of two units, which is within experimental error. Thermal response factors are not absolute values; rather they are instrumental values that will differ from system to system. It is also important to recognize that there is an age factor involved, meaning it is likely that the thermal response factors will change over time as the TCD ages. The new values for thermal response factors are used throughout this report.

Table 23. Thermal Response Factors of Pertinent Oxygenated Reagents and Products.

Compound	New TRF	Old TRF
Methanol	50	55
Isobutanol	115	97
MTBE	127	125
DME	75	100
Isobutene	93	82

GC Operating Conditions. The usual operating conditions that have been used to achieve separation of reaction products are given in Table 24. The column was a Wall Coated Open Tube (WCOT) capillary column with a chemically bonded 5.0 μm thick methyl silicone coating purchased from Chrompack Inc. These conditions allow for separation of

isobutene from both 1-butene and 2-butene. These three products are also separated from methanol and DME. Several iso-octenes can be separated from each other, but exact identification of the iso-octenes has yet to be resolved. C-8 ethers such as ditertiary butyl ether (DTBE) and diisobutyl ether (DIBE) can be resolved from one another, as well as from the iso-octenes. The chromatograms were not very well resolved towards the higher weight products, meaning after approx. 16 min, but two distinct groups of peaks could be seen. These groups are believed to be different kinds of C-12 compounds, and GC-MS will give a more complete identification of these products.

Table 24. Usual GC Operating Conditions

	Column pressure	0.5 MPa
	Injector temperature	250°C
	Detector temperature	275°C
Oven conditions:	Initial temperature	50°C
	Initial time	2 min
	Temp. ramp A	8°C/min to 110°C
	Hold time at 110°C	0 min
	Temp. ramp B	20°C/min to 250°C
	Hold time at 250°C	9 min
	Total analysis time	25 min

B. Gas Chromatographic Analysis with Mass Spectrometric Detection

Mass spectrometry is very useful in conjunction with gas chromatographic separation. It has the power of obtaining many spectra within a chromatographic peak, which can be used for detecting the products in unresolved GC peaks. It also serves as a more or less absolute indication of substances present in a mixture.

Reaction products from a standard test over Amberlyst-15 were collected in a cold trap and stored in a sealed container. The sample was transferred by syringe and analyzed by GC-MS using a similar column as mentioned above and the same operating conditions.

Attention was focused on resolving methyl tertiary butyl ether (MTBE) from methyl isobutyl ether (MIBE) and tertiarybutyl-isobutyl ether (TIBE) from diisobutyl ether (DIBE). No C-12 compounds were detected in this sample. MTBE and MIBE show very different mass spectrometric fragmentation patterns and therefore distinction between the two was unambiguous.

The mass spectrum of DIBE showed a perfect fit with the library spectrum and is therefore determined beyond any doubt. Through this mass spectrometric analysis, the other C_8 isomer produced and seen by GC, as described in this report, was recently identified unambiguously as TIBE and not DTBE (ditertiarybutyl ether).

C. ^{1}H NMR to Resolve Whether 1-Butene was a Product

Our main technique to identify reactants and products was gas chromatography. Isobutene was an abundant product when isobutanol was dehydrated over acid catalysts. As shown, other possible dehydration products were *cis*-2-butene, *trans*-2-butene, and 1-butene. By GC analysis with our present method of separation, isobutene could be separated from *cis*-2-butene and *trans*-2-butene but not from 1-butene. To resolve if and how much 1-butene was present as a product over the sulfated zirconia, ^{1}H NMR was utilized to further distinguish the C_4 products.

Products from dehydration of isobutanol over sulfated zirconia were collected in a N_2 (*l*) cooled trap. The product stream was dried with molecular sieves prior to the trap to remove as much water as possible. As standards, individual samples of pure 1-butene, isobutene, *cis*-2-butene, and *trans*-2-butene were collected from their respective gas cylinders.

A 500 MHz Bruker AM500 NMR instrument was utilized for these analyses. The spectra were acquired from 0 to 8 ppm at approximately -20°C. All samples were diluted

approximately 1:4 with $CDCl_3$. The pure butene samples were used to calibrate peak positions.

Isobutene has distinctive ^1H NMR peaks at 4.65 and 1.7 ppm (Figure 67), whereas 1-butene has groups of peaks at approximately 5.9, 4.9, 2.1, and 1.0 ppm (Figure 68). The spectra of the pure butenes were compared to the spectrum of the dehydration products of isobutanol (Figure 69).

From the NMR spectra, it was concluded that 1-butene was indeed present in the product stream in a small amount. By integrating the NMR peaks at 5.9 and 4.65 ppm, the quantity of 1-butene could be determined since neither *cis*-2-butene nor *trans*-2-butene have any peaks in this region. It was found that the butene product stream produced by the sulfated zirconia catalyst contained ≤3% 1-butene.

D. Liquid Phase Alcohol Coupling Reactions

The dehydrative coupling of ethanol/isobutanol over the very active Amberlyst-35 catalyst resin, obtained from Rohm & Haas, was carried out in the liquid phase with an autoclave reactorfor comparison with the gas phase reaction and as a basis for suture liquid phase reactions. The reactor (300 cc EZE-SEAL), purchased from Autoclave Engineers, Inc., is capable of running between 25-450°C and 0.1-20 MPa. In the current study, 10 ml ethanol, 90 ml isobutanol and 2.0 grams of the Amberlyst-35 catalyst were charged into the 300 ml reactor. The reactor was then pressurized with 0.5 MPa of nitrogen, which also served as the internal standard for the GC analysis of the gas phase products. The reaction temperature was set at 100 °C, and the magnetic stirring rate was set at 1000 rpm. The liquid and gas phase samples were taken at designated times, and the analyses were performed with a HP5890 series II GC equipped with TCD and FID detectors.

Figure 67. NMR spectrum of pure isobutene in $CDCl_3$.

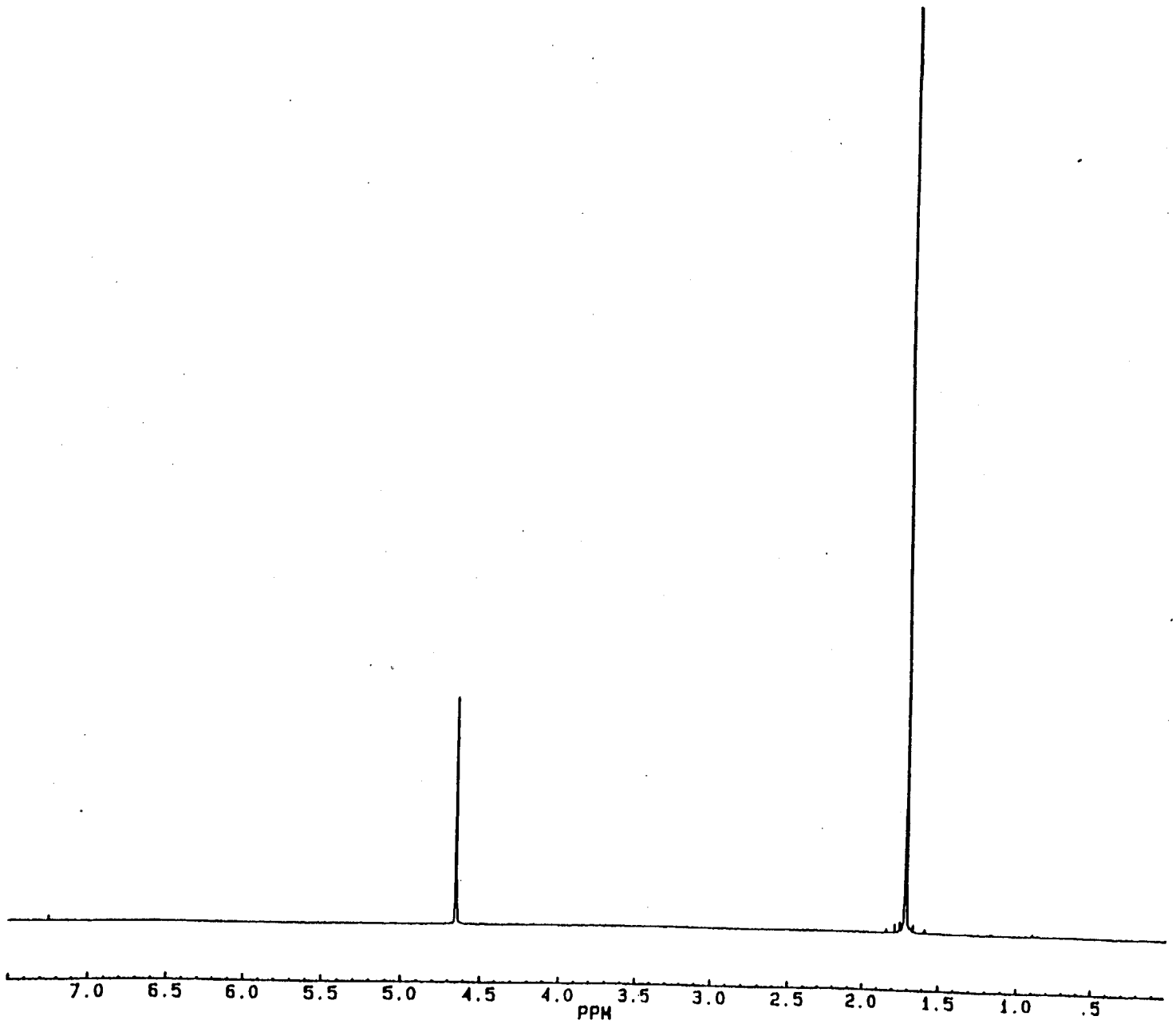

BRUKER

```
MARISTD1
DATE 21-12-92
TIME 9:26

SOLVENT CC13
SF     500.135
SFO    500.130
SFO2   500.130
SF2    500.135
SY 166.0
O1    7941.000
SI   32768
TD   32768
SW    6024.096
SW2   6024.096
HZ/PT     .368
VO        0.0

PW        1.0
AD        0.0
AQ        2.720
RG          1
NS         16
TE        300

DE      106.3
DR         12
DW         83
FW       7600
O2   50000.000
OP   63L PO

LB        0.0
GB        0.0
NC          0
CX        20.00
CY        15.00
F1         7.500P
F2           .001P
MI           .01
DC         1.000
HZ/CM  187.536
PPM/CM     .375
IS          1
SR     5432.62
```

Figure 68. NMR spectrum of pure 1-butene in $CDCl_3$.

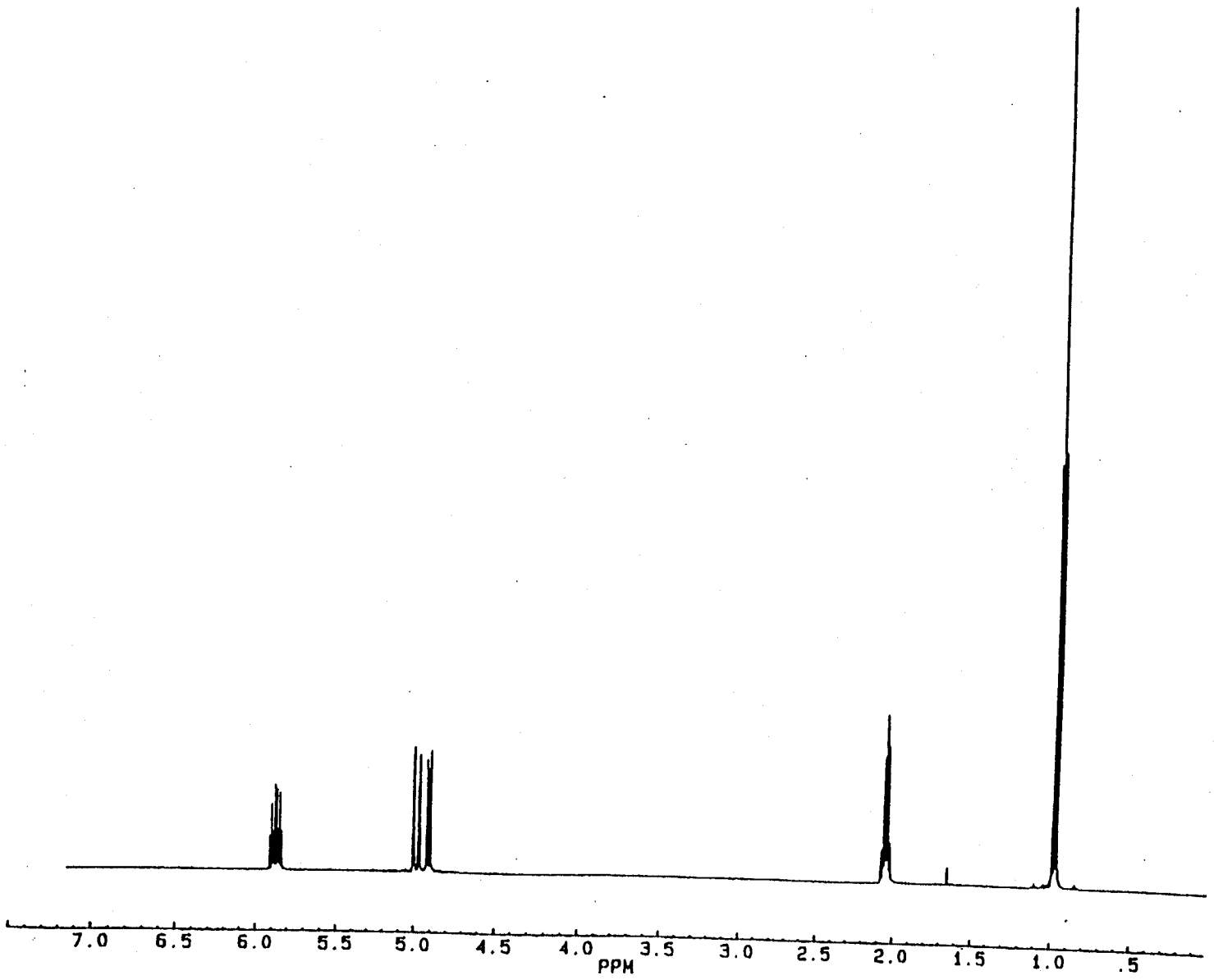

HQ.DMSO
DATE 21-12-92
TIME 8:59

SOLVENT CC13
SF 500.135
SFO 500.130
SFO2 500.130
SF2 500.135
SY 166.0
O1 7941.000
SI 32768
TD 32768
SW 6024.096
SW2 6024.096
HZ/PT .368
VD 0.0

PW 1.0
RD 0.0
AQ 2.720
RG 1
NS 16
TE 300

DE 106.3
DR 12
DW 83
FW 7600
O2 50000.000
DP 63L PO

LB 0.0
GB 0.0
NC -1
CX 20.00
CY 15.00
F1 7.500P
F2 .001P
MI .01
DC 1.000
HZ/CM 187.536
PPM/CM .375
IS 1
SR 5432.62

Figure 69. NMR spectrum of isobutanol dehydration products in $CDCl_3$.

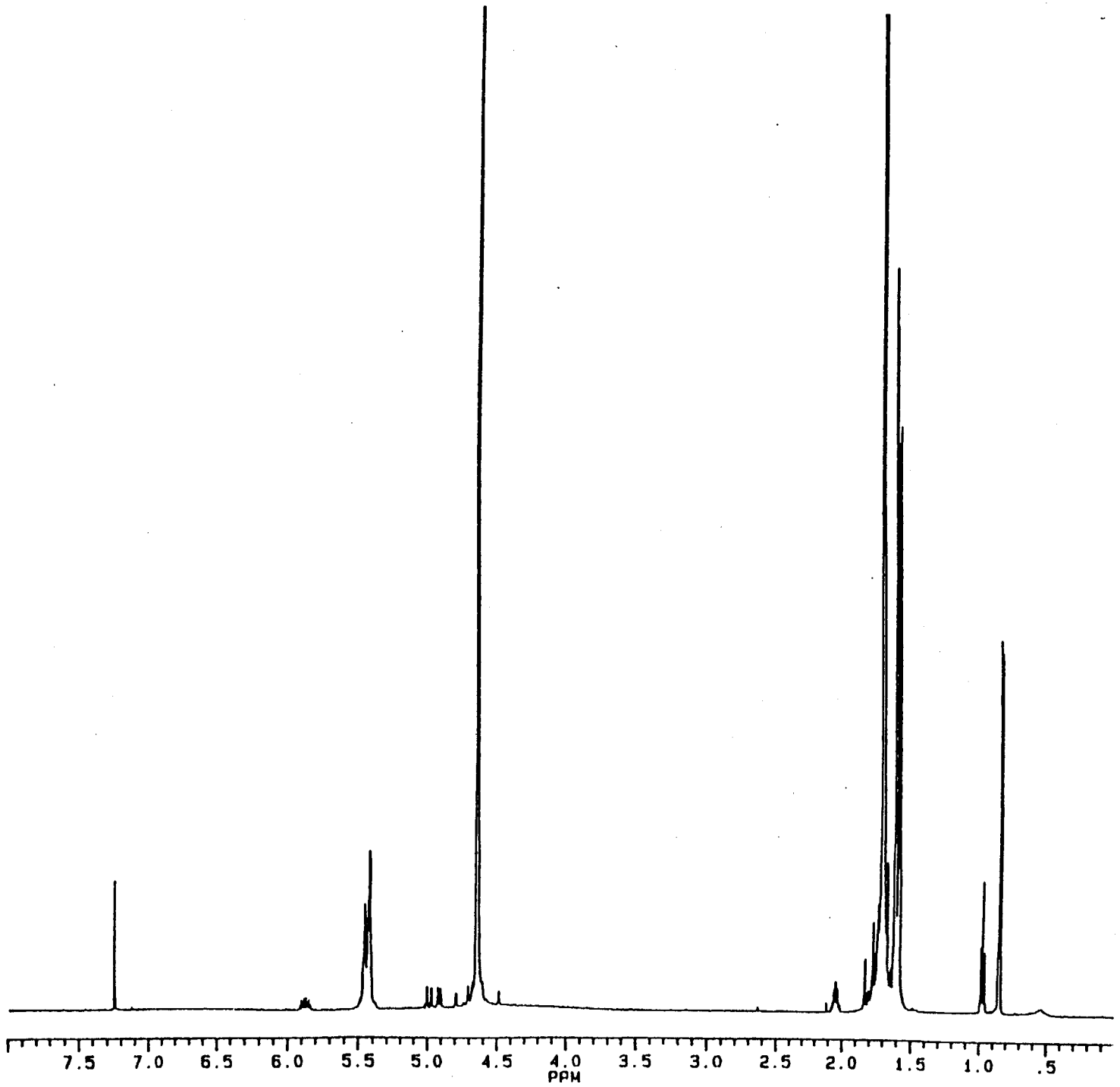

BRUKER

```
FID3
DATE 14-12-92
TIME 9:59

SOLVENT CDCl3
SF     500.135
SFO    500.130
SFO2    500.130
SF2    500.135
SY 166.0
O1    7941.000
SI   32768
TD   32768
SW    6024.096
SW2   6024.096
HZ/PT      .368
VD          0.0

PW          2.0
RD          0.0
AQ          2.720
RG          4
NS        228
TE        300

DE        106.3
DR         12
DW         83
FW       7600
O2    50000.000
DP    63L PO

LB          0.0
GB          0.0
NC          5
CX         20.00
CY          0.0
F1          8.000P
F2           .000P
MI           .01
DC          1.000
HZ/CM 200.056
PPM/CM     .400
IS          1
SR     5433.73
```

The products present in the liquid phase mixture include diethylether (DEE), ethylisobutyl ether (EIBE), ethyltertiarybutyl ether (ETBE), tertiarybutyl-isobutylether (TIBE), diisobutylether (DIBE), and a small amount of isobutene (IB). The isobutene was principally detected in the gas phase. However, since the gas phase product analysis was not very reliable, isobutene was determined based on the production of water and the rest of the liquid products. The isobutene value reported here should represent the maximum quantity of isobutene that could be formed. The results are listed in Table 25 in terms of reactant conversions and product selectivities, where Sel.(%EtOH) and Sel.(%iBuOH) are the product selectivities calculated on the basis of ethanol and isobutanol, respectively. The product space time yields obtained in this liquid phase batch reactor are in comparable amounts to that from the continuous flow reactor. For example, the space time yield of EIBE produced in the liquid phase at 100°C is 0.18 mol/kg cat/hr, as compared with the 0.6 mol/kg cat/hr from the continuous flow gas phase reactor (obtained at 110°C).

Table 25. Conversion and selectivity of the liquid-phase ethanol/isobutanol batch reaction at 100 °C as a function of time.

Time (hr):	4.0	9.0	21.5	31.5
EtOH Conversion (%)	1.8	3.8	8.3	11.4
iBuOH Coversion (%)	0.7	1.5	2.4	2.8
Sel.(%EtOH) DEE	46.0	42.4	42.8	39.5
Sel.(%EtOH) EIBE	46.0	50.8	51.2	54.4
Sel.(%EtOH) ETBE	7.2	6.2	6.8	6.1
Sel.(%iBuOH) IB	33.0	40.4	29.5	12.8
Sel.(%iBuOH) EIBE	20.0	18.6	25.2	30.6
Sel.(%iBuOH) ETBE	5.4	2.5	3.0	3.4
Sel.(%iBuOH) TIBE	38.6	34.2	40.1	46.7
Sel.(%iBuOH) DIBE	3.0	4.3	2.2	6.5

IX. Conclusions

A wide range of organic resin catalysts and inorganic oxide and zeolite catalysts have been investigated for activity and selectivity in directly coupling alcohols, principally methanol and isobutanol, to form ethers and in the dehydration of isobutanol to isobutene in the presence of methanol. All of these catalysts are strong acids, and it was found that the organic and inorganic catalysts operate in different, but overlapping, temperature ranges, i.e. mainly 60-120°C for the organic resins and 90-175°C for the inorganic catalysts. For both types of catalysts, the presence of strong acid centers is required for catalytic activity, as was demonstrated by lack of activity of fully K^+ ion exchanged Nafion resin and zirconia prior to being sulfated by treatment with sulfuric acid.

Testing the organic resin catalysts in a gas phase continuous downflow reactor with a methanol/isobutanol = 1/1 reactant mixture in a He/N_2 carrier gas at ambient pressure and 90°C demonstrated that the overall catalytic activity followed the order of Amberlyst-35 > Amberlyst-36 > Amberlyst-15 ≈ Purolite C-150 > BioRad AG 50W X-2 > Amberlyst-1010 > Nafion-H MS. The resins showed differing selectivity patterns as a function of temperature, but the most selective catalyst was observed to be the fluorocarbon sulfonic acid polymer Nafion-H that exhibited over 60% selectivity toward MIBE, with decreasing quanitities of DME, DIBE, butenes, and MTBE as side products. It was demonstrated with the Nafion-H and Amberlyst-35 resins that increasing the partial pressures of the reactant alcohols (with the total reactor pressure in the 0.1-1.3 MPa range) depressed the catalyst productivity toward butenes while enhancing the productivities (and selectivities) of the ethers formed, principally MIBE and DME.

Mechanistic studies carried out over the Nafion-H resin catalyst at 90°C by using ^{18}O-labelled methanol showed that MIBE and MTBE are formed by two different pathways that

do not contain a common intermediate. In particular, in the reaction of $CH_3{}^{18}OH$ + $(CH_3)_2CHCH_2{}^{16}OH$, the products (with >90% isotopic purity) were observed to be ^{16}O-MIBE, ^{18}O-MTBE, and ^{18}O-DME. These isotopic results, along with reaction studies centered on providing insight into the kinetics of the reaction pathways, are consistent with MIBE being formed by a S_N2-type of reaction, but where high concentrations of either reactant cause self-poisoning of the catalyst, i.e. saturation of the active acid centers. This is a feature of a dual site reaction mechanism, which also applies to the scheme of dehydration of isobutanol to isobutene that subsequently reacts with methanol to form MTBE.

The inorganic catalysts were generally less active than the resin catalysts, and higher reaction temperatures were required to achieve significant dehydration of the alcohols. The overall order of activities for the dehydration reactions over the inorganic solid acids was SO_4^{2-}/ZrO_2 > H-ZSM-5 zeolite > H-mordenite > SiO_2/Al_2O_3 > H-montmorillonite >> γ-Al_2O_3. Of special note are the findings that from a methanol/isobutanol = 1/1 reactant mixture,

1. **H-mordenite** was active in selectively dehydrated methanol with near total conversion to dimethylether (DME) while not converting isobutanol to products at temperatures ≤150°C, and
2. the **SO_4^{2-}/ZrO_2** catalyst was very active, with near total conversion, in dehydrating isobutanol to isobutene at 175°C without significantly activating methanol.

The former observation could be the basis for a process for separating isobutanol from methanol while at the same time producing DME. The latter experimental result could be the basis for a 2-step process for the selective conversion of methanol/isobutanol to MTBE, wherein the first step would be carried out over the SO_4^{2-}/ZrO_2 catalyst, e.g. at 175°C, and the second step would couple the isobutene with the unreacted methanol over

a resin catalyst at lower temperature, e.g. Amberlyst-15 or -35 resin at 60-90°C.

Molecular modelling *via* computer graphics of the selective activation and conversion of methanol to DME, in the presence of isobutanol, over H-mordenite indicates that the active acid sites are located in the side pockets of the zeolite structure and not in the large channels. Thus, the active acid centers are not accessible to isobutanol because the pockets are perpendicular to the larger channels, and the isobutanol molecule does not have room to rotate to interact with the acid centers nor to interact with activated methanol in the pockets. It appears that poisoning of the accessible acid centers in the larger channels by the basic isobutanol molecule must also occur at low reaction temperatures because experimentally isobutanol begins to be activated and to form isobutene and MIBE (if methanol is present) at ≈150°C.

Extensive testing and characterization of the active SO_4^{2-}/ZrO_2 catalyst that selectively dehydrates isobutanol to isobutene has been carried out. It was shown that this catalyst was much more active for dehydration of isobutanol to isobutene than for dehydration of ethanol, n-propanol, and n-butanol to olefins. Elevated pressures tended to inhibit the isobutanol dehydration reaction, but high space time yields of isobutene could be obtained by using high isobutanol feed rates and high reaction temperature, e.g. >11 mol isobutene/kg catal/hr at 225°C. The presence of small quantities of water in the reactant alcohol mixture had no effect on the activity in converting isobutanol to isobutene.

It was found that the sulfating treatment signficantly increased the surface area of the zirconia, and XPS analysis indicated that the surface contained 1 S/2 Zr (≈0.5 monolayer coverage), which agreed with the chemical analysis of the catalyst. Therefore, the sulfate groups are located on the surface of the catalyst, and titration showed that there was 1 H^+/SO_4^{2-} group in an aqueous environment. Using pyridine as a probe for acid sites, XPS

analysis using resolved positions of the N 1s line showed that there were both Lewis and Brönsted acid sites on the catalyst, and to-date no difference has been found between dry (calcined to 620°C) and wet (H_2O exposed) samples of this catalyst. In contrast, analogous XPS analyses showed that the Nafion-H catalyst had only Brönsted acid sites, while γ-alumina had only Lewis acid sites.

Using samples of MIBE prepared by us, it was found that MIBE has low blending research and motor octane numbers in unleaded regular gasoline. It was shown that a 1/1 mixture of MIBE/MTBE could be added to gasoline to enhance the oxygenate content while not changing the research and motor octane numbers of the gasoline. With respect to cetane numbers, it was found that MIBE has an elevated cetane number of ≈53, which is significantly above the 40-45 cetane level of diesel fuel used in the U.S.

X. Acknowledgements

The experimental research reported here was principally carried out by Owen C. Feeley and Marie A. Johansson. Contributions to the research were also made by Stefaan DeTavenier, Roy D. Bastian, Mark Kieke, Jamie Menszak and Dan Kim.

We appreciate the determination of octane numbers of ether/gasoline blends for us by the AMOCO Oil Co. and of the cetane number of MIBE for us by the Southwest Research Institute.

XI. References

1. "*Critical Technologies: The Role of Chemistry and Chemical Engineering*," National Research Council, National Academy Press, Washington, D.C., pp 22-23 (1992).

2. Chase, J. D., and Galvez, B. B., Hydrocarbon Process., 60(3), 89 (1981).

3. Chase, J. D., in "*Catalytic Conversions of Synthesis Gas and Alcohols to Chemicals*," ed. by R. G. Herman, Plenum Press, New York, 307 (1984).

4. Hydrocarbon Process., 68(11), 96 (1989); and Satterfield, C. N., "*Heterogeneous Catalysis in Industrial Practice*," 2nd Ed., McGraw-Hill, Inc., New York, 260 (1991).

5. Haggin, J., Chem. Eng. News, 67(23), 31 (1989).

6. Monfils, J. L., Barendregt, S., Kapur, S. K., and Woerde, H. M., Hydrocarbon Process., 71(2), 47 (1992).

7. Krishna, A. S., Hsieh, C. R., English, A. R., Pecoraro, T. A., and Kuehler, C. W., Hydrocarbon Process., 70(11), 59 (1991).

8. Chem. Eng. News, 70(15), 17 (1992).

9. Chem. Eng. News, 70(19), 26 (1992).

10. Abraham, O. C., and Prescott, G. F., Hydrocarbon Process., 71(2), 51 (1992).

11. Klier, K., Herman, R. G., and Young, C.-W., Preprints, Div. Fuel Chem., ACS, 29(5), 273 (1984).

12. Klier, K., Herman, R. G., Nunan, J. G., Smith, K. J., Bogdan, C. E., Young, C.-W., and Santiesteban, J. G., in "*Methane Conversion*," ed. by D. M. Bibby, C. D. Chang, R. F. Howe, and S. Yurchak, Elsevier, Amsterdam, 109 (1988).

13. Nunan, J. G., Bogdan, C. E., Klier, K., Smith, K. J., Young, C.-W., and Herman, R. G., J. Catal., 116, 195 (1989).

14. Nunan, J. G., Herman, R. G., and Klier, K., J. Catal., 116, 222 (1989).

15. Herman, R. G., in "*New Trends in CO Activation*," ed. by L. Guczi, Elsevier, Amsterdam, 265 (1991).

16. Nunan, J. G., Klier, K., and Herman, R. G., J. Chem. Soc., Chem. Commun., 676 (1985).

17. Nunan, J. G., Klier, K., and Herman, R. G., J. Catal., 139, 406 (1993).

18. Baba, T., Ono, Y., Ishimoto, T., Moritaka, S., and Tanooka, B., Bull. Chem. Soc. Jpn., 58, 2155 (1985).

19. Dorfner, K., "*Ion Exchangers*," ed. by K. Dorfner, Walter de Gruyter, Berlin, 22 (1990).

20. Arnett, E. M., Haaksma, R. A., Chawla, B., and Healey, M. H., J. Am. Chem. Soc., 108, 4888 (1986).

21. Tanabe, K., Misano, M., Ono, Y., and Hattori, H., "*New Solid Acids and Bases*," Elsevier, Amsterdam, 175 (1989).

22. Knözinger, H., Angew. Chem. Intern. Ed., 7, 791 (1968).

23. Pines, H. and Manassen, J., Advan. Catal., 16, 49 (1966).

24. Herman, R. G., Klier, K., Young, C.-W., Nunan, J. G., Feeley, O. C., and Johansson, M. A., Proc. 9th Intern. Pittsburgh Coal Conf., 409 (1992).

25. Erwin, J., Southwest Research Institute, private communication (1993); determined with a sample of MIBE synthesized by us.

26. Cornu, A., and Massot, R., "*Compilation of Mass Spectral Data*," Second Edition, Heyden, London (1975).

27. Ingold, C. K., "*Structure and Mechanism in Organic Chemistry*," Second Edition, Cornell University Press, Ithaca, New York (1969) Chap. 7.

28. Ancillotti, F., Mauri, M. M., and Pescarollo, E., J. Catal., 46, 49 (1977); Ancillotti, F., Mauri, M. M., Pescarollo, E., and Romagnoni, L., J. Mol. Catal., 4, 37 (1978).

29. Gicquel, A., and Torck, B., J. Catal., 83, 9 (1983).

30. Hino, M., Kobayashi, S., and Atara, K., J. Am. Chem. Soc., 101, 6439 (1979).

31. Hino, M., and Atara, K., J. Chem. Soc., Chem. Comm., 851 (1980).

32. Yamaguchi, T., Tanabe, K., and Kung, Y.C., Mater. Chem. Phys., 16, 67 (1986).

33. Schlenker, J. L., Pluth, J. J., and Smith, J. V., Mater. Res. Bull., 13, 901 (1978); 14, 751 (1979).

34. Breck, D. W., "*Zeolite Molecular Sieves: Structure, Chemistry, and Use*," John Wiley & Sons, Inc., New York (1974).

35. Knözinger, H., and Scheglila, A., J. Catal., 17, 252 (1969).

36. Herling, J., and Pines, H., Chem. & Ind., 984 (1963).

37. Peri, J. B., J. Phys. Chem., 69, 231 (1965).

38. Kotsarenko, S., and Malysheva, L. V., Kinet. Katal., 24, 877 (1983).

39. Weisz, P. B., Frilette, V. J., Maatman, R. W., and Mower, E. B., J. Catal., 1, 307 (1962).

40. Csicsery, S. M., J. Catal., 19, 394 (1970).

41. Chen, N. Y., Mazuik, J., Schwartz, A. B., and Weisz, P. B., Oil & Gas J., 154 (Nov. 18, 1968).

42. Tanabe, K., Misano, M., Ono, Y., and Hattoir, H., "*New Solid Acids and Bases,*" Elsevier, Amsterdam, 199 (1989).

43. Hsu, C.-Y., Heimbuch, C. R., Armes, C. T., and Gates, B. C., J. Chem. Soc., Chem. Commun., 1645 (1992).

44. Lin, C.-H., and Hsu, C.-Y., J. Chem. Soc., Chem. Commun., 1479 (1992).

45. Rohrbaugh, W. J., and Wu, E. L., in "*Characterization and Catalyst Development,*" ed. by S. A. Bradley, M. J. Gattuso, and R. J. Bertolacini, ACS Symp. Ser., 411, 279 (1989).

46. Mortier, W. J., "*Compilation of Extra Framework Sites in Zeolites,*" Butterworth, New York (1982).

47. Chu, P.-J., Gerstein, B. C., Nunan, J., and Klier, K., J. Phys. Chem., 91, 3588 (1987).

48. Feeley, O. C., Johansson, M. A., Herman, R. G., and Klier, K., Preprints, Div. Fuel Chem., ACS, 37(4), 1817 (1992).

49. Kotsarenko, S., and Malysheva, L.V., Kinet. Katal., 24, 877 (1983).

50. Keim, W., and Falter, W., Catal. Letters, 3, 59 (1989).

51. Arata, K., Adv. Catal., 37, 165 (1990).

52. Tanabe, K., Misono, M., Ono, Y., and Hattori, H., "*New Solid Acids And Bases,*" Elsevier, Amsterdam, 201 (1989).

53. Forni, L., Catal. Rev., 8(1), 65, (1973).

54. Defosse, C., and Canesson, P., J. Chem. Soc., Faraday Trans. 1, 2565 (1976).

55. Chang, C. C., Surface Sci., 48, 9 (1975).

56. Dreiling, M. J., Surface Sci., 71, 231 (1978).

57. Vedage, G. A., Himmelfarb, P. B., Simmons, G. W., and Klier, K., ACS Symp. Ser., 279, 295 (1985).

58. Seah, M. P., and Dench, W. A., Surface Interface Anal., 1, 2 (1979).

59. Spindelbalker, C., and Schmidt, A., Erdol, Erdgas und Kohle, 102 469 (1986).

60. Dietz, W. A., J. Gas Chromatogr., 5, 68 (1967).